UNIVERSIDADE FEDERAL DE PELOTAS
Centro de Ciências Químicas, Farmacêuticas e de Alimentos
Programa de Pós-Graduação em Bioquímica e Bioprospecção

TESE

A efetividade do composto 1,4-anidro-4-seleno-D-talitol (SeTal) e biomateriais poliméricos no tratamento de lesões semelhantes a dermatite atópica em camundongos

Guilherme Teixeira Voss

Pelotas, 2022

Universidade Federal de Pelotas / Sistema de Bibliotecas
Catalogação na Publicação

V969e Voss, Guilherme Teixeira

A efetividade do composto 1,4-anidro-4-seleno-D-talitol (SeTal) e biomateriais poliméricos notratamento de lesões semelhantes a dermatite atópica em camundongos / Guilherme Teixeira Voss ; Ethel Antunes Wilhelm, orientadora ; Cristiane Luchese, coorientadora. — Pelotas, 2022.

159 f.

Tese (Doutorado) — Bioquímica e Bioprospecção, Centro de Ciências Químicas, Farmacêuticas e de Alimentos, Universidade Federal de Pelotas, 2022.

1. Selênio. 2. Dermatite atópica. 3. Tratamento cutâneo. 4. Biopolimero. 5. Hidrocortisona. I. Wilhelm, Ethel Antunes, orient. II. Luchese, Cristiane, coorient. III. Título.

CDD : 616.5

Elaborada por Ubirajara Buddin Cruz CRB: 10/901

Guilherme Teixeira Voss

A efetividade do composto 1,4-anidro-4-seleno-D-talitol (SeTal) e biomateriais poliméricos no tratamento de lesões semelhantes a dermatite atópica em camundongos

Tese apresentada ao Programa de Pós-Graduação em Bioquímica e Bioprospecção do Centro de Ciências Químicas, Farmacêuticas e de Alimentos da Universidade Federal de Pelotas, como requisito parcial à obtenção do título de Doutor em Ciências com ênfase em Bioquímica e Bioprospecção.

Orientadora: Prof.ª Drª. Ethel Antunes Wilhelm
Coorientadora: Prof.ª Drª. Cristiane Luchese

Pelotas, 2022

Guilherme Teixeira Voss

Título: A efetividade do composto 1,4-anidro-4-seleno-D-talitol (SeTal) e biomateriais poliméricos no tratamento de lesões semelhantes a dermatite atópica em camundongos

Tese apresentada ao Programa de Pós-Graduação em Bioquímica e Bioprospecção do Centro de Ciências Químicas, Farmacêuticas e de Alimentos da Universidade Federal de Pelotas, como requisito parcial à obtenção do título de Doutor em Ciências com ênfase em Bioquímica e Bioprospecção.

Data da defesa: 20 de dezembro de 2022

Banca examinadora:

.....

Profª. Drª. Ethel Antunes Wilhelm (Orientadora)
Doutora em Ciências Biológicas (Bioquímica Toxicológica) pela Universidade Federal de Santa Maria, UFSM, Brasil.

.....

Profª.Drª. Lucielli Savegnago
Doutora em Ciências Biológicas (Bioquímica Toxicológica) pela Universidade Federal de Santa Maria, UFSM, Brasil.

.....

Drª. Gabriela Klein Couto
Doutora em Bioquímica e Bioprospecção pela Universidade Federal de Pelotas, UFPel, Brasil.

.....

Prof. Dr. Diogo La Rosa Novo
Doutor em Química pela Universidade Federal de Pelotas, UFPel, Brasil.

Dedico essa tese
à minha família .

Agradecimentos

Agradeço primeiramente a minha família por todo apoio e incentivo durante a minha jornada, em especial os meus pais **Rosi** e **Beto** que nunca mediram esforços para me ajudar durante este processo, sem vocês nada disso teria acontecido.

A minha noiva, **Renata,** que sempre me deu apoio em todas as horas, principalmente nas mais difíceis. Esse agradecimento é principalmente para você que além de todo o amor e cuidado que tens comigo, me ajudou diretamente em toda minha vida acadêmica, por onde passamos por todas as etapas da graduação até o doutorado, e realizamos o nosso sonho de nos formarmos e concluir esta etapa juntos.

A minha orientadora **Ethel,** por todo suporte que me deu, por estar sempre disposta a me ajudar, por todas as correções e incentivo. Obrigado por tudo professora!

A minha coorientadora e professora **Cristiane,** pela disponibilidade e incentivo desde o período da graduação. Obrigado **Cris**!

A todos meus colegas de laboratório**,** e a todos os outros envolvidos neste processo, por todo apoio e parceria.

Aos laboratórios parceiros, **Laboratório de Genômica Estrutural**, **Laboratório Regional de Diagnóstico da Faculdade de Veterinária**, **Department of Biomedical Sciences of University of Copenhagen, Laboratório de Tecnologia e Desenvolvimento de Compósitos e Materiais Poliméricos e a Seleno Therapeutics.**

Ao **Biotério Central** da Universidade Federal de Pelotas e seus funcionários.

À todos os professores do Programa de Pós-Graduação em Bioquímica e Bioprospecção, e também à Universidade Federal de Pelotas.

À CAPES pelo auxílio financeiro no decorrer do trabalho.

Enfim agradeço, a todos que de uma forma ou de outra colaboraram para a realização deste trabalho.

Resumo

VOSS, Guilherme Teixeira. **A efetividade do composto 1,4-anidro-4-seleno-D-talitol (SeTal) e biomateriais poliméricos no tratamentos de lesões semelhantes a dermatite atópica em camundongos**. Orientadora: Ethel Antunes Wilhelm. 2022. 159 f. Tese (Doutorado em Ciências com ênfase em Bioquímica e Bioprospecção) - Centro de Ciências Químicas, Farmacêuticas e de Alimentos, Universidade Federal de Pelotas, Pelotas, 2022.

A dermatite atópica (DA) é uma das doenças crônicas mais comuns da pele que se caracteriza por lesões avermelhadas, com elevado prurido e escamação (lesões eczematosas), desencadeadas por processo inflamatório e alérgico. Os corticosteroides de uso tópico (não específicos para a DA), têm sido a base dos tratamentos, porém, a eficácia é limitada, e a aplicação a longo prazo acarreta no risco de desenvolver efeitos adversos (afinamento da pele, fissuras e sangramento). Frente a isso, estudos experimentais têm buscado terapias que possam atuar nessa patologia complexa. Assim, o objetivo da presente tese consistiu-se na busca por uma nova estratégia terapêutica para o tratamento de lesões semelhantes à DA induzida por 2,4-dinitroclorobenzeno (DNCB) em camundongos. Inicialmente, no artigo 1,avaliou-se a eficácia de um composto orgânico de selênio, o 1,4-anidro-4-seleno-D-talitol (SeTal) na redução das lesões e dos sintomas encontrados na DA por meio da modulação de parâmetros inflamatórios em um modelo experimental utilizando camundongos. Além disso, neste estudo foi comparado o efeito do SeTal com um dos medicamentos de referência da classe dos corticosteroides utilizados para tratar a DA, a hidrocortisona (HC), no qual o SeTal apresentou efeitos positivos e menores efeitos adversos em comparação com a HC. Tendo em vista, que a HC apresenta efeitos adversos relevantes quando utilizada por períodos prolongados, outro objetivo dessa tese foi melhorar o tratamento já utilizado, buscando uma maneira de reduzir estes efeitos. Sendo assim, no artigo 2 foi desenvolvido um sistema de administração de HC, por meio da utilização de um filme biopolimérico composto de gelatina e/ou amido, capaz de atuar nas lesões semelhantes a DA, modulando parâmetros inflamatórios e com mínima absorção sistêmica. E por fim, no manuscrito avaliou-se o efeito associativo do SeTal com a HC ou com a vitamina C encapsulados em biomateriais de gelatina e alginato

de sódio, como uma abordagem para tratar lesões semelhantes a DA localmente. Dessa forma, os resultados dessa tese contribuem para um melhor entendimento da fisiopatologia da DA, assim como para o desenvolvimento de um novo tratamento para as suas lesões e sintomas. Portanto, o SeTal pode ser uma importante alternativa terapêutica para o tratamento das lesões semelhantes a DA. Além disso, enquanto a busca por um tratamento eficaz é realizada os filmes biopoliméricos tornan-se uma alternativa promissora para melhorar a eficiência e reduzir os efeitos adversos do tratamento já utilizado (HC).

Palavras-chave: Selênio. Dermatite atópica. Tratamento cutâneo. Biopolimero. Hidrocortisona.

Abstract

VOSS, Guilherme Teixeira. **The effectiveness of the compound 1,4-anhydro-4-selene-D-thalitol (SeTal) and polymeric biomaterials in the treatment of lesions similar to atopic dermatitis in mice.** Advisor: Ethel Antunes Wilhelm. 2022. 159 f. Thesis (Doctorate in Science an emphasis on Biochemistry and Bioprospecting) - Center for Chemical, Pharmaceutical and Food Sciences, Federal University of Pelotas, Pelotas, 2022.

Atopic dermatitis (AD) is one of the most common chronic skin diseases that is characterized by reddish lesions, with high itching and scaling (eczematous lesions), triggered by an inflammatory and allergic process. Topical corticosteroids (non-specific for AD) have been the basis of treatments, however, their effectiveness is limited, and long-term application carries the risk of developing adverse effects (thinning of the skin, fissures and bleeding). Faced with this, experimental studies have sought therapies that can act in this complex pathology. Thus, the objective of this thesis consisted in the search for a new therapeutic strategy for the treatment of lesions similar to AD induced by 2,4-dinitrochlorobenzene (DNCB) in mice. Initially, in article 1, the effectiveness of an organic selenium compound, 1,4-anhydro-4-seleno-D-thalitol (SeTal) was evaluated in the reduction of lesions and symptoms found in AD through the modulation of inflammatory parameters in an experimental model using mice. In addition, this study compared the effect of SeTal with one of the reference drugs in the corticosteroid class used to treat AD, hydrocortisone (HC), in which SeTal showed positive effects and fewer adverse effects compared to HC. Bearing in mind that HC has relevant adverse effects when used for prolonged periods, another objective of this thesis was to improve the treatment already used, seeking a way to reduce these effects. Therefore, in article 2, a CH administration system was developed, through the use of a biopolymeric film composed of gelatin and/or starch, capable of acting on AD-like lesions, modulating inflammatory parameters and with minimal systemic absorption. Finally, the manuscript evaluated the associative effect of SeTal with HC or vitamin C encapsulated in gelatin and sodium alginate biomaterials, as an approach to locally treat AD-like lesions. Thus, the results of this thesis contribute to a better

understanding of the pathophysiology of AD, as well as to the development of a new treatment for its lesions and symptoms. Therefore, SeTal may be an important therapeutic alternative for the treatment of AD-like lesions. In addition, while the search for an effective treatment is carried out, biopolymer films become a promising alternative to improve efficiency and reduce the adverse effects of the already used treatment (HC).

Keywords: Selenium. atopic dermatitis. Skin treatment. Biopolymer. Hydrocortisone.

Lista de figuras

Revisão Bibliográfica

Artigo 1

Fig. 1 Chemical structure of 1,4-anhydro-4-seleno-D-talitol (SeTal).

Fig. 2 Summary of experimental protocol for the development of atopic AD-like skin lesions in DNCB treated mice.

Fig. 3 The effect of SeTal treatment on (**A)** dermatitis scores, (**B)** scratching incidence and (**c)** ear swelling, after DNCB exposure. Data are means ± SEMs (one-way ANOVA followed by the Tukey's test). # $p < 0.05$ compared with the control group, * $p < 0.05$ compared with the DNCB group, & $p < 0.05$ compared with the HC group.

Fig. 4 The effect of SeTal treatment on (**A)** ear swelling, (**B)** ear MPO activity and **(C)** dorsal skin MPO activity. Data are means ± SEMs (one-way ANOVA followed by the Tukey's test). # $p < 0.05$ compared with the control group, * $p < 0.05$ compared with the DNCB group, & $p < 0.05$ compared with the HC group.

Fig. 5 The effect of SeTal treatment on mRNA expression levels of cytokines: (**A)** TNF-α, (**B)** IL-18 and **(C)** IL-33 in mouse dorsal skin. Data are means ± SEMs. (one-way ANOVA followed by the Tukey's test). # $p < 0.05$ compared with the control group, * $p < 0.05$ compared with the DNCB group, & $p < 0.05$ compared with the HC group.

Fig. 6 Photomicrographs showing the severity of ear and dorsal-skin morphological alterations caused by treatment exposure. (**1)**, (**2)**, (**3)** and (**4)** represent control animals, which show a normal aspect; (**5)**, (**6)**, (**7)** and (**8)** represent animals exposed to DNCB – [vascular congestion (*), dilated lymphatic vessels (arrow), and the presence of a crust on the inner and outer faces (arrowhead), C (cartilage) and subepidermal pustules (arrow)]. (**9)**, (**10)**, (**11)** and (**12)** represent 1% HC + DNCB group – [thickened ear with vascular congestion (*), dilated lymphatic vessels (arrow), and the presence of intraepidermal pustules (arrowhead), C (cartilage), presence of intraepidermal (long arrow) and subepidermal (short arrow) pustules]. (**13)**, (**14)**, (**15)** and (**16)** represent 1%

SeTal + DNCB group and (**17)**, (**18)**, (**19)** and (**20)** 2% SeTal + DNCB group - [a thick crust is present (*) as well as bacterial colonies and subepidermal pustules (arrow)]. (HE staining - 100X and MT - 100X and 400X).

Artigo 2

Fig. 1 Summary of experimental protocol for the development of atopic dermatitis-like (AD-like) skin lesions in 2,4-dinitrochlorobenzene (DNCB) treated mice. The dorsal skin of the mice was shaved and between days 1-3 were topically treated with 0.5% DNCB. The mice were then challenged with 1% DNCB on days 14, 17, 20, 23, 26, and 29. AD-like mice were treated with topical film loaded or not with HC (Gel, Gel@HC, Gel/St or Gel/St@HC), or hydrocortisone (HC) on each 3 days, between diads 14-27.. Finally, the mice were euthanized on day 30.

Fig. 2 FTIR spectra of (a) starting materials (pure gelatin, starch, hydrocortisone) and (b) biopolymeric films loaded (Gel@HC and Gel/St@HC) or not (Gel and Gel/St) with hydrocortisone.

Fig. 3 (a) TGA and (b) DTG curves of HC, Gel, Gel/ST, Gel@HC, and Gel/St@HC.

Fig. 4 SEM images recorded from (a) Gel, (b) Gel/St, (c) Gel@HC, and (d) Gel/St@HC films**.**

Fig. 5 Light microscopy images of (a) pure HC, (b) Gel@HC, and (c) Gel/St@HC films.

Fig. 6 Photographic images recorded from (a–c) Gel@HC and (d–f) Gel/St@HC films.

Fig. 7 Swelling profile of the prepared biopolymeric films in SWF (pH 7.4) at 37 °C.

Fig. 8 (a) In vitro dissolution profile of HC (control) and HC released from Gel@HC and Gel/St@HC in SWF (pH 7.4) at 37 °C. (b) Korsmeyer-Peppas plots for Gel@HC and Gel/St@HC.

Fig. 9 The effect of topical treatment with film loaded or not with hydrocortisone (HC) (Gel, Gel@HC, Gel/St or Gel/St@HC), or HC (cream) on atopic dermatitislike (AD-like) symptoms in mice. (a) Images of dorsal skin and ear lesions from groups of mice taken on the last day of the experiment (day 30), (b) signs of skin lesions, and (c) scratching incidence time. Data represent the mean ± S.E.M. (one-way ANOVA followed by the Newman-Keuls' test). * $p < .05$ compared with the control group, # $p < .05$ compared with the 2,4-dinitrochlorobenzene (DNCB) group, & $p < .05$ compared with the HC group.

Fig. 10 The effect of topical treatment with film loaded or not with hydrocortisone (HC) (Gel, Gel@HC, Gel/St or Gel/St@HC), or hydrocortisone (HC, cream) on (a) ear swelling, (b) myeloperoxidase (MPO) activity in ears and (c) dorsal skin of mice. Data represent the mean ± S.E.M. (one-way ANOVA followed by the Newman- Keuls' test). *$p < .05$ compared with the control group, #$p < .05$ compared with the 2,4-dinitrochlorobenzene (DNCB) group, &$p < .05$ compared with the HC group.

Fig. 11 The effect of topical treatment with film loaded or not with hydrocortisone (HC) (Gel, Gel@HC, Gel/St or Gel/St@HC), or HC (cream) on corticosterone levels in mice. Data represent the mean ± S.E.M. (one-way ANOVA followed by the Newman-Keuls' test). * $p < .05$ compared with the control group, # $p < .05$ compared with the 2,4-dinitrochlorobenzene (DNCB) group, & $p < .05$ compared with the HC group.

Manuscrito

Fig.1 Summary of experimental protocol for the development of AD-like skin lesions in DNCB-sensitized mice.

Fig.2 (a) FTIR spectra and (b) XRD patterns of Gel-Alg, Gel-Alg/SeTal, Gel-Alg/SeTal/HC, and Gel-Alg/SeTal/VitC.

Fig.3 (a) TGA and (b) DTG curves of Gel-Alg, Gel-Alg/SeTal, Gel-Alg/SeTal/HC, and Gel-Alg/SeTal/VitC.

Fig.4 Photografics of (a) Gel-Alg, (b) Gel-Alg/SeTal, (c) Gel-Alg/SeTal/HC, and (d) Gel-Alg/SeTal/VitC. (e) Photography of the Gel-Alg/SeTal/HC film applied on backhand skin.

Fig.5 (a) Swelling profile of the prepared films immersed in SWF at 37 ºC. (b) SeTal relase profile from Gel-Alg/SeTal, Gel-Alg/SeTal/HC, and Gel-Alg/SeTal/VitC in SWF (pH 7.4) at 37 ºC.

Fig.6 The effect of topical treatment with films (Gel-Alg, Gel-Alg/SeTal, Gel-Alg/SeTal/HC, and Gel-Alg/SeTal/VitC) or Hydrocortisone (cream) on atopic dermatitis-like (AD-like) symptoms in mice. (a) Photographics of dorsal skin, (b) skin lesion score, (c) scratching time, (d) back thickness, (e) spleen length, and (f) spleen weight after DNCB sensitizing. Data are means ± SEMs (One-way ANOVA followed by Tukey's test). * $p < 0.05$ compared with the control group, # $p < 0.05$ compared with the vehicle-DNCB group and & $p < 0.05$ compared with the Hydrocortisone group.

Fig.7 The effect of topical treatment with films (Gel-Alg, Gel-Alg/SeTal, Gel-Alg/SeTal/HC and Gel-Alg/SeTal/VitC) or Hydrocortisone (cream) on (a) ear swelling, (b) ear MPO activity and (c) dorsal skin MPO activity Data are means ± SEMs (One-way ANOVA followed by the Tukey's test). * $p < 0.05$ compared with the control group, # $p < 0.05$ compared with the vehicle-DNCB group, + $p < 0.05$

compared with the Gel-Alg/SeTal group and & $p < 0.05$ compared with the Hydrocortisone group.

Fig.8 The effect of topical treatment with films (Gel-Alg, Gel-Alg/SeTal, Gel-Alg/SeTal/HC and Gel-Alg/SeTal/VitC) or Hydrocortisone (cream) on nitric oxide level in mouse dorsal skin. Data are means ± SEMs (One-way ANOVA followed by Tukey's test). * $p < 0.05$ compared with the control group, # $p < 0.05$ compared with the vehicle-DNCB group, + $p < 0.05$ compared with the Gel-Alg/SeTal group, & $p < 0.05$ compared with the Hydrocortisone group.

Fig.9 Photomicrographs showing the severity of dorsal-skin morphological alterations caused by sensibilization with DNCB and treatments. (a) and (b) represent control animals; (c) and (d) represent animals sensitized with DNCB; (e) and (f) represent the HC cream group; (g) and (h) represent the Gel-Alg group; (i) and (j) represent Gel-Alg/SeTal group; (k) and (l) represent Gel-Alg/SeTal/HC and (m) and (n) Gel-Alg/SeTal/VitC group. Insets: Epidermis (E), Dermis (D), Subcutaneous (S), and Muscle layer (M). (H.E. staining - 100X - 200X).

Lista de tabelas

Artigo 1

Artigo 2

Table 1 Mechanical properties of the prepared biopolymeric films loaded or not with hydrocortisone.

Table 2 Kinetic constants and correlation coefficients (R2) obtained from different kinetic models for HC release from Gel@HC and Gel/St@HC films.

Table 3 Effect of treatment with topical film loaded or not with HC (Gel, Gel@HC, Gel/St or Gel/St@HC) or HC (cream, 1%) on the plasma biochemical markers in mice.

Manuscrito

Table 1 Composition of each prepared Gel-Alg film.

Table 2 Thickness and mechanical properties of the films based on Gel-Alg.

Table 3 Kinetic constants and determination coefficients (R2) were calculated from different release models for SeTal release from the prepared films.

Lista de abreviaturas e siglas

DA	Dermatite atópica
Th0/TCD4+	Linfócito auxiliar tipo 0
Th1	Linfócito auxiliar tipo 1
Th2	Linfócito auxiliar tipo 2
IgE	Imunoglobulina E
SeTal	1,4-anhydro-4-selene-D-talitol
HC	Hidrocortisona
IL	Interleucina
INF-gama	Interferon-gama
TNF-alfa	Fator de necrose tumoral alfa
MPO	Mieloperoxidase
DNFB	Dinitrofluorobenzeno
DNCB	2,4-dinitroclorobenzeno
TNP	1,1,1-tricloroetano
APC	Célula apresentadora de antígeno
Se	Selênio
4-PSQ	7-cloro-4-(fenilselanil) quinolina
Gel	Gelatina
ATP	Adenosina trifosfato
Alg	Alginato de sódio
VitC	Vitamina C
NOx	Níveis de nitrito e nitrato
RS	Espécies reativas
TGA/DTG	Teste de análise termogravimétrica
ANVISA	Âgencia Nacional de Vigilância Sanitária
IL-4Rα	Receptor alfa de interleucina 4
SEM	Microscopia eletrônica de varredura
NF-κB	Fator Nuclear Kappa B
HPA	Eixo Hipotálamo-hipófise Adrenal

SUMÁRIO

1. INTRODUÇÃO

A pele reúne uma complexidade própria no que diz respeito à sua constituição, representando o maior órgão do corpo e tendo como principal função atuar como barreira anatômica e fisiológica entre o organismo e o meio ambiente (Lai-Cheong & McGrath, 2017). Enquanto desempenha a sua função de proteção, a pele é exposta a diversos fatores externos, o que pode levar a uma série de problemas e doenças. Entre essas doenças, destaca-se a dermatite atópica (DA), que é uma das doenças inflamatórias crônicas mais comuns da pele, caracterizada por prurido intenso e lesões eczematosas recorrentes (H. Kim et al., 2014). Os pacientes com DA sofrem de estresse psicológico grave, o que aumenta acentuadamente a taxa de prevalência de depressão e transtornos de ansiedade na vida adulta, reduzindo a qualidade de vida dos portadores dessa doença (Bruno et al., 2016).

A fisiopatologia da DA é complexa e não está totalmente esclarecida. Acredita-se que a ativação exacerbada de linfócitos T (responsáveis pela defesa do organismo contra agentes desconhecidos (antígenos)), especialmente linfócitos auxiliares tipo 2 (linfócitos Th2), podem levar à indução da resposta alérgica e inflamatória na DA (Turner et al., 2012). Células Th2 ativam linfócitos B para produção de imunoglobulina E (IgE), induzindo assim a ativação de mastócitos desencadeando uma reação alérgica (Brandt & Sivaprasad, 2011). Além disso, as células Th2 são responsáveis pela infiltração de eosinófilos no tecido (Eyerich et al., 2013). Dessa forma, uma inibição na atividade de linfócitos Th2 pode acarretar em uma melhora nos sintomas ocasionados pela DA.

A classe de fármacos dos corticosteroides, principalmente de uso tópico, têm sido a base dos tratamentos farmacológicos para DA, mas para muitos pacientes com essa doença na sua forma moderada ou grave, a eficácia dos tratamentos tópicos é limitada, e a aplicação a longo prazo acarreta no risco de desenvolver efeitos colaterais como afinamento da pele (atrofia), estrias, vasos sanguíneos dilatados e clareamento ou escurecimento da pele. (Ring et al., 2012; Eichenfield et al., 2014). Corroborando, as drogas imunossupressoras sistêmicas são geralmente mais eficazes que os tratamentos tópicos, mas também possuem um potencial de gerar efeitos tóxicos mais graves como cansaço, aumento dos níveis de açúcar no sangue, diminuição das defesas corporais, agitação, insônia, aumento de colesterol e de triglicerídeos, dor de cabeça e glaucoma. (Ring et

al., 2012; Sidbury et al., 2014). Com base na relevância da DA e no interesse em alcançar uma eficácia terapêutica para esta doença, o nosso grupo de pesquisa tem se dedicado ao estudo de compostos contendo selênio, bem como na utilização de filmes poliméricos.

Estudos prévios realizados por um grupo de pesquisa parceiro (*Department of Biomedical Sciences, Faculty of Health and Medical Sciences, University of Copenhagen*), demonstraram que o composto 1,4-anidro-4-seleno-D-talitol (SeTal), um derivado de carboidrato contendo selênio solúvel em água, tem atividade antioxidante em um tratamento para feridas crônicas, pois melhora a cicatrização em camundongos normais e diabéticos, e melhora a perfusão vascular (Davies & Schiesser, 2019; Ng et al., 2017; Corin Storkey, 2018). Além disso, estudos preliminares do nosso grupo de pesquisa revelaram que um composto orgânico de selênio apresentou propriedades farmacológicas positivas em modelos experimentais de inflamação e de lesões semelhantes a DA em camundongos (Voss et al., 2018; Wilhelm et al., 2019).

Além da prospecção de um novo composto, nesse estudo também dedicamos esforços em buscar uma alternativa para melhorar o tratamento à base de corticosteroides já existente, bem como investigar a encapsulação do SeTal e sua associação com outros agentes farmacológicos utilizados no tratamento dos sintomas da DA. Alguns estudos utilizam dispositivos de liberação controlada de base polimérica visando melhorar as propriedades farmacológicas de alguns medicamentos, como por exemplo a hidrocortisona (HC) (Dehkharghani et al., 2018; Azandaryani et al., 2018; Malekhosseini et al., 2020). No entanto, o uso de dispositivos de liberação constituídos majoritariamente por biopolímeros como a gelatina, amido e o alginato de sódio tem sido pouco explorado. A gelatina é um biopolímero derivado do colágeno amplamente utilizado pelas indústrias alimentícia, farmacêutica e médica (Young et al., 2005; Radosinski et al., 2019). O amido é um biopolímero que consiste predominantemente em dois polissacarídeos (amilose e amilopectina), que exibe excelentes propriedades de formação de filme. O Alginato é um polissacarídeo linear natural, extraído comercialmente de algas marrons, com reconhecidas propriedades biológicas (K. Y. Lee & Mooney, 2012). Os biopolímeros (gelatina, amido e alginato), existem em abundância, possuem baixo custo, são

biocompatíveis e biodegradáveis, o que estimula seu uso em aplicações médicas e farmacêuticas (Youssef & El-Sayed, 2018; Young et al., 2005).

Tendo em vista as propriedades promissoras do composto SeTal em reduzir às lesões cutâneas semelhantes a DA em camundongos (Voss et al., 2021), decidiu-se ampliar o conhecimento em torno deste composto por meio da sua incorporação em um biomaterial (constituídos de gelatina e alginato). Ainda, para explorar o efeito associativo do SeTal com outros agentes farmacológicos, também foram avaliados filmes biopoliméricos contendo SeTal e HC ou vitamina C, como uma abordagem para tratar as lesões semelhantes à DA localmente. Ademais, objetivou-se melhorar as propriedades farmacológicas da HC, bem como reduzir os seus efeitos adversos através de um filme biopolimérico de gelatina ou gelatina associado ao amido (incorporado com HC), de liberação controlada, ambos estudos utilizando um modelo de DA em camundongos.

2. REVISÃO BIBLIOGRÁFICA

2.1 Dermatite atópica

Segundo a Sociedade Brasileira de Dermatologia (2022), a DA é um dos tipos mais comuns de alergia cutânea caracterizada por eczema atópico. Além disso, a DA se caracteriza por ser uma doença genética, crônica e que apresenta pele seca, erupções e crostas. Seu surgimento é mais comum nas dobras dos braços e na parte de trás dos joelhos. Ademais, a DA pode também vir acompanhada de asma ou rinite alérgica, porém, com manifestação clínica variável.

O termo atopia tem como significado a tendência pessoal e/ou familiar para tornar-se sensibilizado e produzir anticorpos específicos da classe IgE em resposta à alérgenos. A sua prevalência tem aumentado nos últimos anos e os fatores provavelmente implicados nesse aumento de casos seriam a predisposição genética, a poluição, as infecções e a exposição alergênica (Zanandréa et al., 2020).

A manifestação da DA está aumentando drasticamente, especialmente nos países desenvolvidos, e chega a afetar até 30% das crianças e 10% dos adultos. Além disso, esta doença tem maior ocorrência na zona urbana quando comparada com ambientes residenciais rurais (Silverberg et al., 2021). Aproximadamente 50% dos pacientes apresentam as manifestações clínicas iniciais da doença antes dos 5 anos de idade (de Bruin Weller et al., 2012). Cerca de 60% das crianças afetadas com essa doença apresentam o início do quadro na fase de lactente. Ademais, a DA pode persistir na idade adulta em cerca de 40% dos pacientes (Ong & Boguniewicz, 2008). Os principais fatores de risco para permanência dos sintomas são gravidade inicial da dermatite e sensibilização atópica (Illi et al., 2004).

Os ataques de DA são caracterizados por feridas com pápulas eritematosas intensamente pruriginosas associadas a escoriações e exsudatos serosos. A pele afetada pelas lesões ocasionadas por essa patologia apresenta vermelhidão e coceira, além disso, o prurido excessivo pode causar feridas e vazamento de fluidos (Tokura, 2010). Em pacientes com DA crônica, a pele vai gradualmente engrossar e se desgastar, afetando sua aparência. Frente a isso, essas características patológicas podem interferir no humor e estilo de vida dos portadores (Berke et al., 2012).

2.1.1 Fisiopatologia da doença

A fisiopatologia da DA é complexa e não totalmente compreendida. Acredita-se que esta doença seja resultado de interações entre genes de suscetibilidade e fatores ambientais (Lee & Park, 2019). Atualmente, sabe-se que a DA possui comprovada predisposição genética (Bin & Leung, 2016). Cho e colaboradores (2014) observaram um aumento de casos em famílias com antecedentes de atopia, podendo chegar a 75% em crianças que tinham pais com esta dermatose.

Em indivíduos saudáveis, o sistema imunológico atua normalmente, existe um balanço na secreção de células linfocitárias T auxiliares do tipo 1 e 2 (Th1, Th2). Foi descoberto que os pacientes com DA possuem um subconjunto de linfócitos T, citocinas e interleucinas (IL)-4, IL-5 e IL-13, que podem ser utilizados como biomarcadores no diagnóstico desta doença (Brandt & Sivaprasad, 2011). Por outro lado, a atopia é um termo que está ligado a reações de hipersensibilidade mediada por IgE, em resposta a antígenos comuns. Além da fisiopatologia complexa da doença, na literatura são encontrados dados sobre a DA com participação ou não do sistema imunológico (Tokura, 2010). Dessa maneira, são descritos dois subtipos observáveis de DA, a intrínseca (ou seja, não alérgica) e a extrínseca (alérgica). A DA extrínseca é caracterizada por eosinofilia, níveis elevados de IgE total e específica, IL-4, IL-5, IL-13, IL-18 e IL-33 quando expostos a alérgenos alimentares e aeroalérgenos. Aproximadamente 85% dos pacientes com DA estão neste grupo. Por outro lado, a DA intrínseca apresenta fenótipo clínico similar, eosinofilia e ausência de anticorpos específicos para sensibilizações alérgicas. As diferenças em relação às ativações imunológicas entre as duas formas de DA são controversas (Suárez-Fariñas et al., 2013)**.**

Em pacientes com DA na fase crônica, verifica-se a secreção predominante de células linfocitárias Th1 e aumento nos níveis de interferon-gama (INF-gama), IL-5 e fator estimulante de colônias de granulócitos e macrófagos (Keet & Wood, 2014). Por fim, o mecanismo em comum que parece estar relacionado com a fisiopatologia da DA (Figura 1), envolve a super ativação dos linfócitos Th2, que irão liberar interleucinas (IL-4, IL-5, IL-13, IL-18 e IL-33), responsáveis por ativarem linfócitos B a fazer a produção de IgE, além da ativação de mastócitos, eosinófilos e neutrófilos, desencadeando a resposta alérgica e inflamatória (Turner et al., 2012).

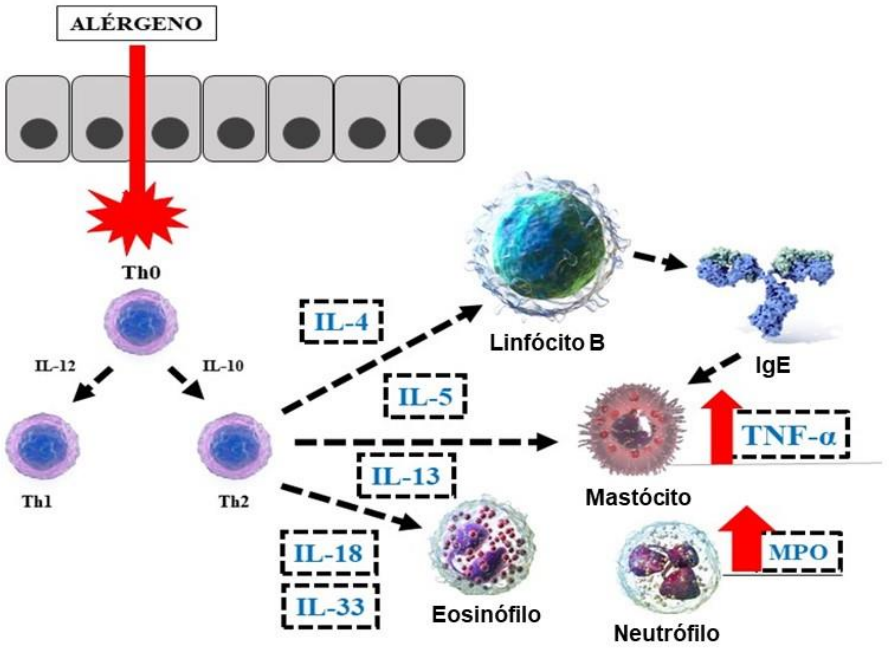

Figura 1. Possível mecanismo atrelado a fisiopatologia da DA (Adaptado do texto de Turner et al., 2012). Abreviações: TNF-α (Fator de necrose tumoral alfa), MPO (Mieloperoxidase). Linfócito Th2 ativado liberando interleucinas responsáveis por ativar células de defesa que irão desencadear o processo alérgico e inflamatório.

2.1.2 Modelos experimentais de indução de DA: 2,4-dinitroclorobenzeno (DNCB)

Modelos de indução de DA são desenvolvidos para melhor compreender a patogênese da doença ou avaliar a eficácia de potenciais terapias (Kim et al., 2019). Os modelos de DA em camundongos são caracterizados em três grupos: *(i)* modelos consanguíneos, no qual os camundongos desenvolvem dermatite eczematosa espontânea sob condições específicas livres de patógenos, com respostas imunes aumentadas contra antígenos percutâneos *(ii)* camundongos geneticamente modificados nos quais os genes de interesse são superexpressos ou deletados e *(iii)* modelos induzidos por aplicação tópica de agentes exógenos (Kim et al., 2019). Neste último modelo, são utilizados sensibilizantes como o dinitrofluorobenzeno (DNFB), 2,4-dinitroclorobenzeno (DNCB), 1,1,1-

tricloroetano (TNP) e oxazolina, estes são indutores que representam uma minoria de substâncias capazes de induzir a DA e são dotados de propriedades pró-inflamatórias potentes (Kalish & Askenase, 1999). A toxicidade desses sensibilizantes fornece um sinal ao sistema imune inato da pele, levando à produção de citocinas inflamatórias, e à ativação de linfócitos T (Kaplan et al., 2012). Os modelos induzidos por aplicação tópica de agentes exógenos são talvez os mais frequentemente utilizados nos campos da pesquisa dermatológica. Embora a aplicação tópica possa ser trabalhosa, ela permite a indução controlada por tempo e dose, além de poder ser utilizada em uma variedade de raças de camundongos, incluindo camundongos geneticamente modificados (Kim et al., 2019).

A aplicação tópica de haptenos, como o DNCB, em camundongos é comumente usada para induzir hipersensibilidade de contato com a pele, além de ser amplamente usado como modelo animal para a DA, uma vez que mimetiza o processo inflamatório da pele envolvido no desenvolvimento e manutenção da doença (Bruno et al., 2016; Kim et al., 2014; Lin et al., 2016). Na hipersensibilidade de contato, os haptenos penetram pela epiderme e se conjugam às proteínas normais do organismo (que funcionarão como proteínas carreadoras). O reconhecimento de um conjugado pelo linfócito T é específico para um conjugado hapteno/carreador. Alguns haptenos, como o DNCB, irão sensibilizar quase todos os indivíduos e por isso esse indutor é amplamente utilizado em modelos animais (Saito et al., 2017).

As células de Langerhans são as principais células apresentadoras de antígenos na hipersensibilidade de contato. Aproximadamente quatro horas após a exposição ao DNCB, estas células aparecem nas áreas corticais dos linfonodos drenantes (De Bezerril, 2014). A hipersensibilidade de contato é dividida em duas fases (fase de sensibilização e fase efetora) (Zhang et al., 2017). A fase de sensibilização ocorre em torno de 10 a 14 dias após a exposição ao DNCB, e nessa fase ocorre a absorção desse hapteno pela pele. Após ser absorvido esse indutor se combina com uma proteína (carreadora), o conjugado hapteno-carreador é internalizado pelas células apresentadoras de antígeno (APC), e essas células vão migrar para as áreas corticais dos linfonodos regionais. As APC vão apresentar o conjugado hapteno-proteína aos linfócitos

TCD4+ (Th0) auxiliares que vão realizar a formação de linfócitos Th0 ativados e um linfócito de memória (Figura 2) (Hennino et al., 2005).

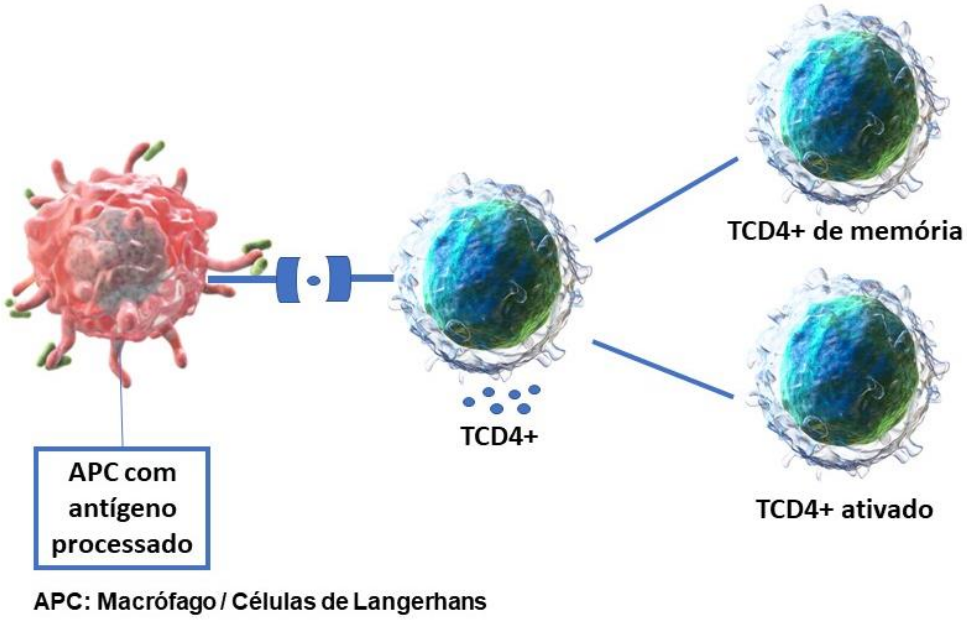

Figura 2. Fase de sensibilização por haptenos. Formação de linfócito TCD4+ ativado e TCD4+ de memória após apresentação do conjugado (Hapteno + receptor), realizado pela APC (Adaptado do texto de Hennino et al., 2005).

Na fase efetora, a manifestação da hipersensibilidade de contato ocorre depois de 4 a 8 horas da exposição ao imunógeno (DNCB). Os linfócitos TCD4+ de memória são ativados pela apresentação do conjugado hapteno-proteína processado pelas células de Langerhans ou macrófagos. A partir desse ponto, essas células passam a produzir e secretar IL-2, IL-4 e IL5, entre outras citocinas importantes para o processo de reação de hipersensibilidade. Segue-se, então, uma proliferação de linfócitos T induzida por estas IL's. Dessa forma, o resultado é uma intensa migração de linfócitos e outras células de defesa para o sítio da inflamação e formação de eczema (Figura 3) (Zhang et al., 2017).

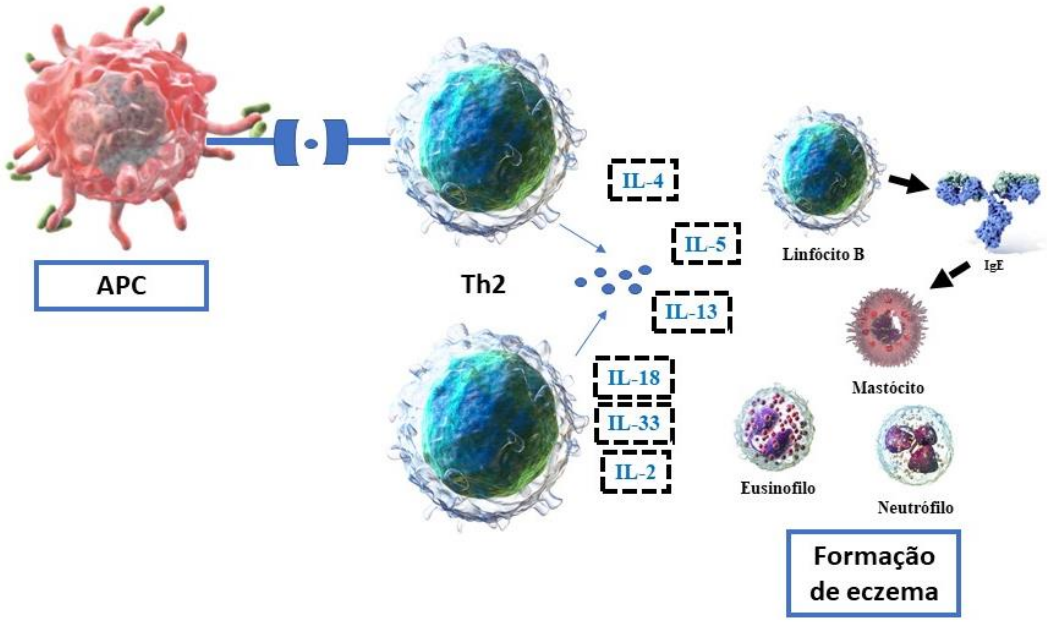

Figura 3. Fase efetora após sensibilização por haptenos. (Adaptado do texto de Hennino et al., 2005).

Frente ao que foi exposto, o modelo de indução utilizando haptenos, no caso o DNCB, mimetiza de forma eficaz os mesmos mecanismos que acreditam-se estar relacionados com a fisiopatologia da DA, tornando esse modelo experimental ideal para o estudo da doença.

2.1.3 Tratamentos para a DA utilizados na atualidade

A DA é uma doença sem cura até os dias atuais (CID 10 - L20). Frente a isso, o portador dessa patologia, deve adotar medidas afim de controlar sua manifestação e tratar as suas complicações (Eichenfield et al., 2014). Normalmente, o primeiro tratamento realizado pelo paciente para controlar as lesões causadas pela DA é o uso de corticosteroides de uso tópico devido a sua ação anti-inflamatória, visando aliviar o prurido. Os corticosteroides potentes, quando aplicados em áreas extensas ou por um período prolongado (mais de sete dias), podem ser absorvidos para a corrente sanguínea. Dessa forma, é preferível interromper o tratamento, pois estes esteroides quando aplicados por um longo período de tempo também levam ao enfraquecimento da pele, rachaduras e sangramentos, facilitando assim a entrada de alérgenos presentes

no meio externo (Tan & Gonzalez, 2012). Os corticosteroides tópicos mais utilizados são: HC, triancinolona e betametasona (Kim et al., 2014).

Por sua vez, essa classe de medicamento quando utilizada por via oral têm uma ação curta e limitada e os efeitos adversos, como reabsorção óssea e renal e inibição da função das glândulas suprarrenais, podem representar um risco superior ao seu benefício (Meena et al., 2017). Em associação com os tratamentos convencionais, podem ser utilizados os anti-histamínicos orais e tópicos que controlam o prurido e permitem o sono, que é perturbado pelo constante ato de coçar (muito característico na DA) (Meena et al., 2017).

Como tratamento de segunda linha na DA são utilizados os imunomoduladores, que são inibidores da proteína ativadora da produção de células T, calcineurina (ciclosporina, tacrolimus e pimecrolimus) e anticorpos monoclonais produzidos por tecnologia de DNA recombinante, que bloqueiam a função da IgE (omalizumab) (Kim et al., 2014). No ano de 2017, a Agência Nacional de Vigilância Sanitária (Anvisa) aprovou no Brasil uma terapia inédita para a DA, o dupilumab, este que é um anticorpo monoclonal totalmente humano dirigido contra a subunidade α (IL-4R α) do receptor IL-4 que inibe a sinalização de IL-4 e IL-13 (Figura 4). Embora outros produtos biológicos, como o omalizumab (anticorpo monoclonal anti-IgE), ustekinumab (anticorpo monoclonal anti-IL-12/IL-23), mepolizumab (anticorpo monoclonal anti-IL-5), BMS-981164 (anticorpo monoclonal anti-IL-31), lebrikizumab (anticorpo monoclonal anti-IL-13) e CIM331 (anticorpo monoclonal anti-IL-31) foram ou estão sendo investigados para DA, o dupilumab é o único, até a presente data, que pode ser comercializado no Brasil para o tratamento dessa patologia (Hamilton et al., 2015).

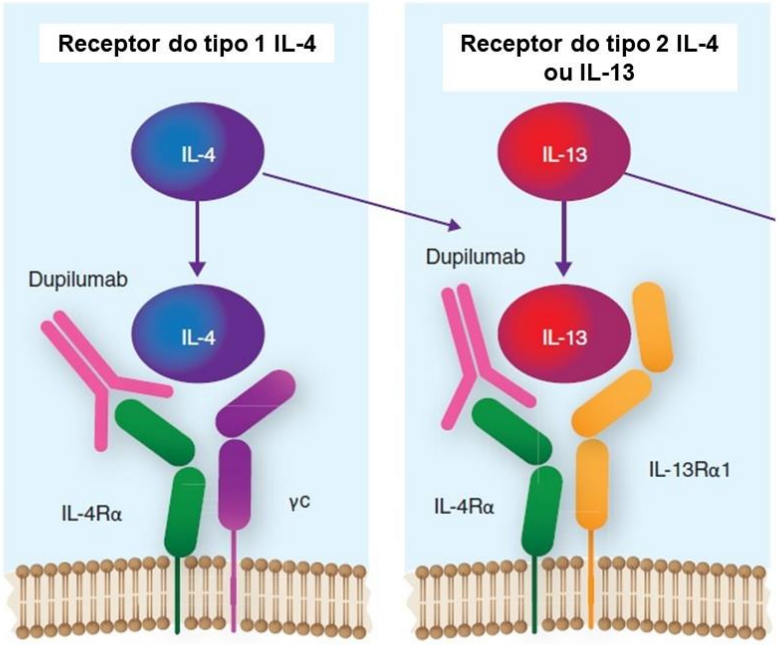

Figura 4. Mecanismo do dupilumab. (Modificado de Hamilton, 2015). Dupilumab inibindo a sinalização através do bloqueio da subunidade α (IL-4R α) do receptor de IL-4 e IL-13.

Além dos tratamentos convencionais e dos novos tratamentos utilizados para amenizar os sintomas da DA, diversos pesquisadores buscam novas alternativas que possam ser utilizadas, tendo em vista que atualmente há uma falta de terapias adequadas, e que a doença não possui cura (Malajian & Guttman-Yassky, 2015). Nesse sentido, diversas moléculas e extratos de plantas foram testadas em modelos animais de DA, buscando auxiliar na melhora dos sintomas dessa patologia (Ju Ho et al., 2018; Tang et al., 2020; Sharma et al., 2020). Embora tenham muitas pesquisas de novas moléculas e extratos que possam vir a tratar a DA, nenhuma delas conseguiu evoluir para se tornar um medicamento exclusivo para o tratamento da patologia, isso provavelmente, devido a fisiopatologia complexa envolvida na doença. Dessa maneira, se faz necessário a utilização de modelos experimentais utilizando animais, visando a busca de uma melhor compreensão da fisiopatologia da doença, assim como a busca de novas estratégias terapêuticas para o seu tratamento.

2.1.4 Hidrocortisona (HC)

A HC é considerada a base do tratamento farmacológico para as lesões da DA (Yuan et al., 2020). Esse medicamento é um análogo sintético do hormônio cortisol que é produzido pela glândula suprarrenal (Prete et al., 2020) (Figura 5). Dentro da classificação dos corticosteroides tópicos de acordo com sua potência, a HC apresenta baixa potência e por isso é a escolha para o tratamento em áreas com alta penetração, incluindo axilas, virilhas, órgãos genitais e face (Chabassol & Green, 2012). De acordo com isso, a HC é um fármaco recomendado para efetuar tratamentos de cunho inflamatório, de origem proliferativa ou de causa imunológica da pele, sendo considerada eficiente no tratamento de sintomas cutâneos com a presença ou não de prurido e sensação de queimadura (Yuan et al., 2020).

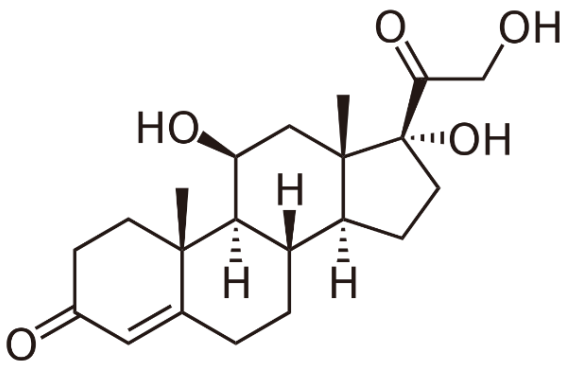

Figura 5. Estrutura da química da hidrocortisona.

.

O mecanismo de ação da HC está ligado a inibição da enzima fosfolipase A2, impedindo a formação de ácido aracdônico e, consequentemente, das prostaglandinas, tromboxanos e leucotrienos. Como agonista do receptor de glicocorticóide, a HC promove o catabolismo proteico, a gliconeogênese, a estabilidade da parede capilar, a excreção renal de cálcio e suprime as respostas imunológicas e inflamatórias (Goodwin et al., 1986). Mesmo a HC sendo a escolha de tratamento para as lesões da DA, quando aplicada em áreas extensas ou por um período prolongado pode desenvolver os efeitos adversos citados no tópico anterior, podendo levar a interrupção do seu uso (Kim et al., 2014). Dessa forma, torna-se importante a pesquisa por novas alternativas

terapêuticas para o tratamento da DA, seja através de novos compostos/moléculas ou alternativas capazes de reduzir os efeitos adversos desta classe de medicamentos utilizados para o tratamento da doença.

2.2 Efeito farmacológico de compostos orgânicos de selênio

O Selênio (Se) é um nutriente essencial para o organismo, que foi descoberto em 1817 pelo químico sueco Jöns Jacob Berzelius. Essa descoberta permitiu que diversos estudos pudessem ser realizados para avaliar a influência de suas formas inorgânicas nos organismos vivos (Kieliszek & Błażejak, 2016). O Se foi reconhecido como um oligoelemento essencial desde 1957, sendo o elemento menos abundante na Terra com finalidade biológica (Schroeder et al., 1970). Na verdade, mais de 25 selenoproteínas foram identificadas em humanos e muitas delas servem a funções críticas (Lu & Holmgren, 2009). Com o passar do tempo, o Se passou a ser empregado em estruturas químicas, uma vez que apresenta diversas propriedades interessantes. Dentre as suas propriedades, destaca-se a antioxidante (Croft et al., 2007).

Este elemento é facilmente introduzido e eliminado de moléculas orgânicas e por isso, a partir da década de 30, os organocalcogênios começaram a ser alvos de interesse para os químicos orgânicos em virtude da descoberta de suas aplicações sintéticas (Comasseto, 1983), e de suas propriedades biológicas e aplicações farmacológicas (Nogueira et al., 2004). Inúmeros estudos demonstram que os compostos orgânicos de Se apresentam propriedades farmacológicas interessantes, como: antioxidantes, anti-inflamatórias, neuroprotetoras, ansiolítica, anti-hiperglicêmica, anti-hipertensiva, anticâncer, antiviral, imunossupressora, antidepressiva, entre outras (Pinz et al., 2018; Wilhelm et al., 2019; Voss et al., 2020; Reis et al., 2020; Luchese et al., 2020; Nogueira et al., 2021; de Oliveira et al., 2022; Reis et al., 2022) . Além disso, em um estudo anterior a esta tese, foram observados efeitos positivos do tratamento oral e tópico com 7-cloro-4-(fenilselanil) quinolina (4-PSQ) (composto orgânico de Se) sobre os sintomas, parâmetros inflamatórios e oxidativos em um modelo de DA induzida com DNCB. Importantemente, a eficácia do tratamento com o 4-PSQ foi semelhante ou até melhor do que a dexametasona, um glicocorticoide frequentemente utilizados no tratamento da DA (Voss et al., 2018).

No estudo dessa tese, foi investigado o efeito de outro composto orgânico de Se, o SeTal (Figura 6), em um modelo de lesões semelhantes a DA induzidas por DNCB. Uma das principais vantagens do SeTal sobre outros compostos de organosselênio é sua alta solubilidade em água. Além disso, ele é altamente estável em soluções que simulam fluidos biológicos e no trato gastrointestinal e não é rapidamente degradado ou metabolizado, ao contrário de outros compostos contendo Se. Dessa forma, permanece intacto durante o armazenamento prolongado e possui disponibilidade por via oral (Zacharias et al., 2020). Ademais, em um estudo realizado anteriormente, o SeTal foi administrado por via oral em camundongos por até 12 semanas a 1 mM, sem qualquer sinal de toxicidade evidente ou efeitos adversos à saúde, e foi demonstrado que permanece intacto no plasma e em vários tecidos (Zacharias et al., 2020). Em relação aos seus efeitos, o SeTal demonstrou atividade antioxidante em camundongos, diminuindo os níveis de superóxido, aumentando a disponibilidade de óxido nítrico basal e normalizando a contribuição de prostanóides vasoconstritores (Ng et al., 2017). Além disso, o SeTal também é um tratamento promissor para feridas crônicas, pois melhora a cicatrização em camundongos não diabéticos e diabéticos e melhora a perfusão vascular (Davies & Schiesser, 2019).

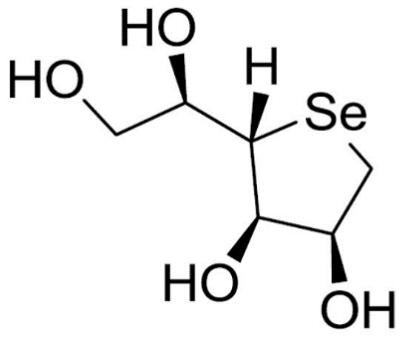

Figura 6. Estrutura química do 1,4-anidro-4-seleno-D-talitol (SeTal).

Sendo assim, a busca e investigação das propriedades farmacológicas dos compostos orgânicos contendo Se, têm crescido nos últimos anos. Nesse contexto, cabe destacar que o SeTal apresentou propriedades farmacológicas interessantes, anteriormente destacadas, e pode tornar-se um promissor

tratamento para lesões semelhantes a DA. Paralelamente a isso, o estudo de novas formas farmacêuticas de uso tópico como os biomateriais são de grande valor no estudo da DA, sendo que estas podem atuar como um curativo capaz de carrear estes compostos de Se, isolar o local da lesão e até mesmo reduzir o efeito adverso dos tratamentos convencionais a base de corticosteróides.

2.3 Biomateriais

No final da década de 1960, estudos começaram a explorar a natureza da biocompatibilidade de materiais, e logo suas aplicações se tornaram visíveis, especialmente no campo da medicina. Sistemas de liberação de fármaco, biossensores e biocurativos, tornaram-se possíveis, em grande parte, por conta dos biomateriais (More et al., 1996). No ano de 1987, surgiu uma das primeiras definições para o termo, que descreve um biomaterial como um material usado em dispositivos médicos, com o objetivo de interagir com os sistemas biológicos. Como complemento, ainda foi descrito que biocompatibilidade é “a habilidade do biomaterial em proporcionar uma resposta hospedeira apropriada para uma aplicação específica” (Ratner et al., 2013). Os biomateriais são classificados de acordo com a sua origem de obtenção, ou seja, natural e artificial. A classificação na forma natural ocorre quando o biomaterial é retirado do meio ambiente sem a necessidade de manipulação em laboratório; na forma artificial ocorre uma combinação de substâncias, manipulação em laboratório ou síntese de novos materiais (O’Brien, 2011).

Para um material ser biocompatível, ele deve possuir como característica a capacidade de promover uma resposta hospedeira adequada para uma aplicação específica, com o mínimo de reações possíveis, levando em consideração as condições de utilização e avaliação (Patel & Gohil, 2012). Esse tipo de material não pode ser tóxico nem liberar substâncias tóxicas, uma vez que entram em contato com fluidos corporais, e precisam ser compatíveis com os tecidos do corpo. Do mesmo modo, um biomaterial não deve causar reação alérgica e/ou inflamatória (Temenoff & Mikos, 2008).

Como mencionado anteriormente, os biomateriais podem ser utilizados como, biossensores e sistemas de hemodiálise, dispositivos para liberação de medicamentos na forma de filmes, implantes subdérmicos e partículas, curativos, entre diversas outras aplicações (Pires et al., 2015). No que diz

respeito a administração de fármaco por meio dos biomateriais, os desafios fundamentais incluem a seleção de fatores ou combinação de fatores necessários para induzir uma resposta desejada, além da dose e da entrega espaço-temporal necessária para a regeneração adequada do tecido (Chen & Liu, 2016).

Polímeros, cerâmicas, metais, entre outros podem ser utilizados como biomateriais, por exemplo, como substitutos desde tecidos ósseos a tecidos moles, como cabeça do fêmur e implantes de mama, respectivamente. Dentre estes materiais, os polímeros vêm se destacando cada vez mais no ramo de aplicações biomédicas (Pires et al., 2015). Como mencionado anteriormente, os biomateriais também podem ser de origem sintética ou natural. O uso de materiais de origem sintética pode levar a formação de resíduos que dificultam a recuperação da lesão. Essa limitação pode ser diminuída pelo uso de dispositivos produzidos a partir de variados tipos de compostos poliméricos naturais, uma vez que estes além de serem biocompatíveis são biodegradáveis (Sionkowska, 2011). Diante do exposto, os biomateriais poliméricos se tornaram uma importante ferramenta na medicina moderna, em doenças de pele ou na cicatrização de feridas eles podem ser utilizados para carrear medicamentos, além de atuar como um curativo (biocurativo). Estes materiais geram um microambiente controlado, além de exercerem a função de barreira física protegendo a lesão contra fatores externos (Basit et al., 2020).

2.3.1 Biomateriais poliméricos (biopolímeros)

Os polímeros são macromoléculas de alta massa molar formadas por meio de ligações covalentes de unidades repetidas menores ao longo da cadeia principal, chamadas de monômeros (Canevarolo, 2002). Os polímeros podem ser obtidos a partir de reações de polimerização ou por meio de organismos vivos, classificando-se, assim, como sintéticos e naturais (biopolimeros). Os biopolímeros, também chamados de polímeros naturais, são macromoléculas provenientes de fontes renováveis que ocorrem na natureza (Hocking, 1992).

Dentre os biomateriais mais empregados no âmbito hospitalar destacam-se os biopolímeros, devido as diversas vantagens que eles apresentam, como: facilidade na fabricação, processamento secundário (reciclagem), baixo custo e disponibilidade em encontrar materiais com propriedades mecânicas e físicas

desejadas para aplicações específicas (Shahid-ul-Islam et al., 2013). Além disso, os biopolimeros são capazes de formar filmes flexíveis, resistentes a ataques biomecânicos, leves e biocompatíveis. Os polímeros de origem natural são encontrados em abundancia e seus produtos de degradação são biocompatíveis e não-tóxicos (Zia et al., 2017).

Existe uma ampla variedade de biopolímeros que são utilizados em aplicações biomédicas, e suas aplicações incluem, principalmente, o tratamento de feridas e liberação controlada de fármacos (Contardi et al., 2019). Estas aplicações são possiveis devido a todas caracteristicas que foram mencionadas anteriormente para esse tipo de material, como biocompatibilidade e biodegrabilidade (Zia et al., 2017). Outra caracteristica importante é que a degradação desses materiais depende de processos enzimáticos. Além disso, estes são mais fáceis de serem metabolizados pelo organismo humano, além de serem formados a partir de grupos funcionais disponíveis para modificações químicas e enzimáticas, disponibilizando grande variedade de produtos com propriedades adaptáveis para vasto campo de aplicação (Jacob et al., 2018).

2.3.1.1 Gelatina, amido e alginato de sódio

Em 1850 a gelatina começou a ser utilizada como aglutinante dos sais de prata na indústria fotográfica (Fakhreddin Hosseini et al., 2013). A gelatina é um polímero natural composto por proteínas e peptídeos, e este biopolimero é derivado da hidrólise parcial do colágeno, correspondente ao principal componente de proteína fibrosa em ossos, cartilagens, pele, tendões (Rivero et al., 2009).

A gelatina é praticamente insípida, inodora e incolor ou ligeiramente amarelada, nas temperaturas entre 45°C a 60°C ela é soluvel em água e a compostos como glicerol e ácido acético. O peso molecular é relativamente alto (20.000-250.000 Da) comparado aos polímeros sintéticos devido ao modo de processamento (Harrington & Von Hippel, 1962). Sob condições específicas como temperatura ambiente, solventes ou pH, a gelatina pode apresentar diferentes modos de geleificação, podendo ser moldada de acordo com o interesse do pesquisador (Huang & Fu, 2010). Existe um grande interesse de aplicação para as indústrias farmacêuticas médicas, devido às suas propriedades de biodegradabilidade e biocompatibilidade com ambientes

fisiológicos e alta resistência à tensões mecânicas.. Sua aplicação se estende à área médica, culinária, industrial, cosmética, entre outras (Gómez-Guillén et al., 2011).

Por outro lado, o amido é um polissacarídeo de reserva de plantas superiores que é acumulado nos cloroplastos das folhas e nos amiloplastos. O amido é oriundo de resíduos de glicose formados durante o processo de fotossíntese. Essas moléculas de glicose unidas pela ação de enzimas, na presença de Adenosina Trifosfato (ATP), formam estruturas complexas, amilose e amilopectina, constituintes majoritários do amido (Forouzandehdel et al., 2020).

Na indústria de alimentos o amido tem ganhado destaque não só pela sua importância nutricional mas também por atuar como um agente de melhoria das propriedades tecnológicas dos alimentos, como a viscosidade, solubilidade, força de gelatinização ou adesão nos produtos alimentares (Cavalcanti et al., 2011). O amido está sendo cada vez mais estudado como substituinte de materiais derivados do petróleo, como na produção de embalagens. E isto se dá pelo fato do amido ser um material de fonte renovável e biodegradável (Dehghan Baniani et al., 2017). A proporção entre a amilose e amilopectina (principais constituintes do amido), afeta a morfologia dos biopolimeros; um alto teor de amilose proporciona a confecção de filmes mais homogêneos, enquanto que um alto teor de amilopectina causará aumento na tendência de separação de fases (Krogars et al., 2003). Ou seja, uma maior concentração de amilose apresentam filmes com melhores propriedades de força mecânica e barreira, por outro lado filmes com maior proporção de amilopectina são mais frágeis e quebradiços (Krogars et al., 2003).

O Alginato é um polissacarídeo linear natural composto por unidades dos ácidos 1,4-β-D-manurônico e α-L-gulurônico, extraído comercialmente de algas, com reconhecidas propriedades biológicas (K. Y. Lee & Mooney, 2012). Este biomaterial apresenta inúmeras aplicações na ciência e engenharia biomédica devido às suas propriedades favoráveis, incluindo biocompatibilidade e facilidade de gelificação. O alginato têm atraído atenção por seus usos na terapia genética, engenharia de tecidos, cicatrização de feridas e administração controlada de drogas, por meio da semelhança estrutural com as matrizes extracelulares nos tecidos (Zdiri et al., 2022).

Os curativos/biomateriais a base de alginato fornecem um microambiente fisiologicamente úmido ao local de aplicação, reduzem a inflamação e infecção bacteriana no local da ferida e consequentemente facilitam a cicatrização (Taskin et al., 2013). Diversas moléculas, desde pequenas drogas químicas até proteínas macromoleculares, podem ser liberadas de géis de alginato de maneira controlada, dependendo dos tipos de reticulantes e métodos de reticulação (K. Y. Lee & Mooney, 2012). Semelhante aos outros biopolímeos, o alginato também é biodegradável, o que estimula seu uso em muitas aplicações médicas e farmacêuticas (Zdiri et al., 2022).

2.3.1.2 Vitamina C

A vitamina C (ácido ascórbico) é um constituinte normal da pele encontrado em níveis elevados tanto na derme quanto na epiderme (Nielsen et al., 2021). Além disso, a vitamina C atua como um antioxidante natural, apresentando propriedades anti-inflamatórias, fotoprotetoras, além de ser um bioestimulador conhecido da síntese de colágeno e síntese de hidroxiprolina e hidroxilisina (Ballaz & Rebec, 2019). Ademais, o efeito antioxidante dessa vitamina desempenha um papel importante auxiliando na proteção contra espécies reativas de oxigênio derivadas da atividade metabólica (Nielsen et al., 2021). Devido as atividades supracitadas, a vitamina C protege componentes biológicos, como lipoproteínas de baixa densidade, contra modificações oxidativas e, assim, pode assumir um papel ateroprotetor (Pawlowska et al., 2019).

Ainda, a vitamina C (Figura 7) é útil para construir uma resistência frente às doenças, sendo essencial na dieta dos seres humanos (Cimmino et al., 2018). Corroborando, essa vitamina está presente no cérebro dos mamíferos, juntamente com várias aminas neurotransmissoras, atuando como um importante cofator (Chang et al., 2020). Frente ao que foi exposto, e devido a sua ampla lista de beneficios para o corpo humano, a vitamina C tem sido utilizada para o tratamento de diversas enfermidades, tais como resfriados, infertilidade e câncer (Nielsen et al., 2021).

Está estabelecido que a deficiência de vitamina C pode desencadear ou agravar a ocorrência e o desenvolvimento de algumas doenças de pele, incluindo a DA (Kaiqin Wang et al., 2018). Além disso, os níveis plamáticos dessa vitamina

estão reduzidos em pacientes comprometidos com DA (Shin et al., 2016). Assim, estudos demonstram que niveis elevados de vitamina C podem reverter quadros inflamatórios crônicos e assim reduzir os sintomas clinicos da DA (Lim et al., 2013; Park & Zippin, 2014). Kaiqin Wang e colaboradores (2018) destacam que a vitamina C pode ser um tratamento coadjuvante para doenças de pele, no entanto, sua administração oral ainda pode causar DA simétrica. Portanto, a incorporação desta vitamina em um biofilme pode oferecer uma via de administração alternativa para o tratamento e atenuação de sintomas semelhantes a DA.

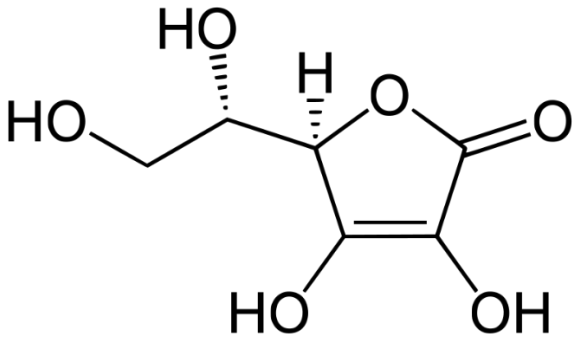

Figura 7. Estrutura química da vitamina C (ácido ascórbico).

3. OBJETIVOS

3.1 Objetivo geral

Investigar o efeito tópico do composto SeTal como uma nova estratégia terapêutica para o tratamento das lesões semelhantes a DA, bem como a utilização de filmes biopoliméricos como moduladores e direcionadores da liberação de fármacos, ambos em um modelo de DA induzida por DNCB em camundongos.

3.2 Objetivos específicos

a) Investigar o efeito tópico do composto SeTal em um modelo de DA induzida por DNCB em camundongos:

- Identificar uma nova estratégia farmacológica para o tratamento da DA;
- Verificar se o SeTal reduz as lesões e o prurido caracteristicos da DA;
- Investigar se o composto SeTal é capaz de modular os parâmetros inflamatórios relacionados com o desenvolvimento das lesões semelhantes a DA nos camundongos;
- Mensurar a expressão de interleucinas que podem ser utilizadas como marcadores fisiopatológicos da DA, bem como avaliar se o composto SeTal é capaz de atenuar estes marcadores;
- Avaliar o efeito do SeTal sobre os infiltrados celulares e a formação de fibras de colágeno na pele, após a indução de lesões semelhantes a DA em camundongos.

b) Investigar o efeito de HC incormporada à um filme biopolimérico (via tópica), em um modelo de DA induzida por DNCB em camundongos:

- Investigar se a incorporação da HC em um filme reduz os seus efeitos adversos;
- Preparar e caracterizar os filmes biopoliméricos de gelatina e gelatina+amido incorporados com HC;
- Avaliar se os filmes biopoliméricos apresentam perfil de liberação controlada de HC *in vitro*;

- Investigar o efeito do filme biopolimérico carregado com HC nas lesões e prurido caracteristicos da DA;
- Avaliar a capacidade dos filmes biopoliméricos de modular parâmetros inflamatórios;
- Mensurar se os filmes biopoliméricos interferem nos níveis de corticosterona, marcador de resposta ao estresse;
- Avaliar se a incorporação da HC nos filmes biopoliméricos reduz a toxicidade hepática.

c) Investigar o efeito da associação do SeTal a HC e a vitamina C incorporados a filmes biopolimericos em um modelo de DA induzida por DNCB em camundongos:

- Investigar se a incorporação do SeTal, SeTal + HC e SeTal + vitamina C; em filmes biopoliméricos aumenta a biodisponibilidade dos compostos *in vitro*, bem como possibilita um tratamento a longo prazo;
- Preparar e caracterizar os filmes biopoliméricos de gelatina e alginato incorporados com SeTal, SeTal + HC e SeTal + vitamina C;
- Avaliar se os filmes biopoliméricos apresentam perfil de liberação controlada de SeTal, SeTal + HC ou SeTal + vitamina C *in vitro*;
- Investigar o efeito dos filmes biopoliméricos carregado com SeTal, SeTal + HC ou SeTal + vitamina C nos sinais clinicos de lesões cutâneas e prurido caracteristicos da DA;
- Verificar se os filmes biopoliméricos modulam a anormalidade imunológica por meio da redução das alterações no baço dos camundongos;
- Avaliar a capacidade dos filmes biopoliméricos em modular parâmetros inflamatórios;
- Investigar se os filmes biopoliméricos modulam os níveis de nitrito e nitrato (NOx);
- Avaliar se a incorporação do SeTal, SeTal + HC ou SeTal + vitamina C nos filmes biopoliméricos reduzem a gravidade das alterações morfológicas induzidas por DNCB.

4. CAPITULOS

Os resultados que fazem parte dessa tese estão apresentados sob a forma de 2 artigos científicos e 1 manuscrito. As seções materiais e métodos, resultados, discussão e referências encontram-se nos artigos e no manuscrito, representando a íntegra desse estudo. Os artigos estão estruturados conforme as revistas no qual foram publicados e o manuscrito está estruturado de acordo com revista na qual foi submetido.

4.1 Artigo 1

Suppressive effect of 1,4-Anhydro-4-seleno-D-talitol (SeTal) on atopic dermatitis-like skin lesions in mice through regulation of inflammatory mediators

O artigo científico encontra-se publicado na revista *International Journal of Trace Elements in Medicine and Biology*

Journal of Trace Elements in Medicine and Biology 67 (2021) 126795

Contents lists available at ScienceDirect

Journal of Trace Elements in Medicine and Biology

journal homepage: www.elsevier.com/locate/jtemb

Suppressive effect of 1,4-anhydro-4-seleno-D-talitol (SeTal) on atopic dermatitis-like skin lesions in mice through regulation of inflammatory mediators

Guilherme T. Voss [a], Renata L. de Oliveira [a], Michael J. Davies [b,c], William B. Domingues [d], Vinicius F. Campos [d], Mauro P. Soares [e], Cristiane Luchese [a], Carl H. Schiesser [c,**], Ethel A. Wilhelm [a,*]

[a] Programa de Pós-graduação em Bioquímica e Bioprospecção, Laboratório de Pesquisa em Farmacologia Bioquímica (LaFarBio), Grupo de Pesquisa em Neurobiotecnologia (GPN), Centro de Ciências Químicas, Farmacêuticas e de Alimentos, Universidade Federal de Pelotas, Pelotas, CEP 96010-900, RS, Brazil
[b] Department of Biomedical Sciences, Faculty of Health and Medical Sciences, University of Copenhagen, Blegdamsvej 3, 2200, Copenhagen, Denmark
[c] Seleno Therapeutics Pty. Ltd., Brighton East, VIC, 3187, Australia
[d] Laboratório de Genômica Estrutural, Centro de Desenvolvimento Tecnológico, Universidade Federal de Pelotas, Pelotas, CEP 96010-900, RS, Brazil
[e] Laboratório Regional de Diagnóstico Faculdade de Veterinária, Universidade Federal de Pelotas, Pelotas, CEP 96010-900, RS, Brazil

ARTICLE INFO

Keywords:
Cytokine
Selenium
4-Anhydro-4-seleno-D-talitol
Inflammation
Hydrocortisone

ABSTRACT

Background: Atopic dermatitis (AD) is a multifactorial chronic inflammatory disease that affects ~20 % of children and 3% of adults globally and is generally treated by the topical application of steroidal drugs that have undesirable side-effects. The development of alternative therapies is therefore an important objective. The present study investigated the effects of topical treatment with a novel water-soluble selenium-containing carbohydrate derivative (4-anhydro-4-seleno-D-tatitol, SeTal) on the symptoms and inflammatory parameters in an AD mouse model.

Methods: Mice were sensitized by applying 2,4-dinitrochlorobenzene (DNCB) to their dorsal skin on days 1–3, then further challenged on their ears and dorsal skin on days 14, 17, 20, 23, 26, and 29. SeTal (1 and 2%) or hydrocortisone (1%) was applied topically to the backs of the mice from days 14–29, and skin severity scores and scratching behavior determined on day 30. The mice were euthanized, and their ears and dorsal skin removed to quantify inflammatory parameters, edema, myeloperoxidase (MPO) activity, and AD-associated cytokines (tumor necrosis factor alpha (TNF-α), interleukins (IL)-18, and IL-33).

Results: DNCB treatment induced skin lesions and increased the scratching behavior, ear edema, MPO activity (ear and dorsal skin), and cytokine levels in dorsal skin. Topical application of SeTal improved inflammatory markers (cytokine levels and MPO activity), cutaneous severity scores, and scratching behavior.

Conclusion: The efficacy of SeTal was satisfactory in the analyzed parameters, showing similar or better results than hydrocortisone. SeTal appears to be therapeutically advantageous for the treatment and control of AD.

1. Introduction

Atopic dermatitis (AD), a multifactorial chronic disease with complex origins, affects approximately 20 % of children and up to 3% of adults worldwide [1–3]. Patients with AD have a hereditary tendency to secrete antibodies (particularly immunoglobulin E (IgE)) excessively in response to a variety of stimuli [4]. The immune response observed during AD is characterized by acute inflammation that presents as

Abbreviations: AD, atopic dermatitis; SeTal, 4-anhydro-4-seleno-D-tatitol; DNCB, 24-dinitrochlorobenzene; HC, hydrocortisone; MPO, myeloperoxidase; IgE, immunoglobulin E; Th2, T helper 2 lymphocytis; ILs, interleukins; P2, pellet; OD, optic density; HE, eosin; MT, masson's trichrome; HPA, hypothalamic-pituitary-adrenal; TNF-α, tumor necrosis factor alpha.

* Corresponding author at: Programa de Pós-graduação em Bioquímica e Bioprospecção, CCQFA, UFPel, Campus Capão do Leão, Pelotas, CEP 96010-900, RS, Brazil.
** Corresponding author at: Seleno Therapeutics Pty. Ltd., 14 Centre Road, Brighton East, VIC, 3187, Australia.
E-mail addresses: carl@selenotherapeutics.com (C.H. Schiesser), ethelwilhelm@yahoo.com.br (E.A. Wilhelm).

https://doi.org/10.1016/j.jtemb.2021.126795
Received 3 September 2020; Received in revised form 21 May 2021; Accepted 25 May 2021
Available online 29 May 2021

outbreaks of eczematous pruritic lesions on skin, beginning with a predominant response of T helper 2 lymphocytes (Th2) [5]. AD skin lesions are also characterized by the overexpression of pro-inflammatory type 2 molecules [6]. Studies have implicated IL-18 in the pathophysiology of AD, as this increases the recruitment of eosinophils to the airways, and enhances the levels of IL-4, IL-13, and histamine, via basophil and mast cell activation [7,8].

The therapeutic strategies used in AD generally consist of treatments capable of relieving the itching [9]. Topical corticosteroids, such as hydrocortisone (HC), are widely used in patients with AD. However, its effectiveness is limited and long-term use results in adverse effects [10,11]. Systemic immunosuppressant drugs for AD are generally more effective than topical treatments, but these are also potentially toxic [10,12]. Consequently, there is interest in identifying new agents that reduce and treat the symptoms of AD [13–15].

1,4-Anhydro-4-seleno-D-talitol (SeTal), a water-soluble selenium-containing carbohydrate derivative, has potent antioxidant activity and is a promising treatment for chronic wounds, as it enhances healing in both normal and diabetic mice and improves vascular perfusion [16,17]. Organoselenium compounds have been previously studied as potential therapeutic agents as they show positive pharmacological actions, as antioxidant, antinociceptive and anxiolytic agents [18–21] and high efficacies in experimental models of inflammation [14,21]. The hypothesis of the present study is that SeTal reduces oxidative stress, especially through the scavenging mechanism on the superoxide radical [16]. In addition, it does not appear to act through induction of selenoenzymes, or through cytotoxic properties like other selenocompounds [18]. SeTal could reduce the inflammatory mediators related to the disease, which are triggered by the hyperactivation of Th2 lymphocytes, and reduce the DA-type skin lesions induced by 2,4-dinitrochlorobenzene (DNCB) in mice.

2. Materials and methods

2.1. Animals

The experiments used BALB/c mice female (6–8 weeks old) kept in a separate animal room, on a 12 h light (07:00–19:00)/dark cycle at 22 ± 1 °C, with free access to food (diet according to the recommended selenium intake for mice) and water. Biological assays were conducted according to institutional and national guidelines for the care and use of animals. The experiments were approved by the Committee on Care and Use of Experimental Animal Resources, Federal University of Pelotas, Brazil (CEEA 4294–2015), following National Institutes of Health guidelines for the care and use of laboratory animals (NIH Publications No. 8023, revised 1978). The number of animals used was the minimum necessary to demonstrate the consistent effects of drug treatment, and all efforts were taken to make them comfortable.

2.2. Drugs

SeTal (Fig. 1) was synthesized and purified in the School of Chemistry at the University of Melbourne, Australia [22]; it was solubilized in

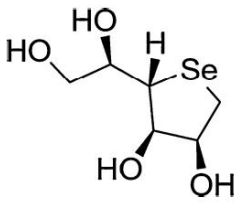

Fig. 1. Chemical structure of 1,4-anhydro-4-seleno-D-talitol (SeTal).

Tween 80 and incorporated in a nonionic cream (pH 5.5; white color, homogeneous, containing cetostearyl alcohol and ethoxylated sorbitan monostearate), for topical application. HC (1%) was obtained commercially in the form of cream (each 1 g of cream contains 11.2 mg of HC acetate and excipients (macrogol stearate 400, stearyl alcohol, liquid petrolatum, white petrolatum, edetate disodium, carbomer 980, sodium hydroxide, methylparaben, propylparaben and purified water)). DNCB was obtained commercially. All other chemicals were of analytical grade and obtained from standard commercial suppliers.

2.3. Experimental protocol

Haptens, such as DNCB, are commonly topically applied to mice to induce skin contact hypersensitivity, and this approach is widely used as an animal model for induction AD. Here, AD-like cutaneous lesions were induced on mice with DNCB according to Chan et al. [23]. Animal were depilated in the dorsal region and 200 μL of 0.5 % (v/v) DNCB in 3:1 (v/v) acetone/olive oil applied on days 1–3. Animals were further challenged with 200 μL of 1% (v/v) DNCB on their backs and 20 μL on their right ears, on days 14, 17, 20, 23, 26, and 29, as shown in Fig. 2. Mice were randomly divided into five groups each of 8 animals. Normal control mice (control group) were sensitized and challenged with acetone/olive oil (3:1) and treated with compound-free nonionic cream. Sensitized control mice (DNCB group) were sensitized and challenged with DNCB and treated with compound-free nonionic cream. Experimental mice were sensitized and challenged with DNCB and received topical treatment with 1% or 2% SeTal incorporated in nonionic cream, or 1% HC (1% SeTal, 2%SeTal, and HC groups). The backs of the mice were treated daily with 0.5 g compound-free nonionic cream, SeTal, or HC, from days 14–29. Signs of toxicity and mortality were evaluated during the experimental protocol. The concentrations of SeTal used in the present study are based on the doses used in previous wound-healing studies (~1%) [17]. The duration of treatment with SeTal was chosen based on previous studies [14,15].

2.4. Clinical skin severity scores

The clinical skin severity score is an important parameter used to identify and classify AD-like skin lesions in DNCB treated mice. On day 30, the skin was photographed, and severity scores were determined according to Park et al. [24]. The five signs of skin lesions are: (1) pruritus/itching, (2) erythema/hemorrhage, (3) edema, (4) excoriation/erosion, and (5) scaling/dryness. The above-mentioned symptoms were graded as follows: 0 (no symptoms), 1 (mild), 2 (moderate), and 3 (severe).

2.5. Scratching behavior

Itching is an important clinical sign in AD, which is related to most complications caused by the disease. Here, the itching caused by AD-like lesions induced by DNCB was evaluated in animals by determining scratching behavior. The amounts of time that the mice spent rubbing their noses, ears, and dorsal skin with their hind paws were measured and recorded for 20 min on day 30 in order to investigate AD-like behavioral changes [25].

3. Inflammatory parameters

3.1. Ear swelling

Inflammatory edema is characteristic of the inflammation observed in AD-like lesions. This phenomenon, associated with increased hydrostatic pressure secondary to vasodilation, results in a marked loss of fluids and an accumulation in the interstitial tissue, which characterizes the edema. The severity of inflammation can easily be evaluated by ear swelling. On day 30, following scratching-behavior assessment, mice

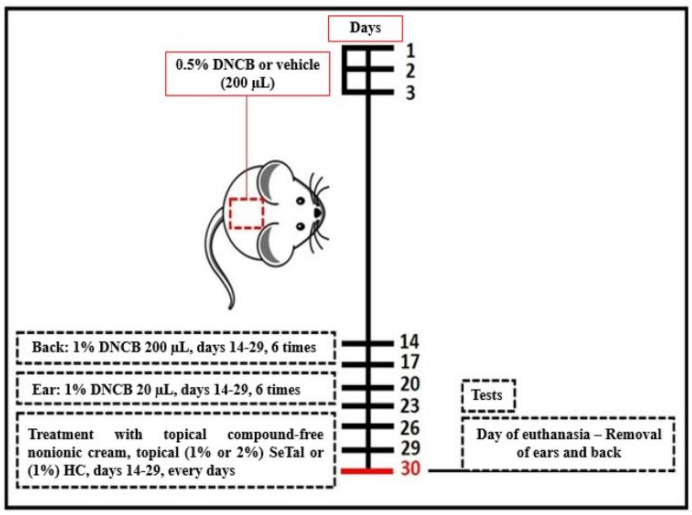

Fig. 2. Summary of experimental protocol for the development of atopic AD-like skin lesions in DNCB treated mice.

were euthanized, and both ears were severed at the base and the mass differences between the control (left) and the DNCB-treated ears (right) determined using an analytical balance. The ears were subsequently used to determine myeloperoxidase (MPO) activity.

3.2. Determination of MPO activity

MPO is an enzyme present in the azurophil granules of polymorphonuclear leukocytes (neutrophils). Polymorphonuclear leukocytes can be estimated by determining MPO activity, a well-established marker of tissue neutrophil influx. In the inflammatory process caused by AD-like lesions, these cells migrate to the animal's tissue. MPO activity was assayed according to the previously described method [26] with some modifications. Mouse ears and back fractions were minced, pooled and homogenized in phosphate-buffered saline (20 mM, pH 7.4) containing ethylenediaminetetraacetic acid (0.1 mM). The homogenates were centrifuged at 900 *g* for 10 min at 4 °C and the pellet discarded. The supernatant (fraction S1) was then re-centrifuged at 24,080 *g* at 4 °C for 15 min to yield the final pellet (P2), which was resuspended in medium containing potassium phosphate buffer (50 mM, pH 6.0) and hexadecyltrimethylammonium bromide (0.5 % w/v). Samples were subjected to three freeze-thaw cycles prior to assaying MPO activity. MPO activity was quantified by adding aliquots of resuspended P2 (100 µL) to solutions containing *N,N,N',N'*-tetramethylbenzidine (1.5 mM). Oxidation of this substrate by MPO was initiated by the addition of H_2O_2 (0.01 vol%) with the absorbance changes at 655 nm monitored over a period of 2 min at 37 °C. Results are expressed as optic density (OD)/mg protein/min. Protein concentration was determined by the Bradford method [27] using bovine serum albumin (1 mg/mL) as the standard.

3.3. RNA extraction, cDNA synthesis, and quantitative real-time polymerase chain reaction

As AD is a chronic multi-factorial inflammatory skin disease, driven by the interplay between genetic predisposition and environmental factors that initiate inflammation, the levels of multiple cytokines involved in the inflammatory process of AD-like lesions were determined. Total mRNA was extracted from thawed samples of back skin (50–70 mg; n = 7 per group) using TRIzol reagent (Invitrogen™, Carlsbad, USA) followed by treatment with DNase I (Amplification Grade, Invitrogen™, Carlsbad, USA) to minimize DNA contamination. The isolated RNA was quantified and its purity (260/280 and 260/230 ratios) determined by spectrophotometry (NanoVue, GE, Fairfield, CT, USA).

cDNA was synthesized using a high capacity cDNA reverse transcription kit (AppliedBiosystems™, UK) according to the manufacturer's protocol. For reverse transcription, 2 µg of total RNA was used in a reaction volume of 20 µL. Amplification was conducted with the GoTaq® qPCR Master Mix (Promega, Madison, WI) with an Agilent Mx3005 P qPCR System (Agilent Technologies Inc., Santa Clara, CA), and the primers listed in Table 1. The qPCR conditions were as follows: 10 min at 95 °C to activate the hot-start Taq polymerase, followed by 35 cycles of denaturation for 15 s at 95 °C, primer annealing for 60 s at 60 °C, and extension for 30 s at 72 °C. Fluorescence signals were recorded at the end of every cycle. Baseline and threshold values were automatically set by the Stratagene MxPro software. The number of PCR cycles required to reach the fluorescence threshold in each sample is defined as the Ct value, and each sample was analyzed in duplicate to obtain an average Ct for each sample. The $2^{-\Delta\Delta CT}$ method was used to normalize the fold change in gene expression [28] using glyceraldehyde-3-phosphate

Table 1
Primers used for quantitative real-time polymerase chain reaction.

Primer Name	Sequence	Reference
TNF-α Forward	5' CCCTCACACTCAGATCATCTTCT 3'	[46]
TNF-α Reverse	5' CTACGACGTGGGCTACAG 3'	
IL- 18 Forward	5' CAACTCAGGAGTCTTGCTCAACA 3'	[47]
IL-18 Reverse	5' CAGGCCTGACATCTTCTGCAA 3'	
IL-33 Forward	5' CTGCAAGTCAATCAGGCGAC 3'	[48]
IL-33 Reverse	5' TGCAGCCAGATGTCTGTGTC 3'	
GAPDH Forward	5'TGCGACTTCAACAGCAACTC 3'	[49]
GAPDH Reverse	5'ATGTAGGCAATGAGGTCCAC 3'	

The forward and reverse primer sequences used to amplify each target gene as well as the GAPDH endogenous control are listed.

dehydrogenase as a housekeeping gene.

3.4. Histological analysis

Histological analysis was used to evaluate tissue changes and cell migration into the affected areas. The back skin and ear samples were fixed in 10 % buffered formalin solution. Tissue samples were embedded in paraffin, sectioned at 3–4 μm and stained with hematoxylin and eosin (HE) or Masson's Trichrome (MT) for optical microscopy.

3.5. Statistical analysis

The normality of the data was evaluated by the D'Agostino and Pearson omnibus normality test. The data were analyzed by one-way analysis of variance (ANOVA) followed by Tukey's test. All analyses were performed using GraphPad software (San Diego, CA, USA). Data are expressed as means ± standard errors of the mean (SEMs); $p < 0.05$ was considered to be statistically significant.

4. Results

4.1. Effect of SeTal on clinical signs of AD-like skin lesions

Clinical skin severity scores were used to investigate the protective effect of SeTal against DNCB-induced AD-like skin damage, with the results displayed in Fig. 3A and B [$F_{4,35} = 114.3$, $p < 0.0001$]. One-way ANOVA followed by Tukey's testing revealed that DNCB significantly increased the skin severity scores when compared with the control group ($p < 0.0001$) (Fig. 3B). Treatment with 1% SeTal ($p < 0.0001$) or 2% SeTal ($p < 0.05$) reduced the severity of the skin-lesions induced by DNCB. No significant difference in the severity of the skin lesions was detected on treatment with HC, when compared to the DNCB group ($p > 0.05$) (Fig. 3B).

Fig. 3C shows the effect of SeTal on scratching behavior [$F_{4,35} = 37.46$, $p < 0.0001$]. One-way ANOVA followed by Tukey's testing revealed that DNCB-exposed animals exhibited increased scratching times when compared with the control group ($p < 0.0001$). SeTal (1%) ($p < 0.01$), SeTal (2%) ($p < 0.0001$) and HC ($p < 0.0001$) reduced the scratching time induced by DNCB, with the protective effect of SeTal (2%) being similar to that of HC.

4.2. Effect of SeTal on inflammatory parameters

Fig. 4A illustrates the effects of SeTal treatment on ear swelling in mice [$F_{4,35} = 21.70$, $p < 0.0001$]. One-way ANOVA followed by Tukey's testing showed that DNCB substantially increased right-ear swelling when compared with the control group ($p < 0.0001$). Treatments with HC ($p < 0.01$), 1% SeTal ($p < 0.001$), and 2% SeTal ($p < 0.001$) partially reduced the ear swelling induced by DNCB. The protective effect of the two SeTal preparations was similar to that of HC.

The results displayed in Fig. 4B and C show the effects of the topical administration of SeTal on ear and dorsal-skin MPO activity, respectively [$F_{4,35} = 33.15$, $p < 0.0001$ (ear); $F_{4,35} = 39.79$, $p < 0.0001$ (dorsal skin)]. One-way ANOVA followed by Tukey's testing revealed that DNCB significantly increased MPO activity in mouse ears ($p < 0.0001$) and dorsal skin ($p < 0.0001$) when compared with the control group. Statistical data analysis reveals that 1% SeTal ($p < 0.001$) and 2% SeTal ($p < 0.001$) partially protected against the increase in MPO activity in ear tissue on exposure to DNCB (Fig. 4B). HC ($p < 0.0001$) also restored the MPO activity of ear tissue to control values, with the protective effect of SeTal similar to that of HC (Fig. 4B).

The data presented in Fig. 4C indicate that treatment with 2% SeTal partially protects against increasing dorsal-skin MPO activity induced by DNCB. Statistical analysis reveals that 1% SeTal ($p < 0.0001$) restores

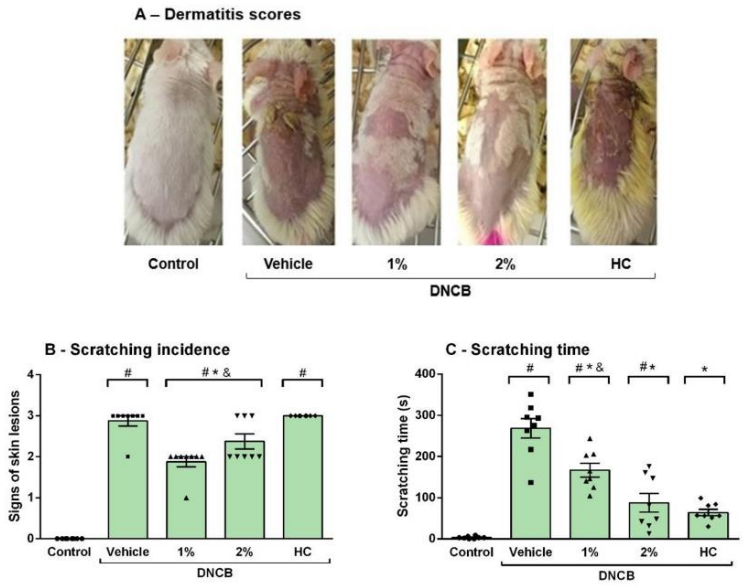

Fig. 3. The effect of SeTal treatment on (**A**) dermatitis scores, (**B**) scratching incidence and (**C**) scratching time, after DNCB exposure. Data are means ± SEMs (one-way ANOVA followed by the Tukey's test). # $p < 0.05$ compared with the control group, * $p < 0.05$ compared with the DNCB group, @ $p < 0.05$ compared with the 1% group, & $p < 0.05$ compared with the HC group.

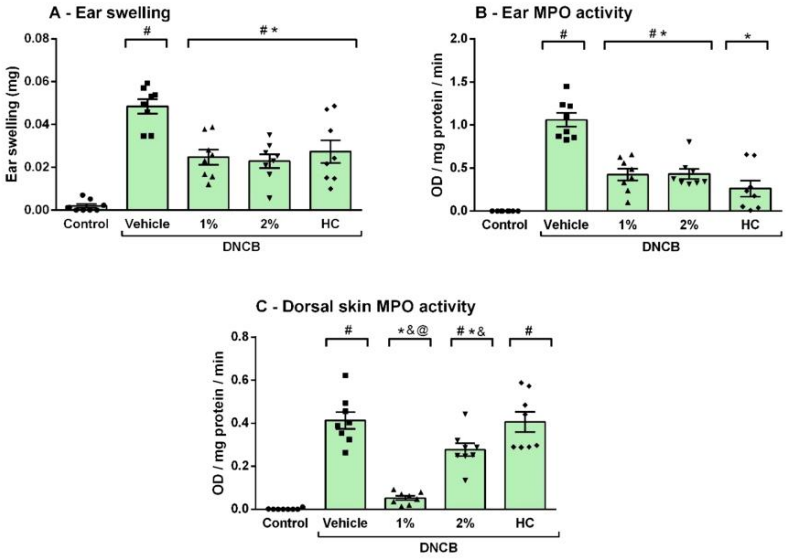

Fig. 4. The effect of SeTal treatment on **(A)** ear swelling, **(B)** ear MPO activity and **(C)** dorsal skin MPO activity. Data are means ± SEMs (one-way ANOVA followed by the Tukey's test). # $p < 0.05$ compared with the control group, * $p < 0.05$ compared with the DNCB group, @ $p < 0.05$ compared with the 2% group & $p < 0.05$ compared with the HC group.

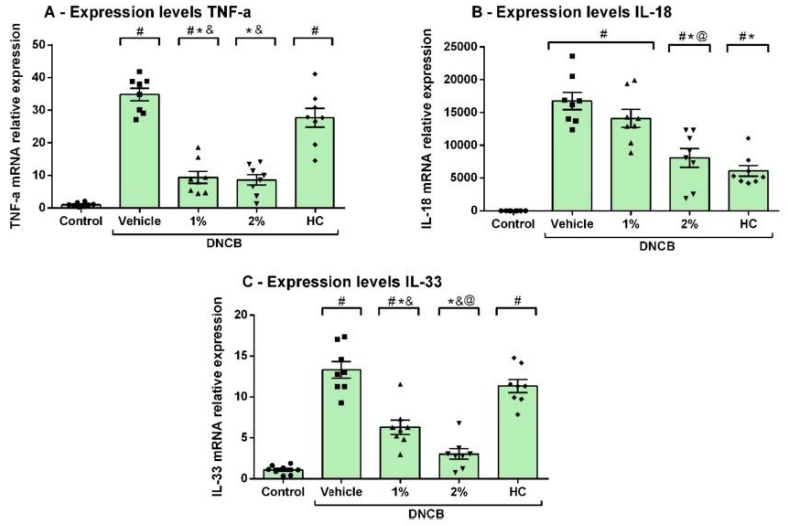

Fig. 5. The effect of SeTal treatment on mRNA expression levels of cytokines: **(A)** TNF-α, **(B)** IL-18 and **(C)** IL-33 in mouse dorsal skin. Data are means ± SEMs. (one-way ANOVA followed by the Tukey's test). # $p < 0.05$ compared with the control group, * $p < 0.05$ compared with the DNCB group, @ $p < 0.05$ compared with the 1% group & $p < 0.05$ compared with the HC group.

dorsal skin MPO activity to control levels. SeTal treatment at both 1% ($p < 0.0001$) and 2% ($p < 0.05$) levels was more effective in reducing dorsal-skin MPO activity than HC (Fig. 4C).

The data presented in Fig. 5(A–C) display the effects of the topical administration of SeTal on the dorsal-skin expression of cytokines tumor necrosis factor alpha (TNF-α) [$F_{4,35} = 56.49$, $p < 0.0001$], IL-18 [$F_{4,35} = 34.78$, $p < 0.0001$], and IL-33 [$F_{4,35} = 47.53$, $p < 0.0001$]. One-way ANOVA followed by Tukey's testing reveals that DNCB significantly increased the expression of TNF-α, IL-18, and IL-33 when compared with the control group; 1% SeTal ($p < 0.0001$) and 2% SeTal ($p < 0.0001$) protected against the increase in TNF-α expression induced by DNCB (Fig. 5A), whilst HC did not.

SeTal at 2% ($p < 0.0001$) partially protected against the increase in IL-18 expression induced by DNCB (Fig. 5B), whilst HC ($p < 0.0001$) reduced the expression of IL-18, when compared to the DNCB group. Treatment with SeTal [1% ($p < 0.0001$) and 2% ($p < 0.0001$)] protected against an increase in IL-33 expression induced by DNCB exposure (Fig. 5C), but HC did not ($p > 0.05$). Treatments with SeTal (1% and 2%) were more effective in reducing the expression of IL-33 than HC.

4.3. Histology

The severity of the morphological alterations to the dorsal skin and ear caused by exposure to the various treatments is shown in Fig. 6. A normal histological architecture was observed for the ears (Fig. 6.1 and 6 .3) and dorsal skin (Fig. 6.2 and 6.4) of the control animals. The ear sections from the DNCB-exposed animals exhibited the formation of crust on a hyperplastic epidermis together with mild hyperkeratosis (Fig. 6.5). The dermis of the dorsal skin was thickened, edematous, contained abundant inflammatory infiltrates of macrophages, lymphocytes, and neutrophils, congested blood vessels, and dilated lymphatic vessels (Fig. 6.6). The collagen fibers of the superficial dermal layer appeared denser than the collagen fibers of the deep dermis when stained with MT (Fig. 6.7 and 6 .8).

The animals treated with HC presented several regions with intra-epidermal and subepidermal pustules. The formation of crust with bacterial colonies was observed on the surface dermises, along with macrophage, neutrophil, and lymphocyte infiltration, vascular congestion, edema, and dilated lymphatic vessels (Fig. 6.9 [ears] and 6.10 [dorsal skin]). The animals treated with 1% HC exhibited lower numbers of collagen fibers, with these appearing mainly as dense bands in the superficial dermis when stained with MT (Fig. 6.11 and 6 .12).

The ear sections of animals treated with 1% SeTal (Fig. 6.13) presented thickened dermises that contained inflammatory lymphocyte and macrophage infiltrates. Non-ulcerated dorsal skin (Fig. 6.14) exhibited epithelial hyperplasia, some foci with crust formation, and mild parakeratotic hyperkeratosis. Inflammatory lymphocyte and macrophage infiltrates were observed in the dermises of animals treated with 1% SeTal. The collagen fibers appeared to be evenly distributed and uniformly colored in the superficial and deep dermal layers (Fig. 6.15 and 6 .16) when stained with MT.

Slight hyperplasia of the epithelium with the presence of crust and the accumulation of bacterial colonies on and intermeshed with keratin filaments was observed in the ear (Fig. 6.17) and dorsal-skin (Fig. 6.18) samples of animals treated with 2% SeTal. When stained with MT, the collagen fibers of the superficial and deep dermal layers were

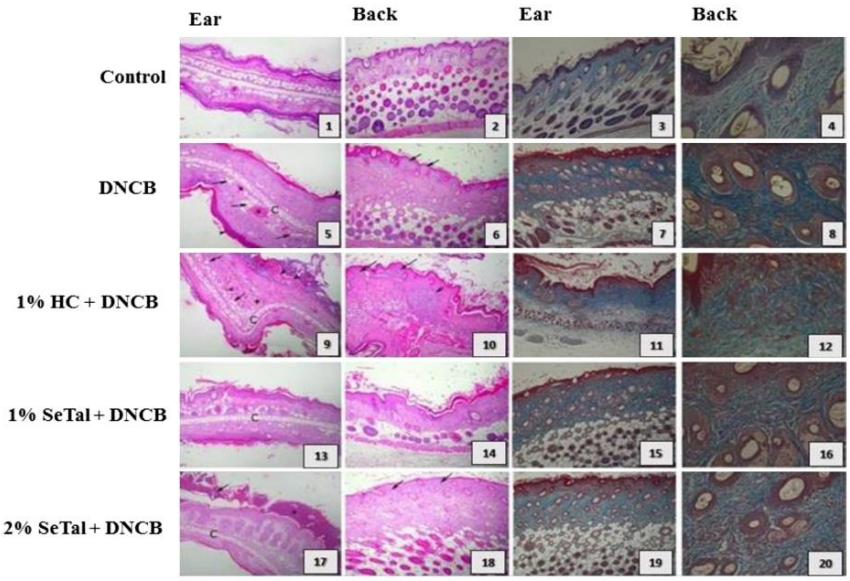

Fig. 6. Photomicrographs showing the severity of ear and dorsal-skin morphological alterations caused by treatment exposure. **(1)**, **(2)**, **(3)** and **(4)** represent control animals, which show a normal aspect; **(5)**, **(6)**, **(7)** and **(8)** represent animals exposed to DNCB – [vascular congestion (*), dilated lymphatic vessels (arrow), and the presence of a crust on the inner and outer faces (arrowhead), C (cartilage) and subepidermal pustules (arrow)]. **(9)**, **(10)**, **(11)** and **(12)** represent 1% HC + DNCB group – [thickened ear with vascular congestion (*), dilated lymphatic vessels (arrow), and the presence of intraepidermal pustules (arrowhead), C (cartilage), presence of intraepidermal (long arrow) and subepidermal (short arrow) pustules]. **(13)**, **(14)**, **(15)** and **(16)** represent 1% SeTal + DNCB group and **(17)**, **(18)**, **(19)** and **(20)** 2% SeTal + DNCB group - [a thick crust is present (*) as well as bacterial colonies and subepidermal pustules (arrow)]. (HE staining - 100X and MT - 100X and 400X).

interspersed with many young fibroblasts (Fig. 6.19 and 6 .20).

4.4. Toxicity and mortality

During the experimental protocol, 50 % of the animals treated topically with 1% HC died. In contrast, no death or sign of toxicity was observed in animals exposed to 1 or 2% SeTal.

5. Discussion

The present study shows, for the first time, the effect of SeTal on AD-like skin lesions in mice. Our findings reveal a suppressive effect of this water-soluble selenium-containing sugar derivative on skin lesions, scratching behavior, and ear swelling induced by exposure to DNCB, probably via a reduction in local inflammatory processes. A summary of these results is shown in Table 2. This finding is extremely important, considering that our research group has dedicated special attention to the study and identification of new agents capable of reducing and treating the symptoms of AD-like pathologies [13–15].

SeTal has therapeutic advantages over other organoselenium compounds due to its high solubility in water (allowing rapid clearance and avoiding any apparent bioaccumulation of the drug in fat deposits which is a limiting factor with some other organoselenium compounds, with lipophilic characteristics), low degradability (remains intact during prolonged storage), little biotransformation and oral availability. In addition, in a previous study SeTal was administered orally in mice for up to 12 weeks at 1 mM, without any sign of evident toxicity, sign of cancer or adverse health effects, and has been shown to remain intact in plasma and in various tissues [18]. The high-water solubility of the compound suggests that selenosis is unlikely to be a major problem, but it was not studied here. As is already known, AD is triggered by the over activation of Th2 lymphocytes, which will release IL that will trigger an allergic and inflammatory process through the activation of B lymphocytes and migration of defense cells such as eosinophils and mast cells [8]. The hypothesis of the SeTal mechanism of action is related to the normalization of Th2 lymphocyte activity and to the decrease in mRNA expression of cytokines involved in the pathophysiology of AD. Another important point that corroborated the choice of SeTal as a treatment for AD, is that it possibly reduces oxidative stress mainly by the scavenging mechanism of the superoxide radical. It is worth mentioning that the present study is in its initial phase, and that future work on the mechanism of action of SeTal, and other possible therapeutic advantages, or disadvantages, are underway. This compound possibly does not act by inducing selenoenzymes or by cytotoxic properties [18]. However, a significant improvement is seen in AD-type lesions.

The primary course of treatment for subjects with AD lesions typically involves the use of topical corticosteroids because of their anti-inflammatory action [29]. Here, mortality was observed in animals sensitized by DNCB and submitted to HC after a long exposure period. In a previous study carried out by our research group, this mortality was also observed [30]. Corticosteroids, when applied over large areas or for prolonged times, can be absorbed into the bloodstream, resulting in systemic effects including the induction of Cushing's syndrome and the suppression of the hypothalamic-pituitary-adrenal (HPA) axis [31]. While the prolonged use of corticosteroids can lead to such complications, the development of symptomatic adrenal insufficiency is rare [32]. Therefore, it is preferable to discontinue treatment, given that long-term topically applied steroids also leads to a weakening of the skin, and formation of cracks and bleeding [29]. Of particular importance, in this study no death was observed during treatment with SeTal at concentrations equal to or higher than that of HC.

Repeated allergic and inflammatory responses over time results in a hardening and thickening of the skin surface [33]. SeTal reduced the scratching behavior induced by DNCB, suggesting a reduction in pruritus. This finding is important, as pruritus is a characteristic aspect of AD and has a significant impact on the quality of life of people with AD [34]. However, further studies to examine the effects of SeTal on the mediators associated with itching are required to confirm and extend the current data.

It is well established that the AD phenotype begins with pruritus, but erythema and dermatitic plaques are also observed. Depending on the duration of the lesions, they may weep, crust, or scale [35]. Here, SeTal (1 and 2%) attenuated the severity of skin lesions induced by DNCB. Surprisingly, HC (1%) did not alter the severity of the lesions induced by this hapten. The SeTal data are consistent with the observed scratching behavior that highlights the possible suppressive effect of SeTal against AD-like skin lesions. In addition, topical and local (dorsal skin) treatment with SeTal or HC reduced the ear edema of animals exposed to DNCB, consistent with both treatments exerting systemic activity.

In an attempt to link the suppressive effects of SeTal with modulation of inflammation, MPO activity was evaluated. MPO is a heme enzyme released from the intracellular granules of activated neutrophils, monocytes, and some macrophages, which generates powerful tissue-damaging oxidants [36]. Since neutrophils are important contributors to immunological disease pathogenesis, MPO protein levels and activity are widely used as markers of inflammation [37]. The importance of

Table 2
Summary of the main behavioral results and inflammatory parameters in mice treated with SeTal.

	Control	Vehicle (DNCB)	DNCB + 1%	DNCB + 2%	DNCB + HC
Behavioral parameters					
Signs of skin lesions	0.0 ± 0.0	2.87 ± 0.12 ↑	1.87 ± 0.12 ↓	2.37 ± 0.18 ↓	3.00 ± 0.00 =
Scratching time	3.25 ± 1.06	268.60 ± 23.37 ↑	166.90 ± 16.62 ↓	87.63 ± 22.78 ↓	64.25 ± 7.81 ↓
Inflammatory parameters					
Ear swelling	0.002 ± 0.0009	0.05 ± 0.003 ↑	0.02 ± 0.003 ↓	0.02 ± 0.003 ↓	0.03 ± 0.005 ↓
MPO (Ears)	0.0 ± 0.0	1.06 ± 0.08 ↑	0.42 ± 0.07 ↓	0.43 ± 0.06 ↓	0.26 ± 0.09 ↓
MPO (Back)	0.001 ± 0.0013	0.41 ± 0.04 ↑	0.05 ± 0.01* ↓	0.28 ± 0.03 ↓	0.41 ± 0.05 =
TNF-α	1.01 ± 0.22	34.84 ± 1.92 ↑	9.40 ± 1.83 ↓	8.62 ± 1.61 ↓	27.68 ± 2.88 =
IL-18	1.00 ± 0.27	16760 ± 1322 ↑	14101 ± 1378 =	8064 ± 1428* ↓	6072 ± 815.3 ↓
IL-33	1.09 ± 0.19	13.31 ± 1.01 ↑	6.29 ± 0.88 ↓	3.02 ± 0.64* ↓	11.33 ± 0.81 =

Data are reported as the mean ± standard error of mean (S.E.M.) of 6 mice in each group. (↑, red) increase in behavioral and inflammatory parameters compared with the control group; (↓, green) reduction in behavioral and inflammatory parameters compared with the induced group (Vehicle – DNCB); (=, green) there was no statistical difference in the behavioral and inflammatory parameters compared to the induced group (Vehicle - DNCB); 1% = 1% SeTal and 2% = 2% SeTal; * statistical difference between 1% SeTal and 2% SeTal.

neutrophils in the pathogenesis of several diseases, and the lack of safe and effective strategies to specifically target them, makes MPO a potential therapeutic target [38]. In the current study, SeTal treatment reduced MPO activity in both the treated dorsal skin and the non-treated ear tissue, consistent with a systemic activity of this selenium compound. 2% SeTal proved to be less efficient than 1% SeTal in the normalization of dorsal skin MPO activity. An explanation for this observation has not yet been obtained. However, based on our set of results, SeTal is promising for the treatment of lesions associated with AD; however, this is a preliminary study. Further studies are underway with the aim of better elucidating the effect of SeTal on AD-like lesions and improving the topical formulation of this compound. However, HC was only effective in reducing MPO activity in the ear. In this way, topical application of SeTal was able to reverse the inflammatory response induced by DNCB, and thereby potentially alleviate the symptoms and skin lesions.

Patients with AD were found to possess a subset of T lymphocytes and cytokines that can be used as biomarkers for AD diagnosis [39]. Here, SeTal decreases the mRNA expression of cytokines involved in the pathophysiology of AD (SeTal at a concentration of 2% - TNF-α (70 %), IL-18 (52 %) and IL-33 (82 %) / SeTal at a concentration of 1% - (TNF-α (70 %), IL-18 (non-significant reduction) and IL-33 (53 %)), thus reducing the inflammatory condition and allergic responses triggered by these mediators. However, no alteration in the expression of TNF-α and IL-33 was observed in animals treated with HC. TNF-α, a well-known potent inflammatory cytokine, is involved in inflammation signal transduction by inducing the migration of NF-kB into the nuclei of keratinocytes, and it is an important factor in controlling cell differentiation and immune responses [40]. IL-18 and IL-33 are believed to be involved in the pathology of AD, as these cytokines belong to the IL-1 family, which is responsible for regulating inflammatory responses [41]. Indeed, IL-18 can stimulate the T-lymphocyte response, given that inflammatory dendritic epidermal cells release IL-18 [42]. In addition, in an earlier study an increase in serum levels of IL-18 was observed in children, adults and in an experimental model using mice [43].

In addition, another important mechanism to be studied is oxidative stress, which seems to be another factor that predisposes the pathogenesis of AD. It occurs by directly damaging the cellular structures of the skin, contributing to the exacerbation of dermal inflammation and by weakening the skin's barrier function favoring infections by pathogens [44]. Here, the effect of SeTal on oxidative stress was not elucidate, however in previous studies, this selenium compound demonstrated potent antioxidant activity in mice, by reducing the levels of superoxide radicals [16]. Thus, the antioxidant effect of SeTal may be involved in the suppressive effect of AD-like skin lesions. In view of this, an exploration of the association between inflammation and oxidative stress in AD may provide a better understanding of the development of the disease, and allow the elucidation of new treatment strategies.

Histological studies reveal that animals treated with SeTal presented collagen fibers in the superficial and deep dermal layers that are interspersed with a large quantity of young fibroblasts. As expected, the use of HC resulted in fewer collagen fibers that formed dense bands mainly in the superficial dermis, which is a known side effect associated with use of corticosteroids [45]. Corticosteroids delay healing because they inhibit the expression of IL and growth factors responsible for neovascularization and fibroblastic migration [45]. Clearly, SeTal provides an advantage over HC in this regard, and has been reported to improve wound healing [17].

In conclusion, these studies reveal that SeTal attenuates AD-like symptoms in mice by suppressing the increase in MPO activity, and mRNA expression levels of TNF-α, IL-18, and IL-33 induced by DNCB. However, further studies are needed to elucidate the best concentration of SeTal (here, a better response was observed with 2% compared to 1% SeTal, with the exception of some of the measurements of MPO activity) and to fully evaluate these processes and other potential mechanisms of action that may contribute to the positive suppressive effects of SeTal in this experimental model. In addition, the results of the present study suggest that the use of this compound can be extended to other studies involving skin/inflammatory diseases and even burns.

6. Limitation of the study

Despite these promising results, it is important to note that the skin barrier of a mouse is considered to be weak compared to that of human skin, and that the surface/volume ratio of a mouse and its physiology are different to that of humans. This is a limitation of the present study. Therefore, the toxicity observed following treatment with HC cream treatment needs to be further studied, since human and mouse skin are different, and the specific properties of mouse skin may make it more sensitive to HC cream. Another important point is that SeTal shows little degradation/biotransformation, and particularly no detectable release of free selenium. It reacts with oxidants but does this in a manner to give the selenoxide that can be readily re-reduced back to the parent compound. Unfortunately, urine collection was not performed to determine SeTal and its metabolites, the focus of the study was to evaluate the effect of SeTal on atopic dermatitis AD-like lesions. In addition, the amount of SeTal and/or Se that may be absorbed by the mice was not evaluated. More studies are necessary to validate this point.

Author statement

The manuscript and the data reported here have not been published previously and they are not under consideration for publication elsewhere. All listed authors have contributed significantly to the research and manuscript preparation. They consent to their names on the manuscript, approving thus the final article. All other authors have read the manuscript and have agreed to submit it in its current form for consideration for publication in the *Journal of Trace Elements in Medicine and Biology*. There is no conflict of interest in the conduct and reporting of research (e.g., financial interests in a test or procedure, funding by pharmaceutical companies for drug research).

Author contributions

G.T.V., R.L.O, C.L and E.A.W. conceived and designed the study. W. B.D. and V.F.C. carried out the qRT-PCR. M.P.S performed the histological analysis. C.H.S. and M.J.D. provided SeTal. G.T.V., R.L.O., M.J. D., C.H.S. and E.A.W. wrote and revised the manuscript. E.A.W and C.L. supervised the study. All authors approved the final version of the manuscript.

Declaration of Competing Interest

The authors declare that they have no conflicts of interest, with the exception of MJD and CSH who are major shareholders and Directors of Seleno Therapeutics Pty. Ltd, which holds patents on the development and use of SeTal.

Acknowledgments

We are grateful for financial support from Seleno Therapeutics Pty. Ltd., and grants and scholarships from the following agencies: CNPq (UNIVERSAL 429859/2018-0), FAPERGS (PqG 17/2551-0001013-2, PRONEM 16/2551-0000240-1), CAPES, the Independent Research Fund Denmark (Danmarks Frie Forskningsfond; DFF-7014-00047) and the Novo Nordisk Foundation (NNF13OC0004294 and NNF15OC0018300). CNPq is also acknowledged for fellowships to E.A.W. and C. L. This study was financed in part by the Coordenação de Aperfeiçoamento de Pessoal de Nível Superior - Brasil (CAPES) - Finance Code 001, and forms part of the activities of the International SeS Redox and Catalysis Network.

References

[1] M. Udompataikul, D. Limpa-o-vart, Comparative trial of 5% dexpanthenol in water-in-oil formulation with 1% hydrocortisone ointment in the treatment of childhood atopic dermatitis: a pilot study, J. Drugs Dermatol. 11 (2012) 366–374.

[2] J.W. Kim, BS, Medscape, Atopic Dermat. Clin. Present, 2019 (Accessed August 14, 2020), https://emedicine.medscape.com.

[3] S. Nutten, Atopic dermatitis: global epidemiology and risk factors, Ann. Nutr. Metab. 66 (Suppl 1) (2015) 8–16, https://doi.org/10.1159/000370220.

[4] C.S.F. do Amaral, M. de F.B.P. March, C.C. Sant'Anna, Quality of life in children and teenagers with atopic dermatitis, An. Bras. Derm. Sifilogr. 87 (2012) 717–723, https://doi.org/10.1590/s0365-05962012000500008.

[5] W. Peng, N. Novak, Pathogenesis of atopic dermatitis, Clin. Exp. Allergy J. Br. Soc. Allergy Clin. Immunol. 45 (2015) 566–574, https://doi.org/10.1111/cea.12495.

[6] V. Aoki, D. Lorenzini, R.L. Orfali, M.C. Zaniboni, Z.N.P. de Oliveira, M.C. Rivitti-Machado, R. Takaoka, M.B. Weber, T. Cestari, B. Gontijo, A.M.C. Ramos, C.M. de R. Silva, S. da C.P. Cestari, S. Souto-Mayor, F.R. Carneiro, A.M.M. de Cerqueira, C. Laczynski, M.C. Pires, Consensus on the therapeutic management of atopic dermatitis - Brazilian Society of Dermatology, An. Bras. Derm. Sifilogr. 94 (2019) 67–75. http://www.scielo.br/scielo.php?script=sci_arttext&pid=S0365-05962019000700067&nrm=iso.

[7] L. Misery, Atopic dermatitis and the nervous system, Clin. Rev. Allergy Immunol. 41 (2011) 259–266, https://doi.org/10.1007/s12016-010-8225-z.

[8] T. Yoshimoto, H. Mizutani, H. Tsutsui, N. Noben-Trauth, K. Yamanaka, M. Tanaka, S. Izumi, H. Okamura, W.E. Paul, K. Nakanishi, IL-18 induction of IgE: dependence on CD4+ t cells, IL-4 and STAT6, Nat. Immunol. 1 (2000) 132–137, https://doi.org/10.1038/77811.

[9] A. Takaoka, I. Arai, M. Sugimoto, Y. Honma, N. Futaki, A. Nakamura, S. Nakaike, Involvement of IL-31 on scratching behavior in NC/Nga mice with atopic-like dermatitis, Exp. Dermatol. 15 (2006) 161–167, https://doi.org/10.1111/j.1600-0625.2006.00405.x.

[10] J. Ring, A. Alomar, T. Bieber, M. Deleuran, A. Fink-Wagner, C. Gelmetti, U. Gieler, J. Lipozencic, T. Luger, A.P. Oranje, T. Schäfer, T. Schwennesen, S. Seidenari, D. Simon, S. Ständer, G. Stingl, S. Szalai, J.C. Szepietowski, A. Taïeb, T. Werfel, A. Wollenberg, U. Darsow, Guidelines for treatment of atopic eczema (atopic dermatitis) Part II, J. Eur. Acad. Dermatol. Venereol. 26 (2012) 1176–1193, https://doi.org/10.1111/j.1468-3083.2012.04636.x.

[11] L.F. Eichenfield, W.L. Tom, T.G. Berger, A. Krol, A.S. Paller, K. Schwarzenberger, J. N. Bergman, S.L. Chamlin, D.E. Cohen, K.D. Cooper, K.M. Cordoro, D.M. Davis, S. R. Feldman, J.M. Hanifin, D.J. Margolis, R.A. Silverman, E.L. Simpson, H. C. Williams, C.A. Elmets, J. Block, C.G. Harrod, W. Smith Begolka, R. Sidbury, Guidelines of care for the management of atopic dermatitis: section 2. Management and treatment of atopic dermatitis with topical therapies, J. Am. Acad. Dermatol. 71 (2014) 116–132, https://doi.org/10.1016/j.jaad.2014.03.023.

[12] E. Roekevisch, P.I. Spuls, D. Kuester, J. Limpens, J. Schmitt, Efficacy and safety of systemic treatments for moderate-to-severe atopic dermatitis: a systematic review, J. Allergy Clin. Immunol. 133 (2014) 429–438, https://doi.org/10.1016/j.jaci.2013.07.049.

[13] N.O. Alves, G.T. da Silva, D.M. Weber, C. Luchese, E.A. Wilhelm, A.R. Fajardo, Chitosan/poly(vinyl alcohol)/bovine bone powder biocomposites: a potential biomaterial for the treatment of atopic dermatitis-like skin lesions, Carbohydr. Polym. 148 (2016) 115–124, https://doi.org/10.1016/j.carbpol.2016.04.049.

[14] G.T. Voss, R.L. Oliveira, J.F. de Souza, L.F.B. Duarte, A.R. Fajardo, D. Alves, C. Luchese, E.A. Wilhelm, Therapeutic and technological potential of 7-chloro-4-phenylselanyl quinoline for the treatment of atopic dermatitis-like skin lesions in mice, Mater. Sci. Eng. C Mater. Biol. Appl. 84 (2018) 90–98, https://doi.org/10.1016/j.msec.2017.11.026.

[15] D. Mroginski Weber, T.G. Voss, L.R. de Oliveira, A.R.C. da Fonseca, J. Paltian, K. C. Rodrigues, F. Rodrigues Ianiski, R.A. Vaucher, C. Luchese, E. Antunes Wilhelm, Topic application of meloxicam-loaded polymeric nanocapsules as a technological alternative for treatment of the atopic dermatitis in mice, J. Appl. Biomed. 16 (2018) 337–343, https://doi.org/10.1016/j.jab.2018.03.003.

[16] H.H. Ng, C.H. Leo, K. O'Sullivan, S.-A. Alexander, M.J. Davies, C.H. Schiesser, L. J. Parry, 1,4-Anhydro-4-seleno-d-talitol (SeTal) protects endothelial function in the mouse aorta by scavenging superoxide radicals under conditions of acute oxidative stress, Biochem. Pharmacol. 128 (2017) 34–45, https://doi.org/10.1016/j.bcp.2016.12.019.

[17] M.J.D. Carl Herbert Schiesser, Corin Storkey, Selenosugars for Skin Tissue Repair, 2018. https://patents.justia.com/patent/9895309.

[18] T. Zacharias, K. Flouda, T.A. Jepps, B. Gammelgaard, C.H. Schiesser, M.J. Davies, Effects of a novel selenium substituted-sugar (1,4-anhydro-4-seleno-d-talitol, SeTal) on human coronary artery cell lines and mouse aortic rings, Biochem. Pharmacol. 173 (2020), 113631, https://doi.org/10.1016/j.bcp.2019.113631.

[19] M.P. Pinz, A.S. dos Reis, A.G. Vogt, R. Krüger, D. Alves, C.R. Jesse, S.S. Roman, M. P. Soares, E.A. Wilhelm, C. Luchese, Current advances of pharmacological properties of 7-chloro-4-(phenylselanyl) quinoline: prevention of cognitive deficit and anxiety in Alzheimer's disease model, Biomed. Pharmacother. 105 (2018) 1006–1014, https://doi.org/10.1016/j.biopha.2018.06.049.

[20] A.S. Reis, M. Pinz, L.F.B. Duarte, J.A. Roehrs, D. Alves, C. Luchese, E.A. Wilhelm, 4-phenylselenyl-7-chloroquinoline, a novel multitarget compound with anxiolytic activity: contribution of the glutamatergic system, J. Psychiatr. Res. 84 (2017) 191–199, https://doi.org/10.1016/j.jpsychires.2016.10.007.

[21] E.A. Wilhelm, P.S. Soares, A.S. Reis, A. Barth, B.G. Freitas, K.P. Motta, B.B. Lemos, A.G. Vogt, C.A.R. da Fonseca, D.R. Araujo, A.M. Barcellos, G. Perin, C. Luchese, Se — [(2,2-Dimethyl-1,3-dioxolan-4-yl) methyl] 4-chlorobenzoselenolate reduces the nociceptive and edematogenic response by chemical noxious stimuli in mice: implications of multi-target actions, Pharmacol. Rep. 71 (2019) 1201–1209, https://doi.org/10.1016/j.pharep.2019.07.003.

[22] C. Storkey, D.I. Pattison, J.M. White, C.H. Schiesser, M.J. Davies, Preventing protein oxidation with sugars: scavenging of hypohalous acids by 5-selenopyranose and 4-Selenofuranose derivatives, Chem. Res. Toxicol. 25 (2012) 2589–2599, https://doi.org/10.1021/tx3003593.

[23] C.-C. Chan, C.-J. Liou, P.-Y. Xu, J.-J. Shen, M.-L. Kuo, W.-B. Len, L.-E. Chang, W.-C. Huang, Effect of dehydroepiandrosterone on atopic dermatitis-like skin lesions induced by 1-chloro-2,4-dinitrobenzene in mouse, J. Dermatol. Sci. 72 (2013) 149–157, https://doi.org/10.1016/j.jdermsci.2013.06.015.

[24] G. Park, M.S. Oh, Inhibitory effects of Juglans mandshurica leaf on allergic dermatitis-like skin lesions-induced by 2,4-dinitrochlorobenzene in mice, Exp. Toxicol. Pathol. Off. J. Gesellschaft Fur Toxikologische Pathol. 66 (2014) 97–101, https://doi.org/10.1016/j.etp.2013.10.001.

[25] H. Kim, J.R. Kim, H. Kang, J. Choi, H. Yang, P. Lee, J. Kim, K.W. Lee, 7,8,4'-Trihydroxyisoflavone attenuates DNCB-induced atopic dermatitis-like symptoms in NC/Nga mice, PLoS One 9 (2014), e104938, https://doi.org/10.1371/journal.pone.0104938.

[26] K. Suzuki, H. Ota, S. Sasagawa, T. Sakatani, T. Fujikura, Assay method for myeloperoxidase in human polymorphonuclear leukocytes, Anal. Biochem. 132 (1983) 345–352, https://doi.org/10.1016/0003-2697(83)90019-2.

[27] M.M. Bradford, A rapid and sensitive method for the quantitation of microgram quantities of protein utilizing the principle of protein-dye binding, Anal. Biochem. 72 (1976) 248–254, https://doi.org/10.1006/abio.1976.9999.

[28] K.J. Livak, T.D. Schmittgen, Analysis of relative gene expression data using real-time quantitative PCR and the 2(-Delta Delta C(T)) Method, Methods 25 (2001) 402–408, https://doi.org/10.1006/meth.2001.1262.

[29] A.U. Tan, M.E. Gonzalez, Management of severe atopic dermatitis in children, J. Drugs Dermatol. 11 (2012) 1158–1165.

[30] G. Voss, M. Gularte, R. Oliveira, C. Luchese, A. Fajardo, E. Wilhelm, Biopolymeric films as delivery vehicles for controlled release of hydrocortisone: promising devices to treat chronic skin diseases, Mater. Sci. Eng. C (2020), 111074, https://doi.org/10.1016/j.msec.2020.111074.

[31] E. Charmandari, N.C. Nicolaides, G.P. Chrousos, Adrenal insufficiency, Lancet (London, England) 383 (2014) 2152–2167, https://doi.org/10.1016/S0140-6736(13)61684-0.

[32] T. Tempark, V. Phatarakijnirund, S. Chatproedprai, S. Watcharasindhu, V. Supornsilchai, S. Wananukul, Exogenous Cushing's syndrome due to topical corticosteroid application: case report and review literature, Endocrine 38 (2010) 328–334, https://doi.org/10.1007/s12020-010-9393-6.

[33] K.B. Yarbrough, K.J. Neuhaus, E.L. Simpson, The effects of treatment on itch in atopic dermatitis, Dermatol. Ther. 26 (2013) 110–119, https://doi.org/10.1111/dth.12032.

[34] A. Torrelo, J. Ortiz, A. Alomar, S. Ros, M. Prieto, J. Cuervo, Atopic dermatitis: impact on quality of life and patients' attitudes toward its management, Eur. J. Dermatol. 22 (2012) 97–105, https://doi.org/10.1684/ejd.2011.1560.

[35] E.L. Simpson, Atopic dermatitis: a review of topical treatment options, Curr. Med. Res. Opin. 26 (2010) 633–640, https://doi.org/10.1185/03007990903512156.

[36] M.J. Davies, C.L. Hawkins, D.I. Pattison, M.D. Rees, Mammalian heme peroxidases: from molecular mechanisms to health implications, Antioxid. Redox Signal. 10 (2008) 1199–1234, https://doi.org/10.1089/ars.2007.1927.

[37] K.C. Navegantes, R. de Souza Gomes, P.A.T. Pereira, P.G. Czaikoski, C.H. M. Azevedo, M.C. Monteiro, Immune modulation of some autoimmune diseases: the critical role of macrophages and neutrophils in the innate and adaptive immunity, J. Transl. Med. 15 (2017) 36, https://doi.org/10.1186/s12967-017-1141-8.

[38] E. Malle, P.G. Furtmüller, W. Sattler, C. Obinger, Myeloperoxidase: a target for new drug development? Br. J. Pharmacol. 152 (2007) 838–854, https://doi.org/10.1038/sj.bjp.0707358.

[39] E.B. Brandt, U. Sivaprasad, Th2 cytokines and atopic dermatitis, J. Clin. Cell. Immunol. 2 (2011), https://doi.org/10.4172/2155-9899.1000110.

[40] M. Jung, T.H. Lee, H.J. Oh, H. Kim, Y. Son, E.H. Lee, J. Kim, Inhibitory effect of 5,6-dihydroergosteol-glucoside on atopic dermatitis-like skin lesions via suppression of NF-κB and STAT activation, J. Dermatol. Sci. 79 (2015) 252–261, https://doi.org/10.1016/j.jdermsci.2015.06.005.

[41] A.S. Paller, K. Kabashima, T. Bieber, Therapeutic pipeline for atopic dermatitis: end of the drought? J. Allergy Clin. Immunol. 140 (2017) 633–643, https://doi.org/10.1016/j.jaci.2017.07.006.

[42] N. Novak, R. Valenta, B. Bohle, S. Laffer, J. Haberstok, S. Kraft, T. Bieber, FcepsilonRI engagement of Langerhans cell-like dendritic cells and inflammatory dendritic epidermal cell-like dendritic cells induces chemotactic signals and different T-cell phenotypes in vitro, J. Allergy Clin. Immunol. 113 (2004) 949–957, https://doi.org/10.1016/j.jaci.2004.02.005.

[43] T. Tanaka, H. Tsutsui, T. Yoshimoto, M. Kotani, M. Matsumoto, A. Fujita, W. Wang, S. Higa, T. Koshimoto, K. Nakanishi, M. Suemura, Interleukin-18 is elevated in the sera from patients with atopic dermatitis and from atopic dermatitis model mice, NC/Nga, Int. Arch. Allergy Immunol. 125 (2001) 236–240, https://doi.org/10.1159/000053821.

[44] P. Ferroni, S. Riondino, O. Buonomo, R. Palmirotta, F. Guadagni, M. Roselli, Type 2 diabetes and breast cancer: the interplay between impaired glucose metabolism and oxidant stress, Oxid. Med. Cell. Longev. 2015 (2015), 183928, https://doi.org/10.1155/2015/183928.

[45] L.M. Howe, Treatment of endotoxic shock: glucocorticoids, lazaroids, nonsteroidals, others, Vet. Clin. North Am. Small Anim. Pract. 28 (1998) 249–267, https://doi.org/10.1016/s0195-5616(98)82004-4.

[46] B. Zhao, B. Ren, R. Guo, W. Zhang, S. Ma, Y. Yao, T. Yuan, Z. Liu, X. Liu, Supplementation of lycopene attenuates oxidative stress induced neuroinflammation and cognitive impairment via Nrf2/NF-κB transcriptional pathway, Food Chem. Toxicol. 109 (2017) 505–516, https://doi.org/10.1016/j.fct.2017.09.050, an Int. J. Publ. Br. Ind. Biol. Res. Assoc.

[47] M. Abu Elhija, E. Lunenfeld, M. Huleihel, LPS increases the expression levels of IL-18, ICE and IL-18 R in mouse testes, Am. J. Reprod. Immunol. 60 (2008) 361–371, https://doi.org/10.1111/j.1600-0897.2008.00636.x.

[48] O. Kurow, B. Frey, L. Schuster, V. Schmitt, S. Adam, M. Hahn, D. Gilchrist, I. B. McInnes, S. Wirtz, U.S. Gaipl, G. Krönke, G. Schett, S. Frey, A.J. Hueber, Full length interleukin 33 aggravates radiation-induced skin reaction, Front. Immunol. 8 (2017) 722, https://doi.org/10.3389/fimmu.2017.00722.

[49] A. Turabelidze, S. Guo, L.A. DiPietro, Importance of housekeeping gene selection for accurate reverse transcription-quantitative polymerase chain reaction in a wound healing model, Wound Repair Regen. 18 (2010) 460–466, https://doi.org/10.1111/j.1524-475X.2010.00611.x. Off. Publ. Wound Heal. Soc. [and] Eur. Tissue Repair Soc.

4.2 Artigo 2

Biopolymeric films as delivery vehicles for controlled release of hydrocortisone: Promising devices to treat chronic skin diseases

O artigo científico encontra-se publicado na revista International *Materials Science & Engineering C*

Materials Science & Engineering C 114 (2020) 111074

Contents lists available at ScienceDirect

Materials Science & Engineering C

journal homepage: www.elsevier.com/locate/msec

Biopolymeric films as delivery vehicles for controlled release of hydrocortisone: Promising devices to treat chronic skin diseases

Guilherme T. Voss[b], Matheus S. Gularte[a], Renata L. de Oliveira[b], Cristiane Luchese[b], André R. Fajardo[a,*,1], Ethel A. Wilhelm[b,*,1]

[a] Laboratório de Tecnologia e Desenvolvimento de Compósitos e Materiais Poliméricos (LaCoPol), Universidade Federal de Pelotas (UFPel), Campus Capão do Leão s/n, 96010-900 Pelotas, RS, Brazil

[b] Laboratório de Pesquisa em Farmacologia Bioquímica (LaFarBio), Universidade Federal de Pelotas (UFPel), Campus Capão do Leão, 96010-900 Pelotas, RS, Brazil

ARTICLE INFO

Keywords:
Atopic dermatitis
Hydrocortisone
Chronic skin disease
Gelatin
Starch
Drug delivery

ABSTRACT

Atopic dermatitis (AD) is the most common chronic inflammatory skin disease with nasty effects on the psychosocial wellbeing of patients. Overall, glucocorticoids, such as hydrocortisone (HC), are the primary pharmacologic drugs used to treat AD and its symptoms. However, the long-term treatment with HC is often accompanied by severe adverse effects. So, this study reports the encapsulation of HC in polymeric films based on gelatin (Gel) and gelatin/starch (Gel/St) and investigates their potential to treat and attenuate 2,4-Dinitrochlorobenzene (DNCB)-induced AD-like symptoms in BALB/c mice model. The prepared films were characterized by different techniques, which indicated that HC was physically entrapped into the polymer matrices. *In vitro* experiments indicate that the HC release process occurs in a controlled manner (up to 48 h) for both films. Regarding the *in vivo* experiments, HC-loaded films (Gel@HC and Gel/St@HC), unloaded films (Gel and Gel/St) and HC cream (1%) (as reference) were applied topically on the back of the DNCB-sensitized animals and skin severity scores and scratching behavior were determined. *Ex-vivo* experiments were done to quantify inflammatory and/or biochemical parameters. As assessed, the topical application of the biopolymeric films (loaded or not with HC) improved the inflammatory parameters, while a lower corticosterone level was observed for the animals treated with Gel and Gel@HC films. In summary, the HC-loaded films showed superior efficiency to treat/attenuate the analyzed parameter than the HC cream (1%). Further, no death or sign of toxicity was observed in animals exposed to HC-loaded films. Thus, the encapsulation of HC in biopolymeric films seems to be a promising alternative for the treatment of injuries caused by chronic skin diseases that require prolonged use of glucocorticoids.

1. Introduction

Chronic skin diseases, such as dermatitis, lupus, and vitiligo, have affected millions of people around the world. In 2019, skin diseases were ranked as the fourth most common cause of human illness and incapacitation [1]. Taking into account that the skin is the primary interface between the human body and the external environment, the presence of skin diseases impact substantially many aspects of the patient's life. For example, patients with severe skin diseases are more susceptible to negative social repercussions resulting in psychological disorders [2]. This scenery gets worst if we consider that children are usually a frequent target of this type of disease.

The clinical manifestation associated with skin diseases varies according to the type of disease. Atopic dermatitis (AD), for example, is a highly pruriginous and recurrent inflammatory disease, while vitiligo is a polygenic autoimmune disease characterized by the progressive skin depigmentation [3]. Overall, the initial treatment of such skin diseases is focused on the use of topical creams and ointments containing anti-inflammatory, antihistaminic, and antibiotic agents [4]. Among these drugs, the corticosteroids constitute a class of primarily synthetic steroids used as anti-inflammatory and antipruritic agents. In particular, hydrocortisone (HC) has been used to reduce dermatosis symptoms (such as redness, itching, swelling, *etc.*) due to its pharmacological properties for decades. Despite the efficient use of HC on the treatment of the different symptoms of skin diseases, its hydrophobic nature may impair its application mainly in exudative lesions [5,6].

* Corresponding authors.
E-mail addresses: andre.fajardo@pq.cnpq.br (A.R. Fajardo), ethelwilhelm@yahoo.com.br, ethelwilhelm@ufpel.edu.br (E.A. Wilhelm).
[1] A.R.F. and E.A.W. contributed equally to this work.

https://doi.org/10.1016/j.msec.2020.111074
Received 18 December 2019; Received in revised form 6 May 2020; Accepted 7 May 2020
Available online 11 May 2020
0928-4931/

Also, a long-term administration of HC may lead to some risks of systemic effects, such as hypothalamus-pituitary-adrenal (HPA) axis suppression [7]. HC is a synthetic analog of cortisol, and a high level of this hormone may be responsible for the suppression of the HPA axis and adrenocorticotropic hormone (ACTH), which leads to adverse effects such as adrenal atrophy [8]. To overcome these drawbacks, we report in this paper the preparation of bio-based films of gelatin (Gel) and gelatin/starch (Gel/St) to act as vehicles for encapsulation and controlled release of HC.

Over the past few years, the use of some polymeric-based devices to release HC in a controlled manner has been reported in the literature [9,10]. Nevertheless, the use of release devices consisting of majorly by biopolymers has been poorly explored. Gelatin (Gel) is a biopolymer derived from collagen widely used by food, pharmaceutical, and medical industries due to its non-toxicity, biodegradability, and biocompatibility properties [11]. More specifically, Gel has been used to formulate different drug delivery devices, such as hydrogels, microparticles, tablets, among others [11,12]. Due to these features, we utilized Gel (pure or blended with starch) to prepared films using a simple protocol. Starch (St) is also a biopolymer consisting predominantly of two polysaccharides, namely amylose and amylopectin. In general, St exhibits excellent film-forming properties as well as natural abundance, low cost and toxicity, and biodegradability [13,14].

Herein, biopolymeric films consisting of Gel and Gel/St were used to encapsulate HC and tested as drug delivery devices. Beyond the full characterization of the obtained films, *in vitro* assays were performed to investigate the HC release profile, kinetics, and mechanism. Furthermore, the biological activity of the HC-containing films was investigated by *in vivo and ex vivo* assays concerning the treatment of 2,4-dinitrochlorobenzene (DNCB)-induced AD-like skin lesions in mice model. Thus, the objective of this study was to develop a corticosteroid administration system, such as HC, capable of acting on the lesions of cutaneous diseases with minimal systemic absorption, leading to fewer adverse effects.

2. Materials and methods

2.1. Materials

Gelatin (Gel, type B) and 2,4-dinitrochlorobenzene (DNCB) were purchased from Sigma-Aldrich (USA). Rice starch (St) with amylose content of 30% was kindly donated by LabGrãos/UFPel (Pelotas-Brazil) [15]. Glycerol (99.5%) was purchased from Synth (Brazil). HC (> 98%, particle size < 20 μm) was purchased from Gemini (Brazil), and HC cream (1%) was obtained commercially (Bayer®) in the form of cream - each 1 g of cream with 11.2 mg of HC acetate and excipients (macrogol stearate 400, stearyl alcohol, liquid petrolatum, white petrolatum, edetate disodium, carbomer 980, sodium hydroxide, methylparaben, propylparaben, and purified water). All other chemicals of analytical grade were used as received without further purification.

2.2. Preparation of Gel and Gel/St films

Gel and Gel/St films were prepared by the solvent casting method [16–18]. Firstly, to prepare the Gel film (without St), 2.5 g of pure gelatin was solubilized in 50 mL of distilled water (stirring of 250 rpm for 1 h at 50 °C). Then, glycerol (100 μL), as a plasticizer, was added to the gelatin solution, which was homogenized under stirring (250 rpm) for 15 min. Next, the resulting solution was poured in a Petri dish (PS, round-shape 85 × 10 mm), which was placed in an oven (40 °C) to evaporate the solvent. After 24 h, the resulting Gel film was carefully peeled-off from the Petri dish, rinsed with distilled water and oven-dried (40 °C, overnight). In parallel, the Gel/St film was prepared by blending the aqueous solutions of gelatin and starch. Briefly, 1.75 g of gelatin was solubilized in 30 mL of distilled water (1 h at 50 °C), while 0.75 g of starch was also solubilized in 30 mL of distilled water (4 h at 85 °C). Both solutions were blended under magnetic stirring (250 rpm for 30 min) at 50 °C. Herein, the gelatin/starch mass ratio was fixed at 70:30 w/w-%, respectively. Next, glycerol (100 μL) was added to the gelatin/starch solution (250 rpm for 30 min), which after homogenization, was poured into a Petri dish. Later, the solvent was evaporated (oven, 40 °C for 24 h), resulting in a Gel/St film, which was recovered, rinsed with distilled water, and oven-dried (40 °C, overnight).

2.3. Preparation of Gel and Gel/St films containing hydrocortisone

The film samples loaded with HC were prepared using a protocol similar to that described in the previous section. However, HC (25 mg) at a fixed mass ratio of 99:1 *w*/w-% (polymer:HC) was added to the film-forming solutions before the solvent evaporation step. The resulting films were denoted as Gel@HC and Gel/St@HC, respectively.

2.4. Characterization

Fourier transform infra-red (FTIR) spectroscopy was used to characterize the chemical nature of the prepared materials. For this, FTIR spectra were obtained in a Shimadzu IR Affinity spectrometer (Japan) in the 4000–400 cm^{-1} range with an average of 64 scans at 4 cm^{-1} resolution. Before the spectra acquisition, the samples were ground with spectroscopic grade KBr and pressed into discs. Thermogravimetric analyses (TGA) were performed using a Shimadzu DTG-60 Analyzer (Japan) in a temperature range of 25–700 °C under N_2 atmosphere at a heating rate of 10 °C min^{-1}. Mechanical properties of the prepared films were investigated by tensile tests using a Stable Microsystems TA.XT2 texturometer equipment (UK). The tests were run using rectangular samples (80 × 25 mm, length x width) in an atmosphere of 50% relative humidity with a test speed of 0.8 mm min^{-1}, according to the ASTM D882-12 method [19]. The morphology of the samples was examined by means of scanning electron microscopy (SEM). Images were obtained in a JEOL JSM-6610LC microscope (USA) using an acceleration voltage of 15 kV. Before the SEM visualization, film samples were cut into rectangular pieces (about 4 × 2 mm), which were attached to sample holders with carbon tapes and, then, gold-coated by sputtering. Microscopic images of the films and the pure HC were also taken using a polarized light microscope (Olympus Germany). Swelling experiments were done to investigate the liquid uptake capacities of the prepared films (loaded or not with HC). Briefly, film samples were weighed and then placed into vials filled with 50 mL of simulated wound fluid (SWF) (2 w/v-% of bovine serum albumin (BSA), 0.02 mol L^{-1} $CaCl_2$, 0.4 mol L^{-1} NaCl, pH 7.4) [20] at 37 °C. At predetermined time intervals, the swollen films were withdrawn, blotted carefully with tissue paper to remove the surface-adhered liquid droplets, and reweighed. The swelling degree of each sample after different time intervals was calculated according to the following equation:

$$\textit{Swelling degree}\ (\%) = \left[\frac{W_s - W_0}{W_0}\right] \times 100 \quad (1)$$

where W_0 is the initial weight of the dry film, and W_s is the swollen weight of the film at time *t*. This experiment was performed in triplicate.

2.5. In vitro hydrocortisone release assays

The release behavior of HC from the Gel@HC and Gel/St@HC films was investigated using a vertical cell diffusion apparatus. Briefly, film samples (50 mg loaded with 0.5 mg of HC) were directly placed over regenerated cellulose dialyses membranes (M_{WCO} 12–14 kDa, Spectra/Por®, USA) with an effective release area of approx. 1.5 cm^2. The acceptor vial was filled with SWF (25 mL, pH 7.4) and the temperature was maintained at ~37 °C. Aliquots (1 mL) were withdrawn at pre-

determined time intervals and analyzed using a Micronal BS82 UV–visible spectrometer (Brazil) at a wavelength of 248 nm (the absorption maximum of HC in aqueous medium). Simultaneously, an equivalent volume (1 mL) of fresh SWF was added to each vial for continuing incubation. The absorbance data were converted into concentration using a calibration curve ($Abs = 0.003 + 0.005[HC]$, $R^2 > 0.999$) that was built using standard concentrations of HC in SWF. Each experiment was performed in triplicate. For comparative purposes, the dissolution profile of pure HC (0.5 mg) was examined under similar conditions (25 mL of SWF at 37 °C).

2.6. In vivo and ex vivo assays

2.6.1. Animals

Herein, BALB/c mice female (6–8 weeks old) were used to perform the experimental protocol. The animals were kept in a 12 h light-dark cycle (7 a.m. to 7 p.m. with light) at 22 ± 1 °C, with free access to food and water. Biological assays were conducted according to institutional and national guidelines for the care and use of animals. The Local Committee for Care and Use of Laboratory Animals of the Federal University of Pelotas (Pelotas, Brazil) approved this research project (code number: 4294–2015). The number of animals used was the minimum necessary to demonstrate the consistent effects of the drug treatment, and all efforts were taken to make them comfortable.

2.6.2. Experimental protocol

DNCB was used as an inducer of AD-like skin lesions, as previously described by Chan et al. [21]. For this, animals were depilated in the dorsal region and 200 μL of 0.5% (v/v) DNCB in 3:1 (v/v) acetone/olive oil applied on days 1 to 3, for sensibilization. Later, animals were further challenged with 200 μL of 1% (v/v) DNCB on their backs and 20 μL on their right ears, on days 14, 17, 20, 23, 26, and 29, as shown in Fig. 1. Mice were randomly divided into seven groups, each one with 7 animals, except for the HC group (n ≈ 14 due to high mortality during the HC treatment). Normal control mice (control group) were sensitized and challenged with acetone/olive oil (3:1) and received no treatment. Sensitized control mice (vehicle group) were sensitized and challenged with DNCB and received no treatment. Experimental mice were sensitized and challenged with DNCB and received topical treatment with either HC-loaded (Gel@HC or Gel/St@HC, 50 mg sample loaded with 0.5 mg of HC) or not-loaded films (Gel or Gel/St) (50 mg samples) or HC (cream, 50 mg containing 0.5 mg of HC (1% w/w)). The backs injuries of mice were treated every 3 days with either HC-loaded or not film (Gel, Gel/St or Gel/St@HC) or HC (cream), the days 14, 17, 20, 23, 26, and 29. Signs of toxicity and mortality were evaluated during the experimental protocol.

2.6.3. Clinical skin severity scores and scratching behavior

On the last day of the experimental protocol (day 30), the skin was photographed, and severity scores were determined, according to Park et al. [22]. The five signs of skin lesions are (1) pruritus/itching, (2) erythema/hemorrhage, (3) edema, (4) excoriation/erosion, and (5) scaling/dryness. The above-mentioned symptoms were graded as follows: 0 (no symptoms), 1 (mild), 2 (moderate), and 3 (severe).

After the clinical skin severity evaluation, the amounts of time that the mice spent rubbing their noses, ears, and dorsal skin with their hind paws were measured and recorded for 20 min to investigate AD-like behavioral changes, according to Kim et al. [23].

2.6.4. Inflammatory parameters

2.6.4.1. Ear swelling. Following scratching-behavior assessment (day 30), mice were euthanized, and both ears were severed at the base and the mass differences between the control (left) and the DNCB-treated ears (right) determined using an analytical balance. Subsequently, the ears were used to determine the myeloperoxidase (MPO) activity.

2.6.4.2. Myeloperoxidase (MPO) activity. The MPO activity was evaluated according to the method previously described by Suzuki et al. [24] with minor modifications. The tissues removed (back and ear) were minced, pooled, and homogenized in phosphate-buffered

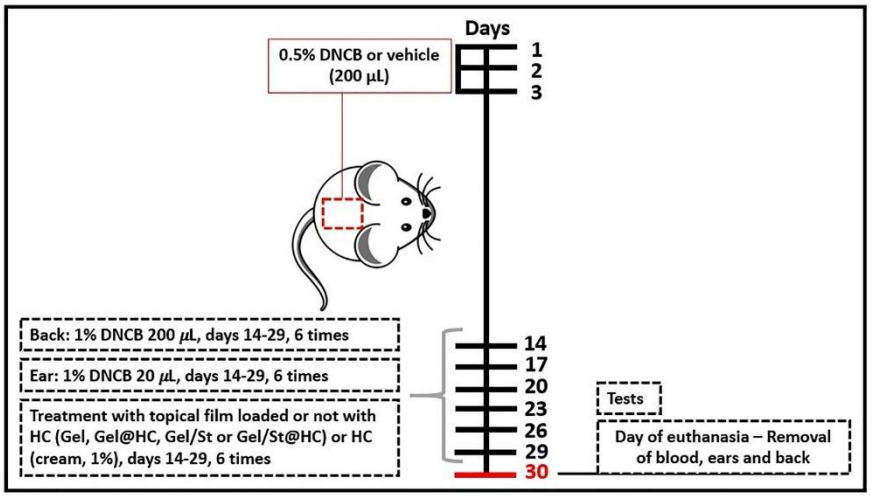

Fig. 1. Summary of the experimental protocol for the development of atopic dermatitis-like (AD) skin lesions in 2,4-dinitrochlorobenzene (DNCB) treated mice. The dorsal skin of the mice was shaved, and between days 1–3 were topically treated with 0.5% DNCB. The mice were then challenged with 1% DNCB on days 14, 17, 20, 23, 26, and 29. AD-like mice were treated with topical film loaded or not with HC (Gel, Gel@HC, Gel/St or Gel/St@HC), or HC (cream) on every 3 days, between days 14–27. Finally, the mice were euthanized on day 30.

saline (PBS) (20 mmol L^{-1}, pH 7.4) containing ethylenediaminetetraacetic acid (0.1 mmol L^{-1}) (EDTA). The homogenates were centrifuged at 900 rpm for 10 min at 4 °C and the pellet discarded. The supernatant (fraction S1) was then re-centrifuged at 24,000 rpm at 4 °C for 15 min to yield the final pellet (P2), which was resuspended in medium containing potassium phosphate buffer (50 mmol L^{-1}, pH 6.0) and hexadecyltrimethylammonium bromide (0.5 w/v-%). Samples were finally frozen and thawed three times prior to the assay. In order to determine the MPO activity, an aliquot of resuspended P2 (100 μL) was added to a medium containing the resuspension medium and *N,N,N′,N′*-tetramethylbenzidine (1.5 mmol L^{-1}). The MPO kinetic analysis was commenced upon the addition of H_2O_2 (0.01 v-%), and the color reaction was followed at 655 nm at 37 °C. Results were expressed as optic density (OD)/mg protein/min. Protein concentration was determined by Bradford's method using BSA (1 mg mL^{-1}) as the standard [25].

2.6.5. Biochemical markers

The estimation of the plasma corticosterone concentration was performed by a fluorometric assay, as described by Zenker and Bernstein [26]. Fluorescence intensity emission, corresponding to plasma corticosterone levels, was recorded at 540 nm (with 247 nm excitation), and corticosterone levels were expressed as ng mL^{-1}. The AST and ALT activities were determined in mice plasma, using commercial kits (Bioclin, Brazil) following the instructions provided by the supplier. ALT and AST activities were expressed as units per liter (U L^{-1}).

2.7. Statistical analysis

The normality of the data was evaluated by the D'Agostino and Pearson omnibus normality test. The data were analyzed by one-way analysis of variance (ANOVA) followed by Newman-Keuls test. All analyses were performed using the GraphPad software (San Diego, CA, USA). Data are expressed as mean ± standard error of the mean (S.E.M.). $p < .05$ was considered statistically significant.

3. Results and discussion

3.1. Characterization

The starting materials used to prepare both films were characterized by FTIR analysis. Briefly, the spectra of gelatin and starch (shown in Fig. 2a) exhibited the main characteristic bands of such compounds corroborating with previous studies [27,28]. The spectrum of HC exhibited bands at 3427 (O—H stretching), 3017 (aromatic C—H stretching), 1742 and 1720 (C=O stretching), 1635, and 1560 (C=C stretching) and 1327 cm^{-1} (C—N stretching) [29]. The bands associated with the C—H stretching modes of CH_2 and CH_3 groups are noticed in the 2980–2870 cm^{-1} region. The FTIR spectroscopy was also utilized to investigate the chemical nature of the prepared films (loaded or not with HC). As shown in Fig. 2b, the Gel film exhibited the main bands proceeding from gelatin with some discrepancies, likely due to the presence of glycerol (the plasticizer) [30]. With the addition of starch, no apparent changes were observed comparing the Gel/St and Gel spectra. Similar results were reported by Wang et al., which explain that the starch does not change the conformational structure of gelatin [31]. The spectrum of Gel/St film showed a slight shifting of the band associated with the O—H stretching likely due to the H-bonds formed between gelatin and starch. Also, the appearing of some new bands and shoulder-type bands in the 1150–1000 cm^{-1} region of the Gel/St spectrum indicates the presence of starch in the film since these bands are assigned to different vibrational modes of typical functional groups of starch (glycoside and pyranose rings, for instance) [32]. Finally, the FTIR spectra of the HC-loaded films (Gel@HC and Gel/St@HC) were similar to the spectra of the unloaded films indicating that HC does not exert a noticeable effect of the films chemical nature. This result may be a result of the small amount of HC present in the film matrices. Additionally, Gel@HC and Gel/St@HC spectra exhibited a band at 1742 cm^{-1} ascribed to the C=O stretching proceeding from HC. The presence of other low intense bands in the region of 1500–1200 cm^{-1} of the Gel@HC and Gel/St@HC spectra can also be associated with HC [29,33]. From these data, it can be inferred that HC was efficiently encapsulated in both films; however, no apparent covalent interactions take place between HC and the film matrices.

TGA and DTG curves o HC and biopolymeric films (loaded or not with HC) are shown in Fig. 3. The pure HC exhibited three weight loss stages that start at 218 °C and end at 635 °C (Fig. 3a), and its major decomposition stage has a maximum temperature at 306 °C (Fig. 3b) [34]. At the end of the analysis (700 °C) the residue of HC corresponded to 5% of its initial weight. The gel film exhibited two stages of weight loss. The first stage (from 30 °C to 120 °C) is attributed to the loss of volatile compounds and water, while the second stage (from 120 °C to 520 °C) is associated with the protein chain breakage and peptide chain rupture of gelatin [35]. Moreover, the thermal decomposition of glycerol (the plasticizer) occurs between 160 and 270 °C [36]. The thermal stability of the Gel film was significantly altered after the addition of HC in the film formulation. As shown in Fig. 3b, the maximum

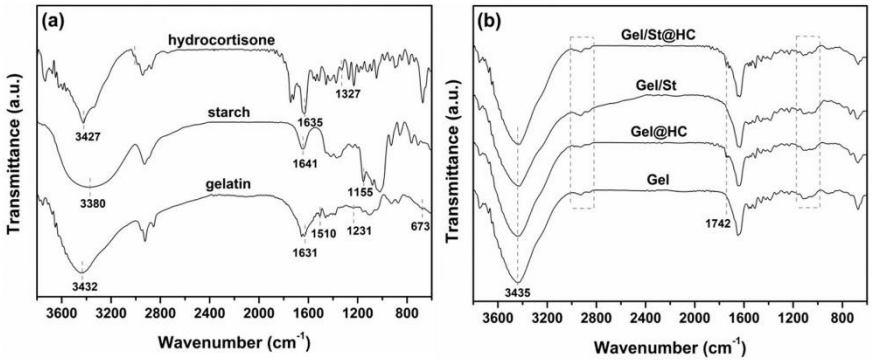

Fig. 2. FTIR spectra of (a) starting materials (pure gelatin, starch, hydrocortisone) and (b) biopolymeric films loaded (Gel@HC and Gel/St@HC) or not (Gel and Gel/St) with hydrocortisone.

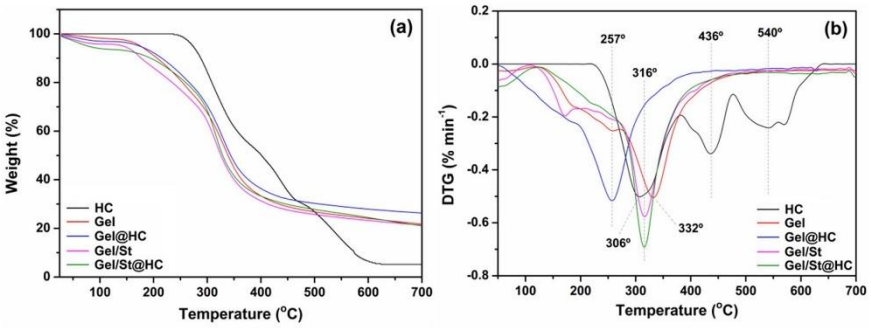

Fig. 3. (a) TGA and (b) DTG curves of HC, Gel, Gel/ST, Gel@HC, and Gel/St@HC.

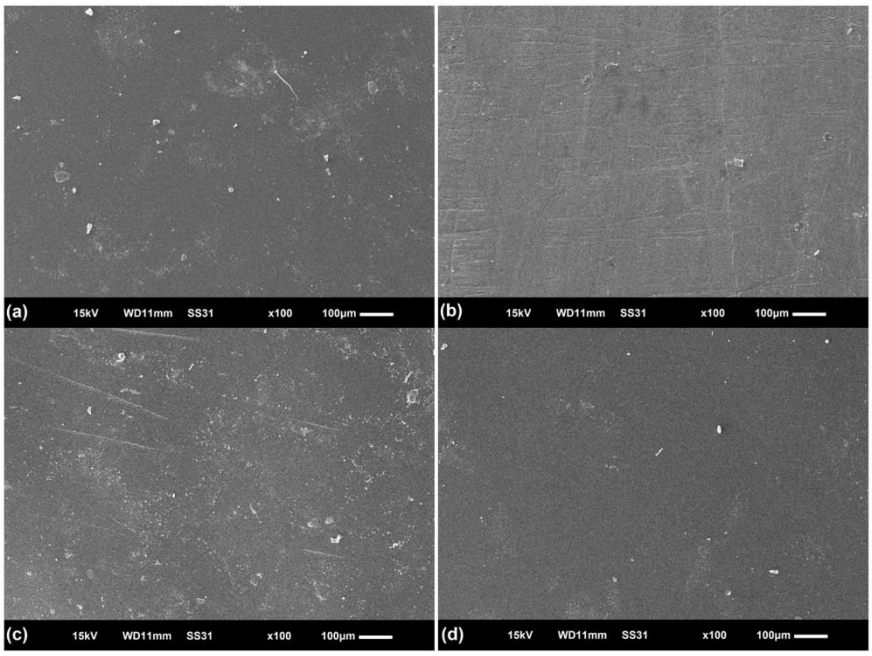

Fig. 4. SEM images recorded from (a) Gel, (b) Gel/St, (c) Gel@HC, and (d) Gel/St@HC films.

temperature associated with the thermal decomposition of the gelatin is shifted from 332 °C to 257 °C for Gel@HC, which may suggest that the drug affects the inter and intramolecular interactions among the gelatin chains. Consequently, the thermal stability of Gel@HC is hammered as compared to Gel film. Additionally, the TGA/DTG curves obtained for Gel@HC did not exhibit the degradation stages of HC, suggesting that the drug is in the amorphous state within the film matrix, which is desirable, taking into account the HC dispersion and subsequent release [34]. Further, the TGA/DTG curves of Gel/St film showed two weight loss stages, where the first is due to the loss of volatile compounds and water (from 30 °C to 130 °C) while the second (from 130 °C to 500 °C) refers to the thermal decomposition of gelatin and starch [37,38]. The absence of a new weight-loss stage indicates high compatibility between the polymers (*i.e.*, miscible blend). Soliman et al. [35] attributed this compatibility to the numerous interactions that occur between gelatin and starch. Likely due to these interactions, the loading of HC did not affect the thermal stability Gel/St@HC film, as observed in Fig. 3. The Gel/St@HC film exhibited thermal behavior similar to the unloaded Gel/St film. Again, the degradation stages associated with HC were not observed.

Scanning electron microscopy (SEM) was used to examine the morphology and microstructure of the prepared films. The images

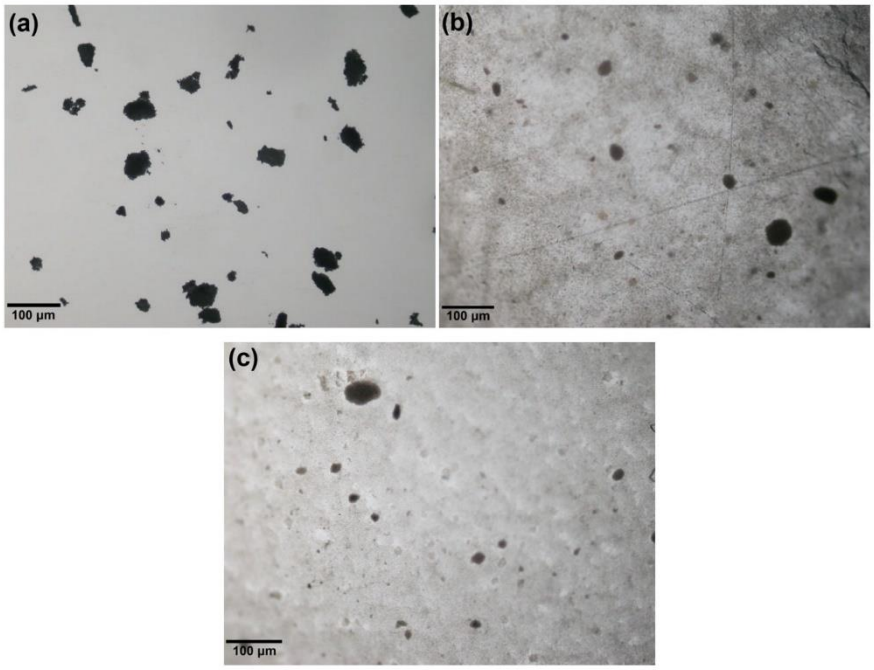

Fig. 5. Light microscopy images of (a) pure HC, (b) Gel@HC, and (c) Gel/St@HC films.

Table 1
Mechanical properties of the prepared biopolymeric films loaded or not with hydrocortisone.

Sample	Film thickness[a] (mm)	Elongation (%)	Tensile strength (MPa)	Young's modulus (MPa)
Gel	0.267 ± 0.04	57.6 ± 5.2	58.1 ± 12.4	5.0 ± 1.0
Gel@HC	0.299 ± 0.05	98.1 ± 14.3	23.7 ± 7.0	1.2 ± 0.3
Gel/St	0.272 ± 0.09	123.3 ± 10.8	17.6 ± 3.7	0.7 ± 0.3
Gel/St@HC	0.302 ± 0.05	116.8 ± 6.7	18.1 ± 3.4	0.7 ± 0.2

[a] The thickness was measured using a digital vernier caliper. The results are given as mean ± S.D. ($n \approx 8$).

recorded from the surface of the films are shown in Fig. 4(a–d). In general lines, all prepared films exhibited uniform, non-porous, and homogenous surfaces, which suggest good compatibility between starting materials (gelatin, starch, and glycerol). According to some authors, the glycerol can act as a plasticizer and a compatibilizer of the gelatin/starch blend [38,39].

The dense structure of the films associated with the absence of roughness suggests a suitable strength property. These observations are in agreement with other previously published studies [40]. Finally, the addition of HC seems to do not exert an effect on the surface morphology of Gel@HC and Gel/St@HC films (Fig. 4b and d). Overall, this result indicates a good dispersion of the drug into the bulk phase of the films.

Fig. 5 shows representative light microscopy images of pure HC and HC-loaded films. The image of pure HC shows irregular dark particles and aggregates with a wide size distribution. In parallel, the images of the loaded films (Gel@HC and Gel Gel/St@HC films) exhibited round dark spots associated with the encapsulated drug. As noticed, the drug is homogeneously distributed through both film samples corroborating the previous data.

The efficiency of polymeric films applied as local drug delivery systems (*i.e.*, topical use) is closely related to a series of physicochemical, biological, and mechanical properties [41]. For instance, a polymeric film can be considered mechanically efficient when it is resistant to handling, transportation, and application processes. Thus, a comprehensive investigation of these properties is required. Different types of equipment and protocols can assess the mechanical properties of polymeric films. Herein, tensile tests were performed using a Texturometer to investigate different mechanical properties of the as-prepared biofilms. The results computed from these tests and the thicknesses of each sample are listed in Table 1.

As demonstrated in Table 1, the thickness increased according to the incorporation of external compounds (starch and/or HC) in the gelatin matrix. This trend is likely due to the volume expansion caused by these compounds [17]. With the addition of starch, the film thickness increased ~10% as compared to the Gel film. Also, the addition of HC increased the thickness of both loaded films as compared to the pristine samples. In general lines, these results corroborate other studies that report the increment of the thickness of gelatin-based films after the addition of external compounds [42].

The mechanical properties of the as-prepared biofilms varied according to their composition, similar to the thickness. The elongation of the films increased considerably after the addition of starch and/or HC, as shown in Table 1. As compared to the pure gelatin film, the elongation of the Gel/St film increased ~114%, while for the Gel@HC film,

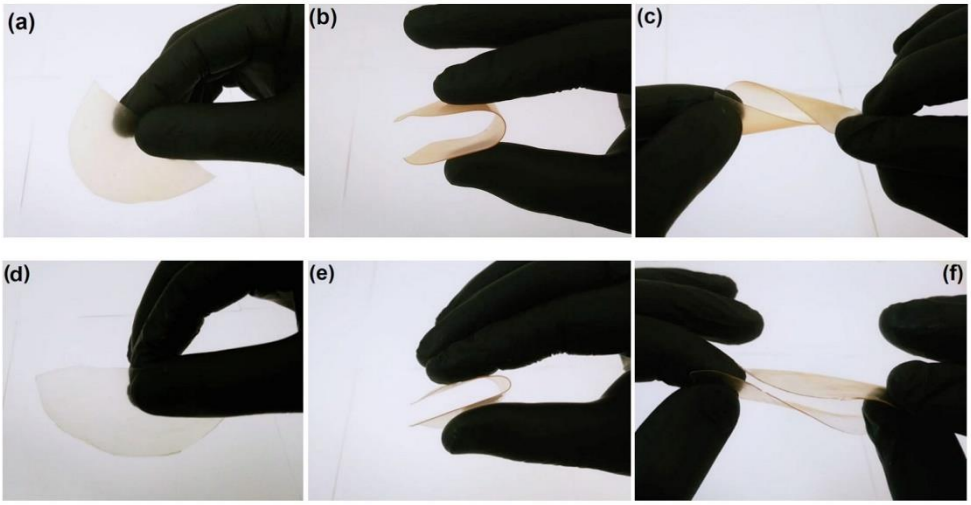

Fig. 6. Photographic images recorded from (a–c) Gel@HC and (d–f) Gel/St@HC films.

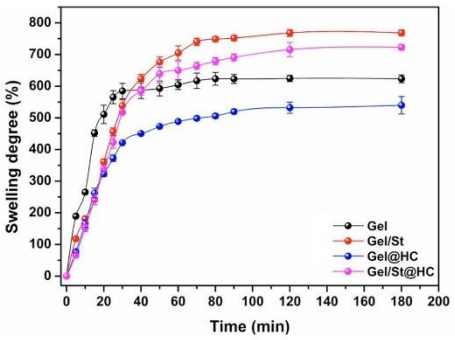

Fig. 7. Swelling profile of the prepared biopolymeric films in SWF (pH 7.4) at 37 °C.

the elongation, increased ~70%. As reported by different authors, the starch chains interact with gelatin by H-bonds that are formed between the hydroxyl groups of starch and carboxyl groups of gelatin [43]. The high amylose content of the starch used in this study enhances the formation of this kind of interaction. So, the enhanced interfacing interactions between the gelatin and starch chains decreases the rigidity of the film matrix and favors the film elongation (*i.e.*, the mobility of polymers chains is enhanced). Further, the thermal analysis showed that the loading of HC in the Gel film exerts a noticeable effect on its thermal behavior, likely due to the impairment of the interactions that occur among the gelatin chains. As a result, the elongation of the Gel@HC film is favored as compared to the pristine Gel film.

Furthermore, the tensile strength and Young's modulus (also known as elastic modulus) of the Gel film are negatively affected by the incorporation of starch. Compared to the Gel film, the tensile strength and Young's modulus values calculated for the Gel/St film were 70% and 86% lower, respectively. At the same time, the Gel@HC film exhibited tensile strength and Young's modulus values 60% and 76% lower than Gel film. The addition of small molecules, such as HC, in the gelatin matrix, can also result in a plasticizer effect due to the interaction of these molecules with the gelatin chains [44]. Conversely, a synergic effect due to the association of starch and HC on the mechanical properties of the gelatin-based films were not observed. As demonstrated in Table 1, the Gel/St and Gel/St@HC did not show a considerable variation of the assessed mechanical properties. It can be hypothesized that the effect caused by the starch chains overcomes the plasticizer action of HC.

Fig. 6 shows some photographic images taken from the Gel@HC and Gel/St@HC films to illustrate their physical aspect and flexibility.

Swelling experiments were performed at 37 °C in SWF (pH 7.4) to investigate the liquid uptake behavior of the as-prepared films. The results are presented in Fig. 7. Overall, all samples (loaded or not with HC) exhibited high liquid uptake capacities (swelling degree > 600%), which can be associated with the hydrophilic nature of the precursor materials. The Gel film exhibited the fastest swelling kinetics achieving a swelling degree of 585% within the first 30 min. After that, the liquid uptaking process slowdown, and the equilibrium is reached after 80 min. For this film sample, the maximum swelling degree was 622%. For the other film samples (Gel/St, Gel@HC, and Gel/St@HC), a discrepant behavior was noticed regarding the initial swelling kinetics when compared to Gel film. The incorporation of starch and/or HC in the gelatin matrix decreased the liquid uptake in the first minutes of the experiment. Two main reasons can explain this behavior: the H-bonds formed between polymers (gelatin and starch) and the drug, which impair the expansion of the film networks and the reduction of hydrophilic groups on the film surface due to these H-bonds limiting the interaction between the film and the water molecules. After the first 20 min, the liquid uptake of the starch-containing films continues increasing, while for the Gel@HC film, the liquid uptake tends to leave off. It may be stated that HC decreases the hydrophilicity of the film due to its hydrophobic nature and due to its interaction with the hydrophilic groups of gelatin. At the end of the experiment, the maximum swelling degree calculated for Gel@HC was 540%.

On the other hand, the starch-containing films exhibited the highest liquid capacity likely due to a large number of hydroxyl groups

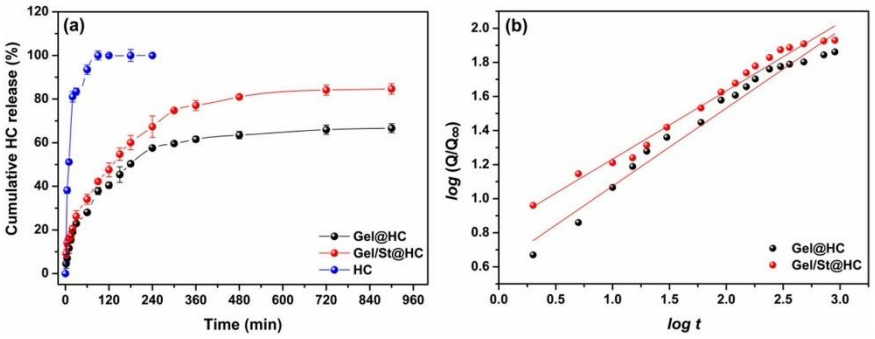

Fig. 8. (a) *In vitro* dissolution profile of HC (control) and HC released from Gel@HC and Gel/St@HC in SWF (pH 7.4) at 37 °C. (b) Korsmeyer-Peppas plots for Gel@HC and Gel/St@HC.

Table 2
Kinetic constants and correlation coefficients (R^2) obtained from different kinetic models for HC release from Gel@HC and Gel/St@HC films.

Model	Parameter	Sample	
		Gel@HC	Gel/St@HC
Zero-order	k_0 (mg min^{-1})	0.005	0.006
	R^2	0.657	0.698
	RSS	14.028	15.662
First-order	k_1 (min^{-1})	0.002	0.002
	R^2	0.433	0.531
	RSS	5.972	3.705
Higuchi	k_H (mg $min^{-0.5}$)	0.171	0.194
	R^2	0.901	0.923
	RSS	4.089	3.992
Korsmeyer-Peppas	k_{KP} (min^{-n})	4.130	6.670
	n	0.458	0.405
	R^2	0.972	0.986
	RSS	0.074	0.026

Note: RSS - Residual sum of squares.

distributed along the starch chains that favor the interaction with the water molecules. The maximum swelling degree calculated for Gel/St film was 768%, while for the Gel/St@HC was 723%. Again, the encapsulation of HC decreases the liquid uptake ability of the Gel/St@HC film as compared to the pristine film (*i.e.*, Gel/St). It is noteworthy that several studies described the use of swellable materials as vehicles for controlled release of HC; however, its effect on the liquid uptake ability of such materials is not investigated.

These finds suggest that both HC-loaded films have appropriate liquid uptake ability, which is desirable to treat chronic skin diseases, such as atopic dermatitis. Swellable materials used as topical drug delivery systems can absorb exudates and provide a moist environment, which reduces the risk of skin maceration and contamination by microorganisms [45].

3.2. In vitro hydrocortisone release

The use of polymeric films as vehicles for encapsulation and controlled release of drugs for topical treatment of chronic skin diseases, such as atopic dermatitis, has gained considerable attention since these materials show several advantages as compared to the conventional system [46]. It is known that the encapsulation of drugs in delivery vehicles based on polymeric matrices can aid in modulating the release process at a predetermined rate for a prolonged time at a target site [47]. In order to investigate this hypothesis, *in vitro* assays are performed under conditions that mimic the biological system. Herein, the release behavior of HC from Gel@HC and Gel/St@HC was examined in a simulated wound fluid (SWF, pH 7.4) at 37 °C. The collected data are shown in Fig. 8a.

As observed, the encapsulation of the HC into the biopolymeric films resulted in a slower release kinetics comparing with the control HC, which was dissolved entirely in the first hour of the experiment. On the whole, this result highlights the ability of Gel and Gel/St films to retain HC, which slow the drug release process (*i.e.*, controlled release). The release profile of HC encapsulated into the biopolymeric films exhibited a similar trend at the beginning of the experiment. Within the first 60 min, 28 ± 1% of HC was released from Gel@HC, while 78 ± 2% was released from Gel/St@HC during this time interval. After that, a faster release trend was observed for Gel/St@HC, where 50% of the encapsulated HC was released in 126 min. In contrast, 50% of the encapsulated HC was released from Gel@HC only after 180 min. Overall, after 180 min the release process slowdown for both films and a well-defined behavior of HC release kinetics was noticed. This trend is vital to the maintenance of an adequate drug concentration level. At the end of the experiment, 66 ± 3% of HC was released from Gel@HC, while 84 ± 1% was released from Gel/St@HC, respectively. As demonstrated by the previous characterization analyses, the incorporation of starch into the gelatin matrix reduces intermolecular interactions impairing the barrier effect of the film. Due to this, the amount of HC release from Gel/St@HC was higher as compared with Gel@HC. It should be mentioned that both samples maintained their flatness during the entire experiment and their dissolution was negligible.

In order to gain insights about the dependence of the HC release in the function of time, the experimental data collected from both film samples were fitted using some mathematical models [48]. Overall, these models are useful tools to evaluate the release kinetics as well as to understand the release mechanisms. Herein, the HC release data were fitted by linear regression analysis according to four different kinetic models: Zero-order (Eq. (2)), first-order (Eq. (3)), Higuchi (Eq. (4)), and Korsmeyer-Peppas (Eq. (5)) models [48,49]. The linearized form of each model is expressed as:

$$Q = k_o t \tag{2}$$

$$lnQ = ln\, Q_o - k_1 t \tag{3}$$

$$Q = k_H t^{0.5} \tag{4}$$

$$log\left(\frac{Q}{Q_\infty}\right) = log\, k_{KP} + n log t \tag{5}$$

where Q is the amount of drug released on time t, Q_∞ is the amount of

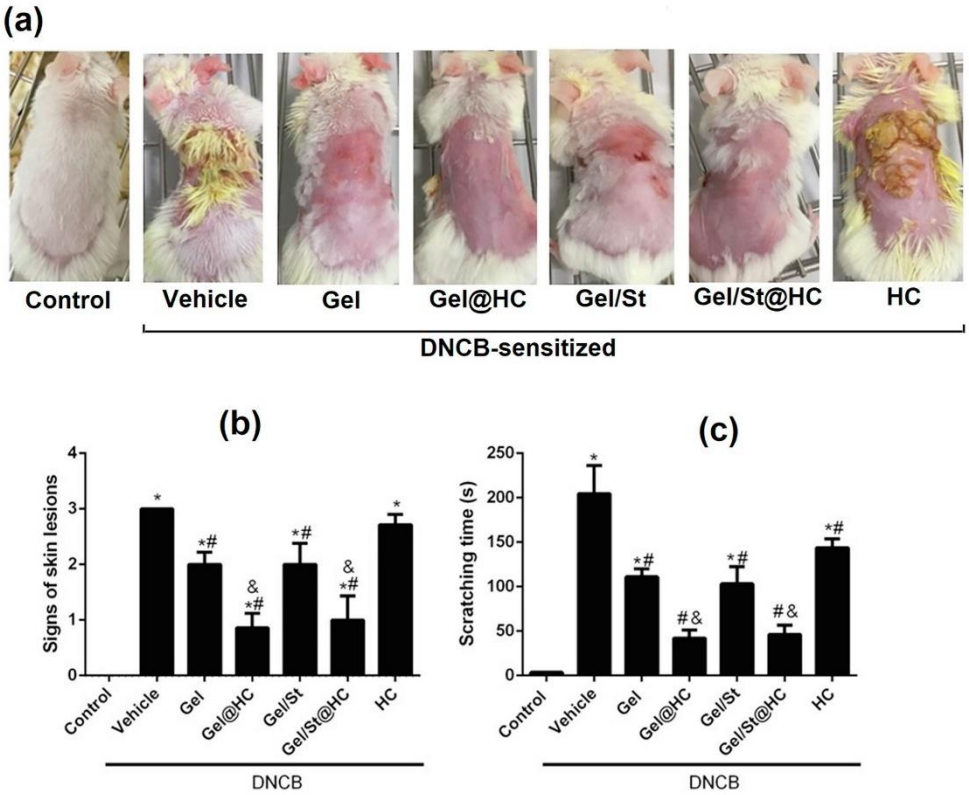

Fig. 9. The effect of topical treatment with film loaded or not with hydrocortisone (HC) (Gel, Gel@HC, Gel/St or Gel/St@HC), or HC (cream) on atopic dermatitis-like (AD-like) symptoms in mice. (a) Images of dorsal skin and ear lesions from groups of mice taken on the last day of the experiment (day 30), (b) signs of skin lesions, and (c) scratching incidence time. Data represent the mean ± S.E.M. (one-way ANOVA followed by the Newman-Keuls' test). * $p < .05$ compared with the control group, # $p < .05$ compared with the 2,4-dinitrochlorobenzene (DNCB) group, & $p < .05$ compared with the HC group.

drug released at the equilibrium. k_0 and k_1 are the zero-order and the first-order constants, while k_H is Higuchi constant. k_{KP} is the Korsmeyer-Peppas constant that incorporates structural and geometrical information of the system, and n is the exponent of release, which is related to the drug release mechanism. It is worth mentioning that the Korsmeyer-Peppas model is limited to the description of the first 60% of the release process [50]. The values of the kinetic constants and correlation coefficients (R^2) values obtained from the linear kinetic plots are given in Table 2.

Examining the values of R^2 given in Table 2, it can be inferred that the HC release data from both films are better fitted by the Korsmeyer-Peppas model (see Fig. 8b). When compared with the other kinetic models, the Korsmeyer-Peppas model resulted in the highest R^2 values ($R^2 > 0.97$) and the lowest RSS values ($RSS < 0.007$). To note, RSS is a statistical parameter that measures the discrepancy between the data and an estimation model. A small RSS indicates a tight fit of the model to the data. It is used as an optimality criterion in parameter selection and model selection [51]. So, the other models were not considered to explain the release kinetics of HC.

Korsmeyer-Peppas model derives from Fick's law of diffusion, and it is mainly used to explain the release mechanism of solutes encapsulated in polymeric matrices [50]. According to this model and considering the planar geometry of the Gel@HC and Gel/St@HC films, if the exponent release n is less 0.5, the release mechanism is driven by Fickian diffusion. On the other hand, the release mechanism is driven by anomalous diffusion when $0.5 < n < 1.0$ or by Case II transport when $n \approx 1.0$. When $n > 1.0$, the drug release is driven by the combination of both diffusional and erosive processes (non-Fickian diffusion) [50]. In this sense, the values of n calculated for Gel@HC and Gel/St@HC (0.458 and 0.400) point out that the HC release mechanism is driven by diffusion. Therefore, the biopolymeric films act as physical barriers through which the HC molecules elute out under diffusion. These data corroborate other similar studies that investigate the release of drugs/biocompounds encapsulated in gelatin-based drug delivery systems [52–54]. Overall, a diffusional release process is characterized by a usual molecular diffusion of the encapsulated drug due to a chemical potential gradient. Simultaneously, phenomenal such as the swelling of the films as water absorbs and the dissolution of the gelatin polymer matrix (polymer disentanglement and erosion), modify the diffusion release rate accordingly [53]. Interestingly, the n values calculated for

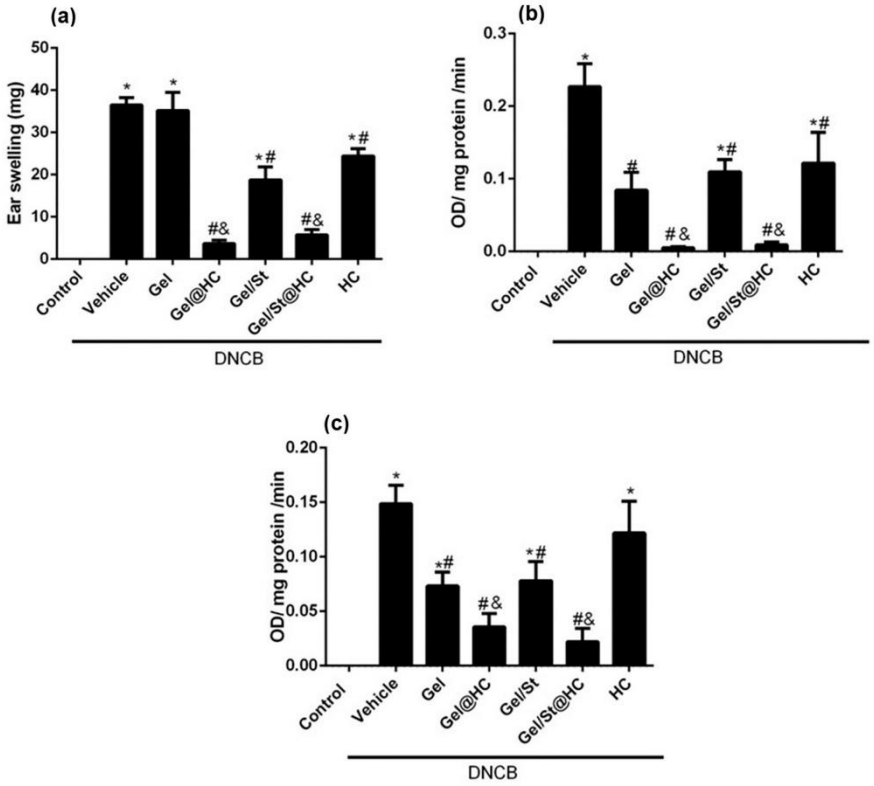

Fig. 10. The effect of topical treatment with film loaded or not with hydrocortisone (HC) (Gel, Gel@HC, Gel/St or Gel/St@HC), or hydrocortisone (HC, cream) on (a) ear swelling, (b) myeloperoxidase (MPO) activity in ears and (c) dorsal skin of mice. Data represent the mean ± S.E.M. (one-way ANOVA followed by the Newman-Keuls' test). $^{*}p < .05$ compared with the control group, $^{\#}p < .05$ compared with the 2,4-dinitrochlorobenzene (DNCB) group, $^{\&}p < .05$ compared with the HC group.

Gel@HC and Gel/St@HC did not show a marked variation with the gelatin/starch blending, suggesting that the HC release mechanism is not affected despite the change in the film composition.

3.3. In vivo assays

3.3.1. Reduction of signs of toxicity and suppressive effect of Gel, Gel/St, Gel@HC and Gel/St@HC films on the severity of injuries and scratching behavior on AD-like symptoms in mice

The high prevalence rates of toxicity after long-term topically applied steroids have encouraged us to search for new biopolymeric films as delivery vehicles for the controlled release of HC. Indeed, during the experimental protocol, 50% of the animals treated topically with 1% HC cream died. No death or sign of toxicity was observed in animals exposed to other treatments (data not shown). It is essential to mention that the mortality observed in the present study was with specific experimental conditions. No mortality study has been conducted in healthy animals. Thus, this toxicity observed after the HC cream treatment should be better studied, since there are peculiarities in the skin of humans differing from the skin of mice.

Intense pruritus and eczematous lesions are characteristic of AD, and these factors cause severe psychological stress and affect the quality of life of patients with the disease [55]. Skin affected by AD has redness and itchy responsive skin, and excessive itching can cause skin sores and fluid leakage [56]. DNCB-induced AD-like lesions were evaluated on day 30 for severity to investigate the protective effect of Gel, Gel/St, Gel@HC, and Gel/St@HC films (Fig. 9a and b) [$F_{6,42} = 16.85$, $p < .0001$]. One-way ANOVA followed by Newman-Keuls' post-hoc testing revealed that DNCB significantly increased the skin severity scores and scratching behavior when compared with the control group ($p < .0001$) (Fig. 9a, b, and c). The topical treatment with film loaded or not with HC (Gel ($p < .5$), Gel@HC ($p < .0001$), Gel/St ($p < .5$) or Gel/St@HC ($p < .0001$) reduced the severity of the skin-lesions induced by DNCB. HC-loaded films (Gel@HC ($p < .001$), Gel/St@HC ($p < .001$)) had a significant improvement as compared to 1% HC cream (reference drug). No significant difference in the severity of the skin lesions was detected after HC treatment when compared to the DNCB-induced group (vehicle) (Fig. 9b). The present study demonstrated, for the first time, that the films reduced the signs of toxicity caused by HC during treatment over a long period and the severity of injuries on AD-like symptoms in mice.

Several forms of dermatosis have pruritus, not different in AD this

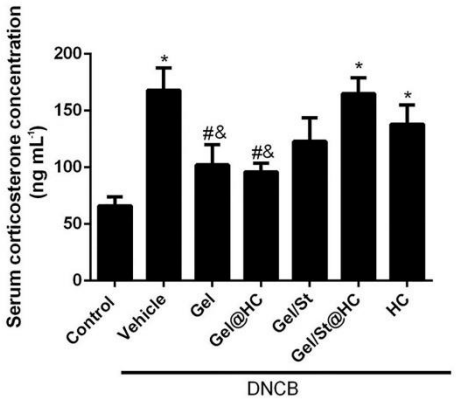

Fig. 11. The effect of topical treatment with film loaded or not with hydrocortisone (HC) (Gel, Gel@HC, Gel/St or Gel/St@HC), or HC (cream) on corticosterone levels in mice. Data represent the mean ± S.E.M. (one-way ANOVA followed by the Newman-Keuls' test). * $p < .05$ compared with the control group, # $p < .05$ compared with the 2,4-dinitrochlorobenzene (DNCB) group, & $p < .05$ compared with the HC group.

becomes an important diagnostic criterion. Then, scratching behavior is a possible approach to evaluate the anti-itching effect of treatments [57]. The effect of film treatments on scratching behavior was shown in Fig. 9c [$F_{6,42} = 18.95$, $p < .0001$]. Treatment with film loaded or not with HC (Gel ($p < .001$), Gel@HC ($p < .0001$), Gel/St ($p < .001$) or Gel/St@HC ($p < .0001$)) and HC cream ($p < .01$) protected against the increase of scratching time induced by DNCB. Treatment with film Gel@HC ($p < .001$) and Gel/St@HC ($p < .001$) were more effective in reducing the scratching time than 1% HC cream. The prolonged use of topical steroids leads to thinning of the skin and cracking, triggering itching, and worsening of the lesion [58]. An important finding in this study was that HC-loaded films did not cause the death of treated animals, unlike animals that were only treated with free HC. Besides, a significant improvement in lesions and scratching behavior was observed. These results demonstrated an improvement in systemic toxicity caused by prolonged use of HC.

3.3.2. Effect of Gel, Gel/St, Gel@HC and Gel/St@HC films on inflammatory responses of AD-like skin lesions in mice

The cause of AD is multifactorial, with the interplay between genetic predisposition and environmental factors initiating inflammation [59]. The skin affected by AD has redness, edema, erythematous papules, and abrasions characteristic of inflammatory processes [56]. The severity of inflammation can be easily evaluated by ear swelling. Fig. 10 illustrates the effects of film treatments on ear swelling in mice [$F_{6,43} = 46.28$, $p < .0001$]. One-way ANOVA, followed by Newman-Keuls' post-hoc testing, demonstrated that DNCB increased the ear swelling as compared with the control group ($p < .0001$) (Fig. 10a). Treatments with films Gel@HC ($p < .0001$), Gel/St ($p < .001$) or Gel/St@HC ($p < .0001$) and HC cream ($p < .01$) reduced the ear swelling induced by DNCB. No alteration on ear swelling after Gel treatment was observed.

The symptoms presented in this study are in line with other experimental investigations that use DNCB skin application to induce AD-like lesions in mice [22,23,60]. AD is a chronic disease characterized by lesions resulting from inflammatory processes, which will trigger edema. According to our findings, there was an increase in ear swelling of mice due to the inflammatory process triggered by the topical application of DNCB, which is also related to the migration of defense cells (polymorphonuclear leukocytes). Polymorphonuclear leukocytes can be estimated by the MPO activity determination, which is well established as a marker of tissue neutrophil influx [61]. Fig. 10b and c show the effect of topical treatment with films (Gel, Gel@HC, Gel/St or Gel/St@HC) on the ear and back skin MPO activity, respectively [$F_{6,42} = 13.15$, $p < .0001$ (ear); $F_{6,42} = 10.59$, $p < .0001$ (back skin)]. One-way ANOVA followed by Newman-Keuls' post-hoc testing revealed that DNCB significantly increased MPO activity in mice ears ($p < .0001$) and dorsal skin ($p < .0001$) when compared with the control group. The films Gel ($p < .001$), Gel@HC ($p < .0001$), Gel/St ($p < .001$), Gel/St@HC ($p < .0001$) and HC cream ($p < .001$) decreased ear MPO activity when compared with DNCB-exposed mice. These results corroborate with ear swelling for Gel@HC, Gel/St, Gel/St@HC and HC cream films. In addition, films incorporated with HC (Gel@HC ($p < .01$) and Gel/St@HC ($p < .01$)) were able to reduce ear MPO activity when compared to HC cream (reference drug). The data presented in Fig. 10c indicated that treatment with Gel ($p < .05$), Gel@HC ($p < .001$), Gel/St ($p < .05$), Gel/St@HC ($p < .001$) films partially protected against the increase in DNCB-induced MPO activity in the dorsal skin. In this case, HC-incorporated film treatments also had a significant improvement when compared with HC cream (Gel@HC ($p < .01$) and Gel/St@HC ($p < .001$)). The reference treatment (1% HC cream) was not able to reduce the MPO activity on the back of the animals. Although the treatment with the HC-loaded films reduces the systemic activity of HC, it did not cause the animals' death. Therefore, the HC-loaded films were more effective in reducing the back and ear MPO activity induced by DNCB exposure.

3.3.3. Effect of Gel, Gel/St, Gel@HC and Gel/St@HC films on biochemical parameters in AD-like skin lesions in mice

When the hypothalamus-pituitary-adrenal axis is stimulated, a substantial increase in plasma glucocorticoid concentration can be observed; therefore, it is considered an adequate parameter to evaluate stress levels of animals [62]. Corticosterone is a permanent stress marker in animals, especially rodents [63,64]. Fig. 11 shows the effect of the films Gel, Gel@HC, Gel/St, Gel/St@HC and HC cream on plasma corticosterone levels. One-way ANOVA, followed by Newman-Keuls' post-hoc testing, reveals that DNCB significantly increased mice plasma corticosterone levels ($p < .001$) when compared with the control group. Treatments with Gel ($p < .01$) and Gel@HC ($p < .01$) films reduced the plasma corticosterone levels when compared with the DNCB-induced group and also when compared with the HC cream treated group. Treatments with Gel/St and Gel/St@HC films were not able to decrease corticosterone levels when compared to the DNCB induced group. As mentioned, plasma corticosterone measurement is the most common way to analyze the stress level of laboratory animals.

Table 3
Effect of treatment with topical film loaded or not with HC (Gel, Gel@HC, Gel/St or Gel/St@HC) or HC (cream, 1%) on the plasma biochemical markers in mice.

	Control	Vehicle	Gel	Gel@HC	Gel/St	Gel/St@HC	HC
ALT	49 ± 2	50 ± 1	45 ± 3	50 ± 2	47 ± 4	50 ± 3	51 ± 1
AST	75 ± 12	78 ± 13	62 ± 16	72 ± 15	59 ± 6	83 ± 12	58 ± 20

Data are reported as mean ± standard error of the mean (SEM) of seven animals per group. AST and ALT activities were expressed as U/L. Statistical analysis was performed using a one-way analysis of variance/Newman-Keuls test. Abbreviations: AST - aspartate aminotransferase; ALT - alanine aminotransferase.

However, plasma corticosterone responds with sensitivity to stressors, especially for small animals [62,65]. Thus, these factors may have influenced the results. Another hypothesis is that corticosterone, being a synthetic corticosterone analog, could be detected as having a higher systemic absorption in some treatments, such as Gel/St@HC treatment. However, the toxic effects observed when there is greater absorption of HC was not observed in any of the film treatments. AST and ALT activities were evaluated as hepatic toxicity markers. No alteration on plasmatic AST and ALT activities were observed after the treatments (Table 3).

Based on the results obtained, we hope that the materials can be an alternative to reduce the adverse effects related to the prolonged use of corticosteroids, such as HC. A highlighted advantage of the gelatin-based film used in this study compared to other proposed technologies lies on the fact that this device consists mainly of a biocompatible and easily obtainable biopolymer that was able to provide a marked decrease in adverse effects when compared to conventional HC formulations. The biopolymeric films also exhibit a simple technology in terms of preparation and use [11]. Also, this biopolymer films provided a dressing that served as a physical barrier capable of preventing the contact of the injured skin with the external environment. However, more studies need to be carried out to elucidate better the action of these materials on DA-like skin lesions. Finally, additional studies should also be conducted in the future to address aspects related to the optimum concentration of HC in the films, skin penetration, and tissue permeation after topical application. All this information is mandatory to obtain a device potentially applicable in the AD treatment.

4. Conclusions

Herein, biopolymeric films based on gelatin and gelatin/starch were prepared and loaded with hydrocortisone (HC), a glucocorticoid, in order to overcome the adverse effects reported to the prolonged use this drug in the treatment of chronic inflammatory skin diseases, like atopic dermatitis (AD). Characterization analysis/experiments showed that the encapsulated HC did not interact with the polymeric matrices, although its presence causes changes in the mechanical and swelling properties of the prepared films. *In vitro* release experiments showed that both film types enable controlling the process. The release data were fitted adequately by the Korsmeyer-Peppas model, which indicated that the HC release mechanism is driven by anomalous diffusion for both film types. *In vivo* and *ex vivo* experiments indicated that all prepared films (loaded or not with HC) exert benign effects on the parameters tested in the DNCB-induced AD model. Overall, the HC-loaded films (Gel@HC and Gel/St@HC) showed enhanced efficiency in the treatment and attenuation of AD-like symptoms as compared to commercial HC cream (1%) (used as reference). According to our results, despite the addition of starch improves the mechanical properties of films, its contribution to the biological experiments seems to be neglected. Finally, it was demonstrated that both HC-loaded films (Gel@HC and Gel/St@HC) exerted less toxicity to the treated animals than the commercial HC cream, which ranks them as promising vehicles to minimize adverse effects associated with the prolonged use of this class of drugs.

CRediT authorship contribution statement

Guilherme T. Voss: Methodology, Formal analysis, Investigation, Writing - original draft.**Matheus S. Gularte:**Methodology, Formal analysis, Investigation.**Renata L. de Oliveira:**Methodology, Formal analysis, Investigation.**Cristiane Luchese:**Supervision, Writing - review & editing.**André R. Fajardo:**Supervision, Project administration, Writing - review & editing.**Ethel A. Wilhelm:**Supervision, Project administration, Writing - review & editing.

Declaration of competing interest

The authors declare that they have no known competing financial interests or personal relationships that could have appeared to influence the work reported in this paper.

Acknowledgments

The authors are thankful for the financial support and scholarships from CNPq (Grant. 404744/2018-4). CNPq is also acknowledged for the PQ-fellowships to A.R.F., E.A.W. and C.L. Also, this study was financed in part by the Coordenação de Aperfeiçoamento de Pessoal de Nível Superior - Brasil (CAPES) - Finance Code 001.

References

[1] L. Tizek, M.C. Schielein, F. Seifert, T. Biedermann, A. Bohner, A. Zink, Skin diseases are more common than we think: screening results of an unreferred population at the Munich Oktoberfest, J. Eur. Acad. Dermatol. 33 (2019) 1421–1428.
[2] J. Hong, B. Koo, J. Koo, The psychosocial and occupational impact of chronic skin disease, Dermatol. Ther. 21 (2008) 54–59.
[3] A. Heratizadeh, Atopic dermatitis: new evidence on the role of allergic inflammation, Curr. Opin. Allergy Clinic. Immun. 16 (2016) 458–464.
[4] V. Aoki, D. Lorenzini, R.L. Orfali, M.C. Zaniboni, Z.N.P. de Oliveira, M.C. Rivitti-Machado, R. Takaoka, M.B. Weber, T. Cestari, B. Gontijos, A.M.C. Ramoss, C.M.D. Silva, S.D.P. Cestari, S. Souto-Mayor, F.R. Carneiro, A.M.M. de Cerqueira, C. Laczynski, M.C. Pires, Consensus on the therapeutic management of atopic dermatitis Brazilian Society of Dermatology, An. Bras. Dermatol. 94 (2019) S67–S75.
[5] A. Abraham, G. Roga, Topical steroid-damaged skin, Indian J. Dermat. 59 (2014) 456–459.
[6] T.S. Nagesh, A. Akhilesh, Topical steroid awareness and abuse: a prospective study among dermatology outpatients, Indian J. Dermat. 61 (2016) 618–621.
[7] H. Schacke, W.D. Docke, K. Asadullah, Mechanisms involved in the side effects of glucocorticoids, Pharmacol. Ther. 96 (2002) 23–43.
[8] L. Kolbe, A.M. Kligman, V. Schreiner, T. Stoudemayer, Corticosteroid-induced atrophy and barrier impairment measured by non-invasive methods in human skin, Skin Res. Technol. 7 (2001) 73–77.
[9] R.A. Dehkharghani, M. Hosseinzadeh, F. Nezafatdoost, J. Jahangiri, Application of methodological analysis for hydrocortisone nanocapsulation in biodegradable polyester and MTT assay, Polym. Sci. A 60 (2018) 770–776.
[10] A.H. Azandaryani, K. Derakhshandeh, E. Arkan, Electrospun nanobandage for hydrocortisone topical delivery as an antipsoriasis candidate, Int. J. Polym. Mater. Polym. Biomater. 67 (2018) 677–685.
[11] S. Young, M. Wong, Y. Tabata, A.G. Mikos, Gelatin as a delivery vehicle for the controlled release of bioactive molecules, J. Control. Release 109 (2005) 256–274.
[12] F. Laffleur, B. Strasdat, Gelatin-based formulations for dermal application, Eur. Polym. J. 118 (2019) 542–550.
[13] A.M. Youssef, S.M. El-Sayed, Bionanocomposites materials for food packaging applications: concepts and future outlook, Carbohydr. Polym. 193 (2018) 19–27.
[14] Q. Chen, H.J. Yu, L. Wang, Z. ul Abdin, Y.S. Chen, J.H. Wang, W.D. Zhou, X.P. Yang, R.U. Khan, H.T. Zhang, X. Chen, Recent progress in chemical modification of starch and its applications, RSC Adv. 5 (2015) 67459–67474.
[15] R. Colussi, V.Z. Pinto, S.L.M. El Halal, N.L. Vanier, F.A. Villanova, R.M.E. Silva, E.D. Zavareze, A.R.G. Dias, Structural, morphological, and physicochemical properties of acetylated high-, medium-, and low-amylose rice starches, Carbohydr. Polym. 103 (2014) 405–413.
[16] F.M. Fakhouri, S.M. Martelli, T. Caon, J.I. Velasco, L.H.I. Mei, Edible films and coatings based on starch/gelatin: film properties and effect of coatings on quality of refrigerated red crimson grapes, Postharvest Biol. Technol. 109 (2015) 57–64.
[17] R. Kumar, G. Ghoshal, M. Goyal, Synthesis and functional properties of gelatin/CA-starch composite film: excellent food packaging material, J. Food Sci. Technol. 5 (2019) 1954–1965.
[18] C. Andreuccetti, R.A. Carvalho, T. Galicia-Garcia, F. Martinez-Bustos, R. Gonzalez-Nunez, C.R.F. Grosso, Functional properties of gelatin-based films containing Yucca schidigera extract produced via casting, extrusion and blown extrusion processes: a preliminary study, J. Food Eng. 113 (2012) 33–40.
[19] M. Tabari, Investigation of carboxymethyl cellulose (CMC) on mechanical properties of cold water fish gelatin biodegradable edible films, Foods 6 (2017) 41–48.
[20] J. Said, C.C. Dodoo, M. Walker, D. Parsons, P. Stapleton, A.E. Beezer, S. Gaisford, An in vitro test of the efficacy of silver-containing wound dressings against Staphylococcus aureus and Pseudomonas aeruginosa in simulated wound fluid, Int. J. Pharm. 462 (2014) 123–128.
[21] C.C. Chan, C.J. Liou, P.Y. Xu, J.J. Shen, M.L. Kuo, W.B. Len, L.E. Chang, W.C. Huang, Effect of dehydroepiandrosterone on atopic dermatitis-like skin lesions induced by 1-chloro-2,4-dinitrobenzene in mouse, J. Dermat. Sci. 72 (2013) 149–157.
[22] G. Park, M.S. Oh, Inhibitory effects of Juglans mandshurica leaf on allergic dermatitis-like skin lesions-induced by 2,4-dinitrochlorobenzene in mice, Experim. Toxic. Pathol. 66 (2014) 97–101.

[23] H. Kim, J.R. Kim, H. Kang, J. Choi, H. Yang, P. Lee, J. Kim, K.W. Lee, 7,8,4 '-Trihydroxyisoflavone attenuates DNCB-induced atopic dermatitis-like symptoms in NC/Nga mice, PLoS One 9 (2014) e104938.
[24] K. Suzuki, H. Ota, S. Sasagawa, T. Sakatani, T. Fujikura, Assay-method for myeloperoxidase in human polymorphonuclear leukocytes, Anal. Biochem. 132 (1983) 345–352.
[25] M.M. Bradford, A rapid and sensitive method for the quantification of microgram quantitites of protein utilizing the principles of protein-dye binding, Anal. Biochem. 72 (1–6) (1976).
[26] N. Zenker, D.E. Bernstein, The estimation of sam amounts of corticosterone in rat pasma, J. Bioinorg. Chem. 231 (1958) 695–701.
[27] K. Ullah, S.A. Khan, G. Murtaza, M. Sohail, Azizullah, A. Manan, A. Afzal, Gelatin-based hydrogels as potential biomaterials for colonic delivery of oxaliplatin, Int. J. Pharm. 556 (2019) 236–245.
[28] A.G.B. Pereira, A.R. Fajardo, S. Nocchi, C.V. Nakamura, A.F. Rubira, E.C. Muniz, Starch-based microspheres for sustained-release of curcumin: preparation and cytotoxic effect on tumor cells, Carbohydr. Polym. 98 (2013) 711–720.
[29] Z. Hussain, H. Katas, M. Amin, E. Kumolosasi, F. Buang, S. Sahudin, Self-assembled polymeric nanoparticles for percutaneous co-delivery of hydrocortisone/hydroxytyrosol: an ex vivo and in vivo study using an NC/Nga mouse model, Int. J. Pharm. 444 (2013) 109–119.
[30] E. Basiak, A. Lenart, F. Debeaufort, How glycerol and water contents affect the structural and functional properties of starch-based edible films, Polymers 10 (2018) 412–418.
[31] K. Wang, W.H. Wang, R. Ye, J.D. Xiao, Y.W. Liu, J.S. Ding, S.J. Zhang, A.J. Liu, Mechanical and barrier properties of maize starch - gelatin composite films: effects of amylose content, J. Sci. Food Agric. 97 (2017) 3613–3622.
[32] N.Z. Zhang, X.X. Liu, L. Yu, R. Shanks, E. Petinaks, H.S. Liu, Phase composition and interface of starch-gelatin blends studied by synchrotron FTIR micro-spectroscopy, Carbohydr. Polym. 95 (2013) 649–653.
[33] O. Adi-Dako, K. Ofori-Kwakye, M. El Boakye-Gyasi, S.O. Bekoe, S. Okyem, In vitro evaluation of cocoa pod husk pectin as a carrier for chronodelivery of hydrocortisone intended for adrenal insufficiency, J. Drug Deliv. (2017) 1–10.
[34] A. Celebioglu, T. Uyar, Hydrocortisone/cyclodextrin complex electrospun nanofibers for a fast-dissolving oral drug delivery system, RSC Med. Chem. 11 (2020) 245–258.
[35] E.A. Soliman, M. Furuta, Influence of phase behavior and miscibility on mechanical, thermal and micro-structure of soluble starch-gelatin thermoplastic biodegradable blend films, Food Nutr. Sci. 5 (2014) 1040–1055.
[36] M.S. Hoque, S. Benjakul, T. Prodpran, Effects of partial hydrolysis and plasticizer content on the properties of film from cuttlefish (Sepia pharaonis) skin gelatin, Food Hydrocoll. 25 (2011) 82–90.
[37] R.F.N. Quadrado, A.R. Fajardo, Microparticles based on carboxymethyl starch/chitosan polyelectrolyte complex as vehicles for drug delivery systems, Arab. J. Chem. 13 (2020) 2183–2194.
[38] A. Podshivalov, M. Zakharova, E. Glazacheva, M. Uspenskaya, Gelatin/potato starch edible biocomposite films: correlation between morphology and physical properties, Carbohydr. Polym. 157 (2017) 1162–1172.
[39] A.A. Al-Hassan, M.H. Norziah, Starch-gelatin edible films: water vapor permeability and mechanical properties as affected by plasticizers, Food Hydrocoll. 26 (2012) 108–117.
[40] V.A.D. García, J.G. Borges, V.B.V. Maciel, M.R. Mazalli, J.D. Lapa-Guimaraes, F.M. Vanin, R.A. de Carvalho, Gelatin/starch orally disintegrating films as a promising system for vitamin C delivery, Food Hydrocoll. 79 (2018) 127–135.
[41] S. Karki, H. Kim, S.J. Na, D. Shin, K. Jo, J. Lee, Thin films as an emerging platform for drug delivery, Asian J. Pharm. Sci. 11 (2016) 559–574.
[42] W. Tongdeesoontorn, L.J. Mauer, S. Wongruong, P. Sriburi, P. Rachtanapun, Mechanical and physical properties of cassava starch-gelatin composite films, Int. J. Polym. Mater. 61 (2012) 778–792.
[43] I. Arvanitoyannis, E. Psomiadou, A. Nakayama, S. Aiba, N. Yamamoto, Edible films made from gelatin, soluble starch and polyols, Food Chem. 60 (1997) 593–604.
[44] N. Suderman, M.I.N. Isa, N.M. Sarbon, The effect of plasticizers on the functional properties of biodegradable gelatin-based film: a review, Food Biosci. 24 (2018) 111–119.
[45] I. Negut, V. Grumezescu, A.M. Grumezescu, Treatment strategies for infected wounds, Molecules 23 (2018) E2392.
[46] T.T.D. Tran, P.H.L. Tran, Controlled release film forming systems in drug delivery: the potential for efficient drug delivery, Pharmaceutics 11 (2019) 290–297.
[47] L.F. Santos, I.J. Correia, A.S. Silva, J.F. Mano, Biomaterials for drug delivery patches, Eur. J. Pharm. Sci. 118 (2018) 49–66.
[48] N.A. Peppas, B. Narasimhan, Mathematical models in drug delivery: how modeling has shaped the way we design new drug delivery systems, J. Control. Release 190 (2014) 75–81.
[49] Y. Fu, W.J. Kao, Drug release kinetics and transport mechanisms of non-degradable and degradable polymeric delivery systems, Expert Opin. Drug Deliv. 7 (2010) 429–444.
[50] R.W. Korsmeyer, R. Gurny, E. Doelker, P. Buri, N.A. Peppas, Mechanisms of solute release from porous hydrophilic polymers, Int. J. Pharm. 15 (1983) 25–35.
[51] K. Ghosal, A. Chandra, R. Rajabalaya, S. Chakraborty, A. Nanda, Mathematical modeling of drug release profiles for modified hydrophobic HPMC based gels, Pharmazie 67 (2012) 147–155.
[52] J.S. Gonzalez, C. Mijangos, R. Hernandez, Polysaccharide coating of gelatin gels for controlled BSA release, Polymers 11 (2019) E702.
[53] I. Dammak, R.A. de Carvalho, C.S.F. Trindade, R.V. Lourenco, P.J.A. Sobral, Properties of active gelatin films incorporated with rutin-loaded nanoemulsions, Int. J. Biol. Macromol. 98 (2017) 39–49.
[54] Z.M. Barzoki, Z. Emam-Djomeh, E. Mortazavian, A.A. Moosavi-Movahedi, M.R. Tehrani, Formulation, in vitro evaluation and kinetic analysis of chitosan-gelatin bilayer muco-adhesive buccal patches of insulin nanoparticles, J. Microencapsul. 33 (2016) 613–624.
[55] Y.X. Li, L. Chen, Y.H. Du, D.C. Huang, H.L. Han, Z.F. Dong, Fluoxetine ameliorates atopic dermatitis- like skin lesions in BALB/c mice through reducing psychological stress and inflammatory response, Front. Pharmacol. 7 (2016) 1–9.
[56] Y. Tokura, Extrinsic and intrinsic types of atopic dermatitis, J. Dermat. Sci. 58 (2010) 1–7.
[57] G. Park, H.G. Kim, S. Lim, W. Lee, Y. Sim, M.S. Oh, Coriander alleviates 2,4-dinitrochlorobenzene-induced contact dermatitis-like skin lesions in mice, J. Med. Food 17 (2014) 862–868.
[58] A.U. Tan, M.E. Gonzalez, Management of severe atopic dermatitis in children, J. Drug Dermat. 11 (2012) 1158–1165.
[59] M. Udompataikul, D. Limpa-o-Vart, Comparative trial of 5% dexpanthenol in water-in-oil formulation with 1% hydrocortisone ointment in the treatment of childhood atopic dermatitis: a pilot study, J. Drug Dermat. 11 (2012) 366–374.
[60] G.T. Voss, R.L. Oliveira, J.F. de Souza, L.F.B. Duarte, A.R. Fajardo, D. Alves, C. Luchese, E.A. Wilhelm, Therapeutic and technological potential of 7-chloro-4-phenylselanyl quinoline for the treatment of atopic dermatitis-like skin lesions in mice, Mater. Sci. Eng. C 84 (2018) 90–98.
[61] D. Odobasic, A.R. Kitching, S.R. Holdsworth, Neutrophil-mediated regulation of innate and adaptive immunity: the role of myeloperoxidase, J Immunol Res 2016 (2016) 1–11.
[62] C. Touma, N. Sachser, E. Mostl, R. Palme, Effects of sex and time of day on metabolism and excretion of corticosterone in urine and feces of mice, Gen. Comparat. Endocr. 130 (2003) 267–278.
[63] K.J. Brown, N.E. Grunberg, Effects of housing on male and female rats - crowding stresses males but calms females, Physiol. Behav. 58 (1995) 1085–1089.
[64] S.S. Arndt, M.C. Laarakker, H.A. van Lith, F.J. van der Staay, E. Gieling, A.R. Salomons, J. van't Klooster, F. Ohl, Individual housing of mice - impact on behaviour and stress responses, Physiol. Behav. 97 (2009) 385–393.
[65] C. Hunt, C. Hambly, Faecal corticosterone concentrations indicate that separately housed male mice are not more stressed than group housed males, Physiol. Behav. 87 (2006) 519–526.

4.1 Manuscrito

Evaluation of gelatin-alginate films containing 1,4-anhydro-4-seleno-*D*-talitol (SeTal) in the treatment of atopic dermatitis-like skin lesions in mice

Manuscrito submetido para Biomaterials Advances

Treating atopic-dermatitis-like skin lesions in mice with gelatin-alginate films containing 1,4-anhydro-4-seleno-D-talitol (SeTal)

Guilherme T. Voss[a], Michael J. Davies[c,d], Carl H. Schiesser[d], Renata L. de Oliveira[a], Andresa B. Nornberg[b], Victória R. Soares[b], Angelita M. Barcellos[b], Cristiane Luchese[a], André R. Fajardo[b*], and Ethel A. Wilhelm[a*]

[a] *Laboratório de Pesquisa em Farmacologia Bioquímica (LaFarBio), Universidade Federal de Pelotas (UFPel), Campus Capão do Leão, 96010-900, Pelotas-RS, Brazil.*

[b] *Laboratório de Tecnologia e Desenvolvimento de Compósitos e Materiais Poliméricos (LaCoPol), Universidade Federal de Pelotas (UFPel), Campus Capão do Leão s/n, 96010-900, Pelotas-RS, Brazil.*

[c] *Department of Biomedical Sciences, Faculty of Health and Medical Sciences, University of Copenhagen, Blegdamsvej 3, 2200, Copenhagen, Denmark.*

[d] *Seleno Therapeutics Pty. Ltd., Brighton East, VIC, 3187, Australia.*

*__Correspondence should be sent to:__

Ethel A. Wilhelm (ORCID 0000-0002-2875-9962) - e-mail: ethelwilhelm@yahoo.com.br

Programa de Pós-graduação em Bioquímica e Bioprospecção (PPGBBio), Centro de Ciências Químicas, Farmacêuticas e de Alimentos, Universidade Federal de Pelotas (UFPel), Campus Capão do Leão s/n, 96010-900, Pelotas-RS, Brazil; Phone: 55-53-32757360.

André R. Fajardo (ORCID 0000-0001-5362-6478) - e-mail: andre.fajardo@pq.cnpq.br

Laboratório de Tecnologia e Desenvolvimento de Compósitos e Materiais Poliméricos (LaCoPol), Universidade Federal de Pelotas (UFPel), Campus Capão do Leão s/n, 96010-900, Pelotas-RS, Brazil; Phone: 55-53-32757360.

Abstract

New compounds and pharmacological strategies offer alternatives for treating chronic skin diseases, such as atopic dermatitis (AD). Here, we investigated encapsulating 1,4-anhydro-4-seleno-D-talitol (SeTal), a bioactive seleno-organic compound, in gelatin and alginate (Gel-Alg) polymeric films as a strategy for improving the treatment and attenuation of AD-like symptoms in a mouse model. Hydrocortisone (HC) or vitamin C (VitC) were encapsulated with SeTal in the Gel-Alg films, and their synergy was investigated. All the prepared film samples were able to encapsulate and release SeTal in a controlled manner. In addition, appreciable film handleability facilitates SeTal administration. A series of *in-vivo*/*ex-vivo* experiments were performed using mice sensitized with dinitrochlorobenzene (DNCB), which induces AD-like symptoms. Long-term topical application of the loaded Gel-Alg films attenuated disease symptoms and pruritus, with suppression of the levels of inflammatory markers, oxidative damage, and the skin lesions associated with AD. Moreover, the loaded films showed superior efficiency in attenuating the analyzed symptoms when compared to hydrocortisone (HC) cream, a traditional AD-treatment, and decreased the inherent drawbacks of this compound. In short, encapsulating SeTal (by itself or with HC or VitC) in biopolymeric films provides a promising alternative for the long-term treatment of AD-type skin diseases.

Keywords: Skin diseases; 1,4-anhydro-4-seleno-D-talitol; hydrocortisone; vitamin C; biomaterials; drug delivery; selenium.

1. Introduction

Atopic dermatitis (AD) is a well-known chronic inflammatory skin disease in which the patient experiences intense itching and recurrent eczematous lesions. Whilst previously regarded as a childhood disorder, AD is now recognized to be a lifelong affliction with various clinical manifestations and expressivities, in which defects of the epidermal barrier play central roles [1]. Currently, AD treatments focus on restoring epidermal barrier function, with first-line therapies including topical corticosteroids that are used as anti-inflammatory and antipruritic agents in acute flare-ups. However, growing concerns regarding the use of this drug class among patients and medical professionals is resulting in decreased treatment compliance, which worsens AD control and patient welfare [2]. Accordingly, new agents are sought for the treatment and attenuation of AD symptoms as alternatives to corticosteroids.

In a previous study, we demonstrated the potential of SeTal (1,4-anhydro-4-seleno-*D*-talitol) to reduce inflammatory mediators associated with AD-type skin lesions induced by 2,4-dinitrochlorobenzene (DNCB) in mice [3]. Importantly, it should be mentioned that SeTal is a patented compound for skin tissue repair applications in addition to its powerful antioxidant effect [4]. To broaden our understanding of this compound and gain insight into its potential, herein we investigated the use of biopolymeric films composed of gelatin (Gel) and sodium alginate (Alg) loaded with SeTal as a local treatment for AD-like lesions. The use of these films as vehicles for the controlled release of SeTal is advantageous because it facilitates administration, increases compound bioavailability, and enables long-term treatment [5]. Furthermore, encapsulating SeTal in a Gel-Alg film overcomes problems related to the fast release and loss of SeTal when applied to exudative lesions, due to the very high water solubility of this compound [6].

The film constituents (Gel and Alg) were chosen as they exhibit attractive properties for preparing biomaterials for topical delivery of drugs to the skin. Gel is a water-soluble biopolymer derived from collagen and is widely used in skin adhesives due to its attractive properties as a biocompatible, biodegradable, non-immunogenic, and naturally abundant material [7–9]. Blending Gel with Alg followed by crosslinking with low amounts of a carbodiimide allows the generation of materials with enhanced stability, mechanical and bioadhesive properties to be prepared [9]. Alg is a natural linear polysaccharide composed of 1,4-β-*D*-mannuronic (M) and α-*L*-guluronic (G) acid units, is commercially extracted from brown algae, and has recognized biological properties [10]. In a similar manner to Gel, Alg is also biocompatible, biodegradable, and non-toxic, which has prompted its use in a number of medical and pharmaceutical applications [11].

Here, we also examined potential additive effects of SeTal and other pharmacological agents used to treat AD symptoms, by also evaluating Gel-Alg films containing SeTal together with hydrocortisone (HC) or vitamin C (VitC). As mentioned above, HC has been used for years to treat and reduce the most common clinical dermatosis symptoms [12]. Despite concerns regarding the topical use of this corticosteroid, encapsulation of HC in a polymeric delivery device is an efficient alternative for controlling its systemic absorption, thereby limiting adverse side effects [13]. On the other hand, VitC is a powerful natural antioxidant that plays a pivotal role in various structural and functional skin processes [14]. VitC deficiency is known to trigger or aggravate the occurrence and development of some skin diseases, including AD [15]. Moreover, lower levels of this vitamin are observed in the plasma of patients afflicted by AD [10]. Wang et al. have reported that VitC can be used as an adjuvant to treat a variety of dermatoses; however, oral administration still can cause symmetrical AD [16]. Therefore, encapsulating VitC in a Gel-Alg film offers an alternative route of

administration. In this study, all prepared films were extensively characterized using a variety of analytic techniques, with systematic *in-vitro*/*in-vivo/ex-vivo* experiments used to evaluate their performance in the treatment and attenuation of AD-like symptoms in an animal model.

2. Experimental section

2.1. Materials

Gelatin (Gel, type B from bovine skin), alginic acid sodium salt (Alg) from brown algae with medium viscosity (molecular mass: 80–120 kDa; M/G units ratio: ~1.56), *N*-(3-dimethylaminopropyl)-*N'*-ethylcarbodiimide hydrochloride (EDC) and DNCB were purchased from Sigma–Aldrich (USA), glycerol (>99%) was purchased from Synth (Brazil), and VitC (L-ascorbic acid, analytical grade) was obtained from Sinopharm (China). Hydrocortisone (HC, purity >98%) was obtained from Gemini (Brazil), and a commercial topical HC cream (1 w/w%, Bayer®) was purchased from a local drugstore (Pelotas, Brazil). Each gram of this cream contains 11.2 mg of HC acetate and excipients (macrogol stearate 400, stearyl alcohol, liquid petrolatum, white petrolatum, edetate disodium, carbomer 980, sodium hydroxide, methylparaben, propylparaben, and purified water). SeTal was prepared according to our previous report [4]. All other chemicals were of analytical grade.

2.2. Preparation of Gel-Alg films

The films (loaded or unloaded) were prepared by a conventional solvent casting method, with the composition of each sample detailed in Table 1. Experimentally, Gel was first solubilized in distilled water (50 mL) with magnetic stirring at 60 °C for 1 h, after which Alg was added to this solution. The Gel:Alg mass ratio was fixed at 10:1

based on previous experiments. After homogenization (stirring for 30 min), glycerol was added to the Gel/Alg solution, with stirring continued at 30 °C for another 30 min. EDC was then added to the solution while being vigorously stirred for 15 min prior to being poured into a Petri dish (polystyrene, 80 × 15 mm, standard round). Solvent casting followed by heating in an oven at 40 °C for 24 h led to a film, which was peeled from the Petri dish and stored in a dissector.

The film samples loaded with SeTal (Figure S1), SeTal/HC, and SeTal/VitC were similarly prepared, with pre-determined amounts of the drug compounds added to the filmogenic solution with magnetic stirring for 30 min prior to the solvent-casting step. Based on previous experiments (not reported), the amounts of these compounds were adjusted to around 1 w/w% based on the total mass of biopolymer.

Table 1. Composition of the prepared Gel-Alg films

Film	Gel (mg)	Alg (mg)	Glycerol (μL)[a]	EDC (mg)	SeTal (mg)	HC (mg)	VitC (mg)
Gel-Alg	900	90	100	5	-	-	-
Gel-Alg/SeTal	900	90	100	5	10	-	-
Gel-Alg/SeTal/HC	900	90	100	5	10	10	-
Gel-Alg/SeTal/VitC	900	90	100	5	10	-	10

[a] This volume refers to 126 μg of glycerol.

2.3. Analytical characterization of films

Fourier-transform infrared (FTIR) spectra were recorded on a Shimadzu IR Affinity-1 spectrometer (Japan) over the 3800–400 cm^{-1} spectral range with a 4 cm^{-1} resolution (64 scans). Samples were powdered (Anton Parr BM500 ball mill, USA) and mixed with KBr and then pressed into disks. Powder X-ray diffraction (XRD) patterns were acquired in the 10–70º 2θ range at 0.05º s^{-1} on a Siemens D500 diffractometer

(Germany) equipped with a Cu-Kα radiation source. The accelerator current and voltage were set to 20 mA and 30 kV, respectively. Thermogravimetric analysis (TGA) was performed using a Shimadzu DTG60 Analyzer (Japan) operating in the 25–600 °C temperature range at 10 °C min^{-1}. Sample were analyzed under 20 mL min^{-1} flowing nitrogen. Mechanical properties were examined using a Stable Microsystems TA.XT2 texturometer (UK) operating in tensile mode according to the ASTM D882-12 standard [17]. Film samples were cut into rectangular shapes (80 × 25 mm) and stored in a 50% relative humidity atmosphere prior to tensile testing.

2.4. Swelling experiments

To evaluate the abilities of the prepared films to absorb physiological fluids, swelling experiments were performed in simulated wound fluid (SWF), which was prepared according to Voss et al. [13]. Dry samples (100 mg) were placed in vials filled with 50 mL of SWF, which were kept under stirring (50 rpm) during the experiment. The swollen samples were recovered from the vials at the desired time, blotted with filter paper to remove the excess liquid and then reweighed. The swelling ratio (SR) at each time was calculated according to Equation (1):

$$SR\ (\%) = \frac{(m_s - m_d)}{m_d} \text{ x } 100 \quad (1)$$

where m_s and m_d refer to the mass of the samples in their swollen and dry states, respectively. These experiments were performed in triplicate.

2.5. In-vitro release experiments

Release experiments were performed using a Franz diffusion cell apparatus. A film sample (100 mg) was directly placed on the surface of a regenerate cellulose dialysis membrane (Mwco: 12,000–14,000; effective release area: 1.5 cm^2), which was placed between the donor and receptor compartments of the Franz diffusion cell. SWF (pH 7.4, 12 mL) was used as release medium, and the temperature of the cell was maintained at ~37 °C throughout the experiment. The release medium was gently magnetically stirred. Aliquots (3 mL) were withdrawn at the indicated time points and analyzed using a PerkinElmer Lambda 35 UV-Vis spectrophotometer (USA) in the 200–700 nm wavelength range. The medium in the receptor compartment of the Franz cell was replaced with an equal amount of fresh SWF. Absorbance data were converted into concentrations using a previously constructed calibration curves. All *in-vitro* experiments were performed in triplicate.

2.6. In-vivo and ex-vivo assays

2.6.1. Animals

Experiments were conducted using BALB/c female mice (6–8 weeks old). The animals were exposed to a 12 h light/dark cycle (with light from 7 a.m. to 7 p.m.) at 22 ± 1 °C and had free access to food and water. Animal experiments were approved by the Committee for Care and Use of Laboratory Animals of the Universidade Federal de Pelotas (Brazil) (CEEA 4294-2015) according the National Institutes of Health guidelines for the care and use of laboratory animals (NIH Publications No. 8023, revised 1978). The minimum number of animals required to demonstrate the consistent effects of the drug treatment regime was used, and all efforts were taken to make ensure their comfort.

2.6.2. Experimental protocol

We used the pre-clinical AD model with DNCB as an inducer of AD-type skin lesions as reported by Chan et al. [18] (Figure 1). The dorsal region of each mouse was shaved and 200 µL of 0.5% (v/v) DNCB in 3:1 (v/v) acetone/olive oil was applied on days 1 to 3 of the experimental protocol in the initial sensitization phase. Each mouse was further challenged with 200 µL of 1% (v/v) DNCB on its back and 20 µL on its right ear on days 14, 17, 20, 23, 26, and 29, as shown in Figure 1. The animals were divided randomly into seven experimental groups each of 7 animals. Normal control mice (control group) were sensitized and challenged with acetone/olive oil (3:1) and received no treatment. Sensitized control mice (DNCB group) were sensitized and challenged with DNCB and received no treatment. Experimental mice were sensitized and challenged with DNCB and were topically treated with films (Gel-Alg, Gel-Alg/SeTal, Gel-Alg/SeTal/HC or Gel-Alg/SeTal/HC/VitC) or HC (cream). The lesions on the back of each mouse was treated every 3 d with loaded or non-loaded film (Gel-Alg, Gel-Alg/SeTal, Gel-Alg/SeTal/HC, or Gel-Alg/SeTal/HC/VitC) or HC (cream), on days 14, 17, 20, 23, 26, and 29. The mice were subjected to behavioral testing on the last day of the experimental protocol (day 30), after which the animals were euthanized and their backs, ears, and spleens were removed for further analysis.

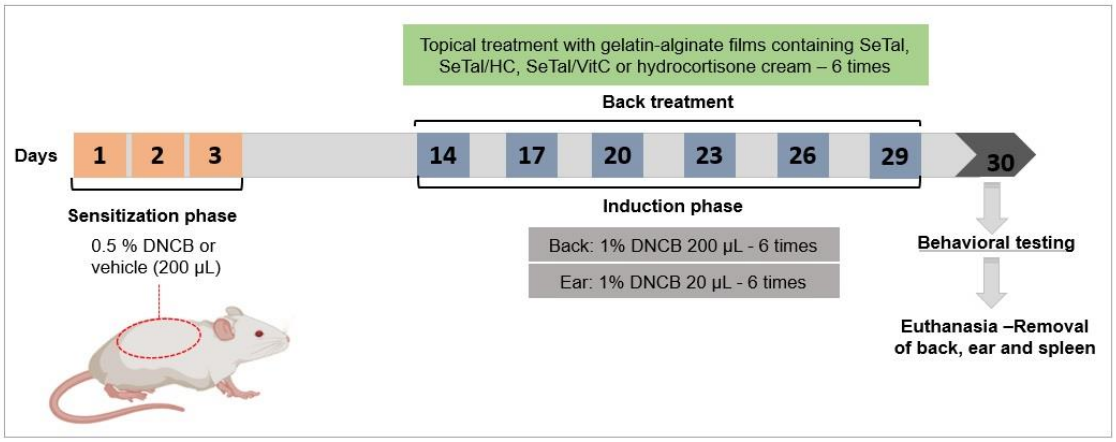

Figure 1. Summary of the experimental protocol used to develop AD-like skin lesions in DNCB-sensitized mice.

2.6.3. Clinical skin severity scores

The lesions on dorsal-skin samples were evaluated and the severity scores were determined by analyzing photographs acquired on the last day of the experiment. Five skin-lesion signs were assessed: pruritus/itching, erythema/hemorrhaging, edema, excoriation/erosion, and scaling/dryness. Each of these symptoms were graded as follows: 0 (no symptoms), 1 (mild), 2 (moderate), and 3 (severe), according to Park et al. [19].

2.6.4. Scratching behavior

Scratching behavior was evaluated on day 30 because pruritus is the main and most-important symptom of AD, with the amount of time that each animal spent rubbing their nose, ears and dorsal skin with their hind legs measured and recorded over a 20 min period, according to Kim et al. [20].

2.6.5. Spleen index

Changes in spleen mass and length were measured using an analytical scale (AUY220- SHIMADZU) and a digital caliper, respectively.

2.6.6. Inflammatory parameters

2.6.6.1. Ear swelling

Following the scratching-behavior assessment (day 30) the thickness of the right ear (central portion of the lobe) was evaluated using a digital caliper. Subsequently, mice were euthanized, both ears were severed at the base and the mass differences between the

control (left) and the DNCB-sensitized ears (right) were determined using an analytical balance to determine the extent of swelling. The tissues were then used to quantify myeloperoxidase (MPO) activity.

2.6.6.2. Determination of MPO enzymatic activity

The activity of MPO was evaluated as described by Suzuki et al. [21] with some modifications. Back and ear tissues were minced, pooled, and homogenized in phosphate-buffered saline (PBS) (20 mmol L^{-1}, pH 7.4) containing ethylenediaminetetraacetic acid (0.1 mmol L^{-1}) (EDTA). The homogenates were centrifuged at 900 *g* for 10 min at 4 °C and the pellet was discarded. The supernatant (fraction S1) was then re-centrifuged at 24,000 *g* at 4 °C for 15 min to yield the final pellet (P2), which was re-suspended in potassium phosphate buffer (50 mmol L^{-1}, pH 6.0) containing hexadecyltrimethylammonium bromide (0.5% w/v). Samples were then subjected to three freeze-thaw cycles before assaying MPO activity by adding an aliquot of resuspended P2 (100 µL) to medium containing the resuspension medium and *N,N,N',N'*-tetramethylbenzidine (1.5 mmol L^{-1}). MPO kinetic activity was initiated by the addition of H_2O_2 (0.01 v/v%), and the absorption measured at 655 nm and 37 °C, with the data expressed as optical density (OD)/mg protein/min. Protein concentrations were determined by the Bradford method [22] using bovine serum albumin (1 g L^{-1}) as the standard.

2.6.7. Nitrate and nitrite (NOx) levels

NOx levels were determined according to Miranda et al. [23]. Back skin samples were used to determine nitrate and nitrite content, an indicator of nitric oxide (NO·) production. The NOx content was determined in a medium containing 2 w/v% VCl_3 (in

5 v/v% HCl), 0.1 w/v% *N*-(1-naphthyl) ethylenediamine dihydrochloride and 2 w/v % sulfanilamide (in 5 v/v% HCl). After incubation at 37 °C, nitrite levels were determined spectrophotometrically at 540 nm, based on the reduction of nitrate to nitrite by VCl_3. Tissue nitrate/nitrite levels are expressed in nmol NOx/mg tissue.

2.6.8. Histological analysis

Histological analysis was used to evaluate tissue changes and cell migration into the affected areas. Skin sections from the backs of mice were collected and fixed in a 10% buffered formalin solution for 24 h. All fragments were cut to 5 μm and stained with hematoxylin and eosin (H.E.) and examined under an optical microscope. The treatment groups were compared to the control group, with assessment of intraepidermal pustules, crust, inflammatory infiltrate in the superficial dermis, deep dermis and subcutaneous inflammatory infiltrate. The extent of these events was assessed qualitatively as: discrete (low), moderate (medium), and accentuated (high).

2.7. Statistical analysis

Data normality was evaluated using the D'Agostino and Pearson omnibus normality test. The data were analyzed by one-way analysis of variance (ANOVA) followed by Tukey's test. All analyses were performed using GraphPad software (San Diego, CA, USA). Data are expressed as means ± standard errors of the means (SEMs), with $p < 0.05$ considered to be statistically significant.

3. Results and discussion

3.1. Characterization of the Gel-Alg films

The chemical nature of the films was studied by FTIR spectroscopy with representative spectra presented in Figure 2a. The spectra of the Gel-Alg films exhibited major bands typically associated with the biopolymers used to prepare it (Figure S2), with those from Gel dominating, as it is present in excess. The band between 3600–3000 cm^{-1} is believed to reflect the high number of hydroxyl and amine groups, as well as the large number of H-bonds among the functional groups of Gel, Alg, and glycerol (the plasticizer). The shoulder-type band at 1689 cm^{-1} is assigned to amide C=O stretching formed through the crosslinking process. As reported by Staroszczyk et al. [24], EDC mediates the formation of iso-peptide bonds between amino groups and activated carboxylic groups of glutamic or aspartic acid residues in Gel. Since carboxylic groups are also available on the Alg backbone, we propose that amide bonds are also formed between the Gel and Alg chains. The spectrum of the film containing SeTal (Gel-Alg/SeTal) is similar to that of the bare film, indicative of weak interactions between this molecule and the polymer matrix, though the bands associated with C–H, C–O, and C–C vibration modes were more intense in the spectrum of Gel-Alg/SeTal compared to Gel-Alg, with these ascribed to contributions from the functional groups of SeTal. The spectrum of Gel-Alg/SeTal/HC exhibited a small band at 1742 cm^{-1} and a shoulder-type band at ~1625 cm^{-1} assigned to the C=O and C=C stretching vibrations of HC. The more intense bands in the 1500–1200 cm^{-1} range are also attributed to HC [25], confirming the presence of this compound in the film. Finally, the spectrum of the film containing VitC exhibited the characteristic bands of Gel-Alg/SeTal with the additional bands observed at 3528, 1741, and 863 cm^{-1} assigned to the O–H, C=O, and C–C ring stretching vibrations of VitC. These findings confirm that VitC had been stably entrapped in the film [26]. Moreover, these spectroscopic data indicate that both the SeTal and VitC in the Gel-

Alg/SeTal/VitC films are physically entrapped in the polymer matrix, with no evidence of any chemical interactions (i.e., covalent bonds).

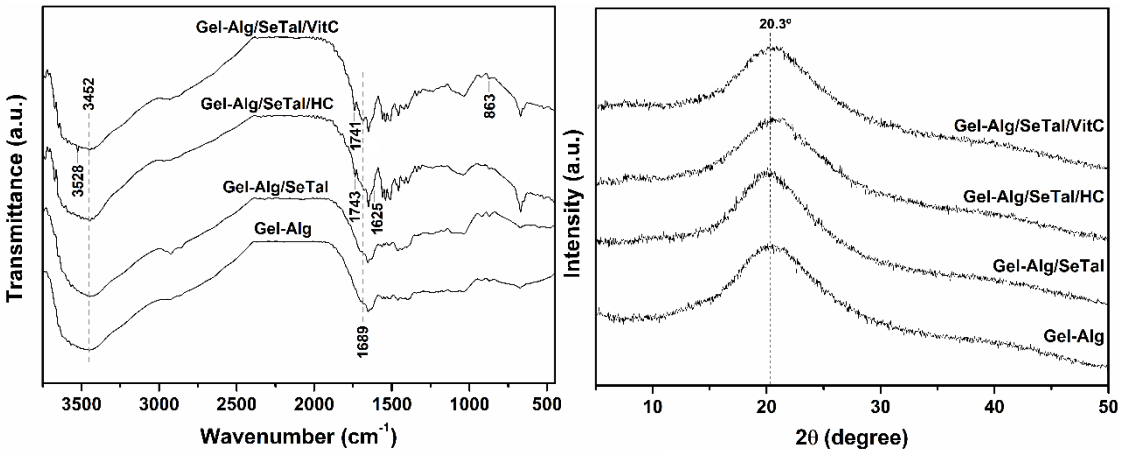

Figure 2. (a) FTIR spectra and (b) XRD patterns of Gel-Alg, Gel-Alg/SeTal, Gel-Alg/SeTal/HC, and Gel-Alg/SeTal/VitC.

The structures of the encapsulated compounds (SeTal, VitC, and HC) were determined by XRD. The data presented in Figure 2b, shows that Gel-Alg exhibits only a broad-halo at around $2\theta \approx 20.3°$ in its XRD pattern, confirming the amorphous nature of this material. No significant changes were observed when the XRD pattern of the bare film was compared with those obtained from the drug-containing films (SeTal, SeTal/VitC, and SeTal/HC). The absence of diffraction peaks from these crystalline compounds (Figure S3) indicates that they undergo structural transitions to amorphous states during encapsulation. Thus, intermolecular interactions among SeTal, VitC, and HC with polymeric matrix appear to limit crystallization of these compounds, which is an advantageous in terms of drug solubility and release (cf. previous reports [27]).

The prepared films were subjected to TGA/DTG to investigate their thermal profiles. Figure 3a shows that all the films exhibited a loss of mass over the 30–150 °C temperature range due to water evaporation. The extent of this loss was dependent on the

film sample, which may indicate that these films have different hydrophilicities. The smallest mass loss (~3%) was observed for the Gel-Alg/SeTal sample, most likely because interactions between SeTal molecules and the polymeric matrix through H-bonding reduces the number of hydrophilic groups able to interact with water molecules. In contrast, the hydrophilicity of the film appeared to return to that observed for the pristine film as other compounds (HC or VitC) were added. This may arise from the presence of HC or VitC restricting interactions between SeTal and the Gel-Alg matrix since these compounds can interact themselves. The mass loss observed in the TGA curves at higher temperatures (> 170 °C) is assigned to thermal decomposition of Alg (maximum ~251 °C) and Gel (maximum ~316 °C). The DTG curves (Figure 3b), reveal that the encapsulated compounds (SeTal, SeTal/HC, and SeTal/VitC) have little effect on the thermal stability of the polymer. As reported above, only weak physical interactions appear to occur between the encapsulated compounds and the film matrix, consistent with the observed thermal trends. However, the DTG curves of Gel-Alg/SeTal and Gel-Alg/SeTal/HC exhibit a shoulder at around 335 °C, which is ascribed to gelatin moieties interacting with SeTal; these moieties are thermally stable, which rationalizes this trend. Such a shoulder was not observed for Gel-Alg/SeTal/VitC, most likely because interactions between SeTal and VitC interfere with those involving the film matrix, with the chemical structures of SeTal and VitC (see Figure S1) favoring interactions between these species. Degradation stages related to the pure compounds (SeTal, HC, and VitC) were not observed in the TGA/DTG curves, indicative of their efficient entrapment. This finding is consistent with the XRD data, which show that these compounds are predominantly amorphous in the film matrix.

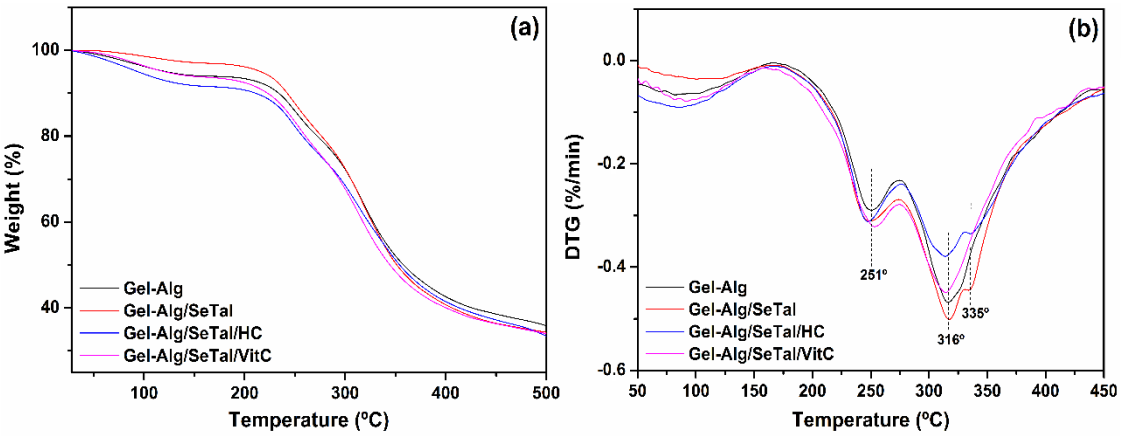

Figure 3. (a) TGA and (b) DTG curves for Gel-Alg, Gel-Alg/SeTal, Gel-Alg/SeTal/HC, and Gel-Alg/SeTal/VitC.

In addition to their physicochemical properties, the mechanical properties of the prepared films may play a significant role in their behavior and drug release capacities. Therefore, tensile testing was used to investigate the mechanical properties of the prepared films. The resulting data are summarized in Table 2 along with the film thicknesses.

Table 2. Thicknesses and mechanical properties of the Gel-Alg-based films.

Film	Thickness (mm)[a]	Young´s modulus (MPa)	Maximum tensile strength (MPa)[b]	Maximum elongation (%)[b]
Gel-Alg	0.13 ± 0.01	22.44 ± 6.10	237.78 ± 17.94	34.67 ± 4.58
Gel-Alg/SeTal	0.15 ± 0.03	26.68 ± 1.53	161.80 ± 9.68	18.05 ± 6.40
Gel-Alg/SeTal/HC	0.16 ± 0.02	25.56 ± 4.10	103.23 ± 37.53	11.13 ± 4.86
Gel-Alg/SeTal/VitC	0.16 ± 0.03	27.85 ± 4.08	142.80 ± 26.82	14.00 ± 5.79

[a] Determined using a digital vernier caliper. [b] Computed at breaking point. All results are given as means ± standard deviations (n = 5).

The prepared films had similar average thicknesses, which demonstrates that incorporating the various compounds did not lead to expansion of the polymeric matrix,

which is possible ascribable to interactions between these compounds and the film polymer, as reported above. The prepared films were determined to have Young's moduli that varied between 22 and 28 MPa, with the loaded films exhibiting slightly higher values, though these were not significantly different, indicating that the encapsulated compounds have minimal effects on the rigidity of the Gel-Alg matrix. These data corroborate previous results that show that the compounds interact weakly with the Gel-Alg matrix (*vide supra*). Compared to other drug-delivery materials, the Young´s moduli determined for the films prepared in this study are comparable or superior to those of other film-like materials tested as drug delivery systems [13,28]. While the encapsulated compounds (SeTal, HC, or VitC) did not appear to affect the Young's modulus significantly, they did affect other mechanical parameters (tensile strength and elongation). Table 2 reveals that SeTal-encapsulated film and those containing SeTal/HC and SeTal/VitC exhibit lower tensile strengths and maximum elongations. Thus, interactions between the various compounds and the film matrix appear to decrease polymer chain mobility during mechanical solicitation Additionally, the encapsulated compounds decrease the free volume in the film matrix [29], especially for the film loaded with SeTal/HC or SeTal/VitC. Despite these small differences, all the films were flexible and easy to handle, as illustrated in Figure 4.

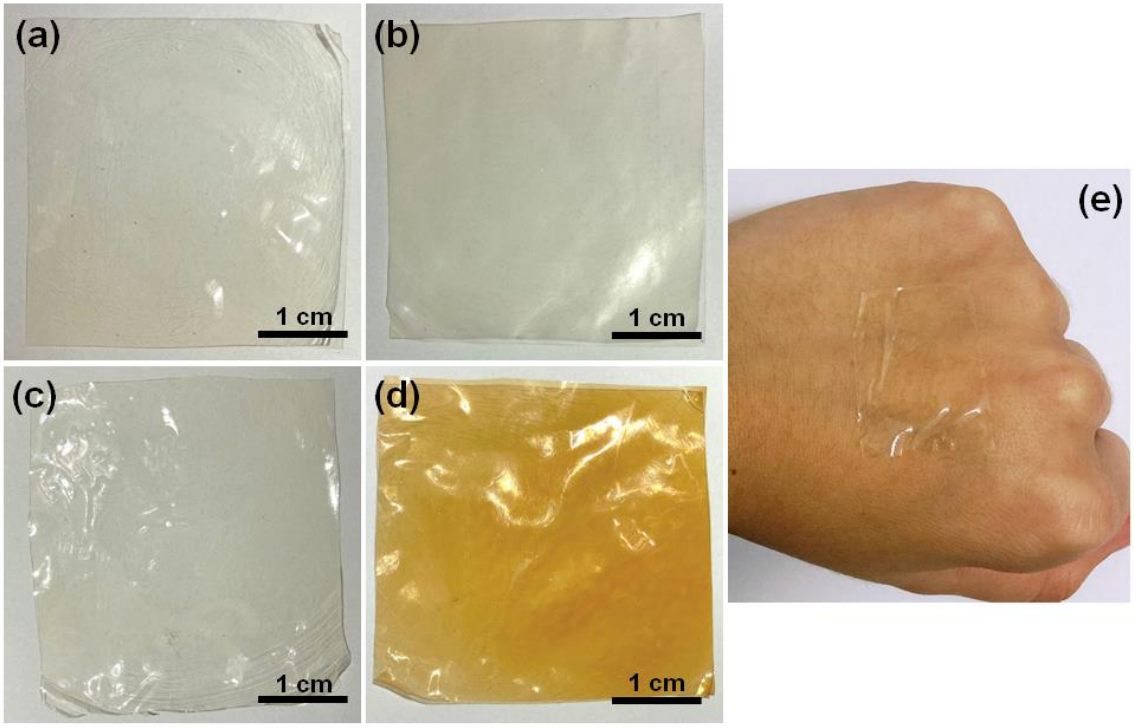

Figure 4. Photographic images of (a) Gel-Alg, (b) Gel-Alg/SeTal, (c) Gel-Alg/SeTal/HC, and (d) Gel-Alg/SeTal/VitC. (e) Photographic image of the Gel-Alg/SeTal/HC film applied to a hand.

3.2. Quantification of film swelling and drug release

The ability of biomaterials to swell is advantageous to treat the exudative lesions caused by AD [30], as it prevents maceration and the accumulation of body fluid at the treated site [30]. At the same time, the swelling process is a feature of the drug-release mechanism [31]. Consequently, we studied the abilities of the prepared films to swell in simulated wound fluid (SWF, pH 5.5) at 37 °C. Figure 5a shows swelling ratios (SRs) for the various films as a function of time, with rapid increases in the SR detected at early time points, with high values achieved by 30 min. This trend is ascribed to the hydrophilic natures of Gel and Alg, which favor the sorption and retention of water molecules. Swelling appears to plateau beyond 30 min as each film approaches equilibrium. The pristine Gel-Alg film achieved an equilibrium earlier (at ~60 min) than the compound-

containing films, which required ~120 min, and the SR values varied minimally once equilibrium had been established. The Gel-Alg film exhibited the highest SR (~490%), which is likely due to the higher number of functional groups in this system that are available for interaction with water molecules, as well as its free volume that accommodates the absorbed liquid. The carboxylic acid groups of Gel and Alg are likely to be deprotonated at the pH value employed (5.5), since their pKa values lie between 3.5–4.5 [32], which results in a high negatively charge density in the polymer matrix that causes it to expand, leading to higher liquid absorption. The maximum SR values of the other films were calculated to be 406% (Gel-Alg/SeTal), 430% (Gel-Alg/SeTal/HC), and 434% (Gel-Alg/SeTal/VitC). The lower SR values for the drug-containing films is ascribed to fewer available hydrophilic groups, due to interaction with the encapsulated molecules, as well as lower the free volume in the film matrix. These results are consistent with the mechanical data. Furthermore, the TGA/DTG data show that Gel-Alg/SeTal is noticeably less hydrophilic compared to the pristine sample; despite this reduction, each drug-containing film exhibited a strong capacity to swell under physiological-like conditions, which is likely to have practical advantages.

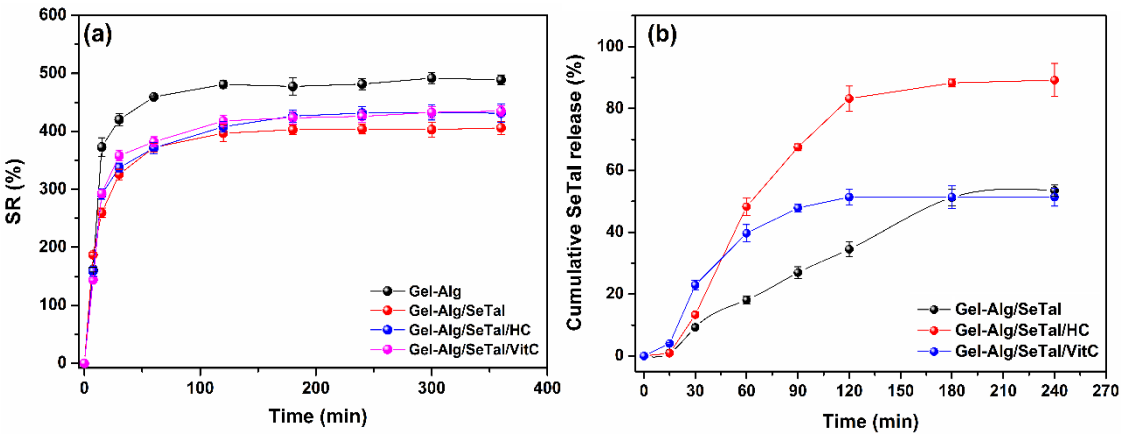

Figure 5. (a) Swelling profiles of the prepared films immersed in SWF at 37 ºC. (b) SeTal-release profiles from Gel-Alg/SeTal, Gel-Alg/SeTal/HC, and Gel-Alg/SeTal/VitC in SWF (pH 7.4) at 37 °C.

Encapsulated-compound release from the various films was investigated using SWF (pH 7.4) as the release medium. These experiments revealed that neither HC nor VitC were released (or not detected by the UV-Vis detector employed) from the Gel-Alg/SeTal/HC and Gel-Alg/SeTal/VitC films over a 24 h period. Only the absorption band assigned to SeTal (at 255 nm) was detected in the spectra of aliquots withdrawn from the acceptor compartment of Franz cells, with the release of this compound being independent of the film sample (Figure S5). Typically, HC and VitC show UV-Vis absorption bands at 248 and 264 nm [33]. As FTIR spectroscopy (see above) provided evidence weak interactions between SeTal and the film matrix, and stronger interactions for HC and VitC (probably through H-bonding), these data rationalize the preferential release of SeTal. Figure 5b shows SeTal release behavior for the three different film samples over time, with this indicating that the release process depends on the film formulation. SeTal was released slowly from Gel-Alg/SeTal at the start of the experiment (< 30 min), with no burst behavior observed; the lower hydrophilicity of Gel-Alg/SeTal helps explain this behavior. The release rate then increased slightly before achieving equilibrium at ~180 min, with ~54% of the encapsulated SeTal released from by the end of the experiment (240 min). In contrast, the Gel-Alg/SeTal/HC and Gel-Alg/SeTal/VitC films released SeTal more rapidly (Figure 5b), with this ascribed to the additional compounds in the matrix reducing the number of SeTal/film interaction sites and facilitating release. Despite their faster release profiles, the Gel-Alg/SeTal/HC and Gel-Alg/SeTal/VitC films achieved a SeTal-release equilibrium faster (~120–150 min) than

Gel-Alg/SeTal, and exhibited maximum SeTal-release extents of 89% and 51%, respectively, after 240 min. The HC molecule possibly interacts intermolecularly with the Gel and Alg chains due to its large size, and blocks interaction between these chains and SeTal, facilitating its release. This suggestion is consistent with the mechanical data (see above), as the Gel-Alg/SeTal/HC film exhibited the lowest elongation rate (i.e., lowest chain mobility) caused by these interactions. The lower molecular mass of SeTal (compared to HC) and its higher aqueous solubility may also contribute to this effect.

The experimental data were fitted to mathematical models to gain insight into the release mechanism, including, zero-order (Equation 3), first-order (Equation 4), Higuchi (Equation 5), and Korsmeyer–Peppas (Equation 6) models:

$$Q = k_0 t \tag{3}$$

$$ln\ Q = k_1 t \tag{4}$$

$$Q = k_H t^{1/2} \tag{5}$$

$$ln\left(\frac{Q}{Q_\infty}\right) = ln\ k_{KP} + n\ ln\ t \tag{6}$$

where Q is the fraction of the compound released at time t, Q_∞ is the fraction of the compound released at infinite time (i.e., equilibrium), while k_0, k_1, k_H, and k_{KP} are the zero-order, first-order, Higuchi, and Korsmeyer–Peppas constants, and n is the release exponent. The values of these parameters determined from this data fitting (Figures S6a–S6d) by simple linear regression analysis are summarized in Table 3.

Table 3. Kinetic data and coefficient of determination (R^2) calculated for SeTal release from each prepared film, for the release model employed.

Release model	Parameter	Film		
		Gel-Alg/SeTal	**Gel-Alg/SeTal/HC**	**Gel-Alg/SeTal/VitC**
Zero-order	k_0 (mg/min)	2.44×10^{-3}	4.18×10^{-3}	2.12×10^{-3}
	R^2	0.953	0.784	0.617
First-order	k_1 (1/min)	1.35×10^{-2}	1.46×10^{-2}	0.79×10^{-2}
	R^2	0.545	0.400	0.320
Higuchi	k_H (mg/min$^{1/2}$)	3.98×10^{-2}	7.30×10^{-2}	3.93×10^{-2}
	R^2	0.930	0.885	0.831
Korsmeyer–Peppas	k_{KP} (1/min^n)	2.59×10^{-4}	1.05×10^{-4}	0.49×10^{-4}
	n	1.66	1.81	1.10
	R^2	0.972	0.951	0.948

The R^2 values in Table 3 suggest that the Korsmeyer–Peppas model is best able to explain SeTal release from the various film samples, with the three Gel-Alg-based films exhibiting R^2 values > 0.94. It is important to note that this model is limited to the first 60% of SeTal release [34]. The value of *n*, which is related to the release mechanism, was determined to be greater than unity for each film, with these values consistent with a super case-II transport mechanism, in which polymer-chain relaxation associated with liquid imbibition is the rate-controlling step [35]. Diffusion and erosion of the polymer material also contribute to this transport mechanism, as reported elsewhere [36]. Our findings are consistent with other studies into drug release from polymer films [37].

3.3. In-vivo and ex-vivo assays

3.3.1. Effect of the prepared films on the clinical signs of AD-like skin lesions

DNCB was used to induce AD-like skin conditions in mice. This small hapten-class molecule penetrates the skin barrier and the intact epidermis of mice to initially cause an acquired immune response. Repeated exposure leads to the development of an AD-like state [38]. DNCB induction causes anaphylaxis and the appearance of AD-like skin lesions, including thicker skin, dryness, swelling, edema, and erythema [39].

The effects of topically applying Gel-Alg, Gel-Alg/SeTal, Gel-Alg/SeTal/HC, and Gel-Alg/SeTal/VitC on skin lesion severity, scratching behavior, and back skin thickness are shown in Figures 6a and 6b. One-way ANOVA followed by Tukey's post-hoc test revealed that DNCB significantly increased skin severity scores [$F_{6,42}$ = 45.79, p < 0.0001], scratching behavior [$F_{6,42}$ = 420.3, p < 0.0001] and back thickening [$F_{6,42}$ = 32.76, p < 0.0001] compared to the control group, consistent with DNCB inducing an AD-like phenotype (Figures 6c and 6d). Topical treatment with film loaded with Gel-Alg (p < 0.0001), Gel-Alg/SeTal (p < 0.0001), Gel-Alg/SeTal/HC (p < 0.0001), and Gel-Alg/SeTal/VitC (p < 0.0001) reduced DNCB-induced skin-lesion severity, scratching behavior, and back thickening. The Gel-Alg/SeTal, Gel-Alg/SeTal/HC, and Gel-Alg/SeTal/VitC films also significantly improved clinical and behavioral parameters compared to those detected with HC cream. DNCB-induced stimulation resulted in typical allergic responses, including the itching, erythema, skin thickening, edema, excoriation, and scaling typical of AD, and the films improved these symptoms and pruritus.

AD induces a variety of immune responses, with the spleen being responsible for the production of immune cells as well as other body functions [40]. Consequently, we measured the length and mass of the spleen on day 30 to assess splenomegaly, an indicator of immunological abnormality [41]. Figures 6e and 6f show that exposure to DNCB causes a significant increase in mouse spleen length [$F_{6,42}$ = 14.83, p < 0.0001] and mass [$F_{6,42}$ = 39.26, p < 0.0001], and that treatment with the Gel-Alg (p < 0.001), Gel-Alg/SeTal (p < 0.0001), Gel-Alg/SeTal/HC (p < 0.0001), and Gel-Alg/SeTal/VitC (p < 0.05) films, as well as HC cream (p < 0.01), diminishing these changes in the animals sensitized with DNCB. The Gel-Alg/SeTal/HC film more effectively modulated these parameters than HC cream. HC is a synthetic cortisol analog and long-term administration

is known to result in suppression of the hypothalamic-pituitary-adrenal (HPA) axis and adrenocorticotropic hormone (ACTH), which leads to adverse effects including adrenal atrophy [42]. In turn, changes in the HPA axis affects the immune system and inflammatory pathways [43], as observed in our study through changes in the spleens of animals sensitized with DNCB. Thus, encapsulating HC in the Gel-Alg film reduced the adverse effects of topical HC, while incorporating SeTal further improved its effects.

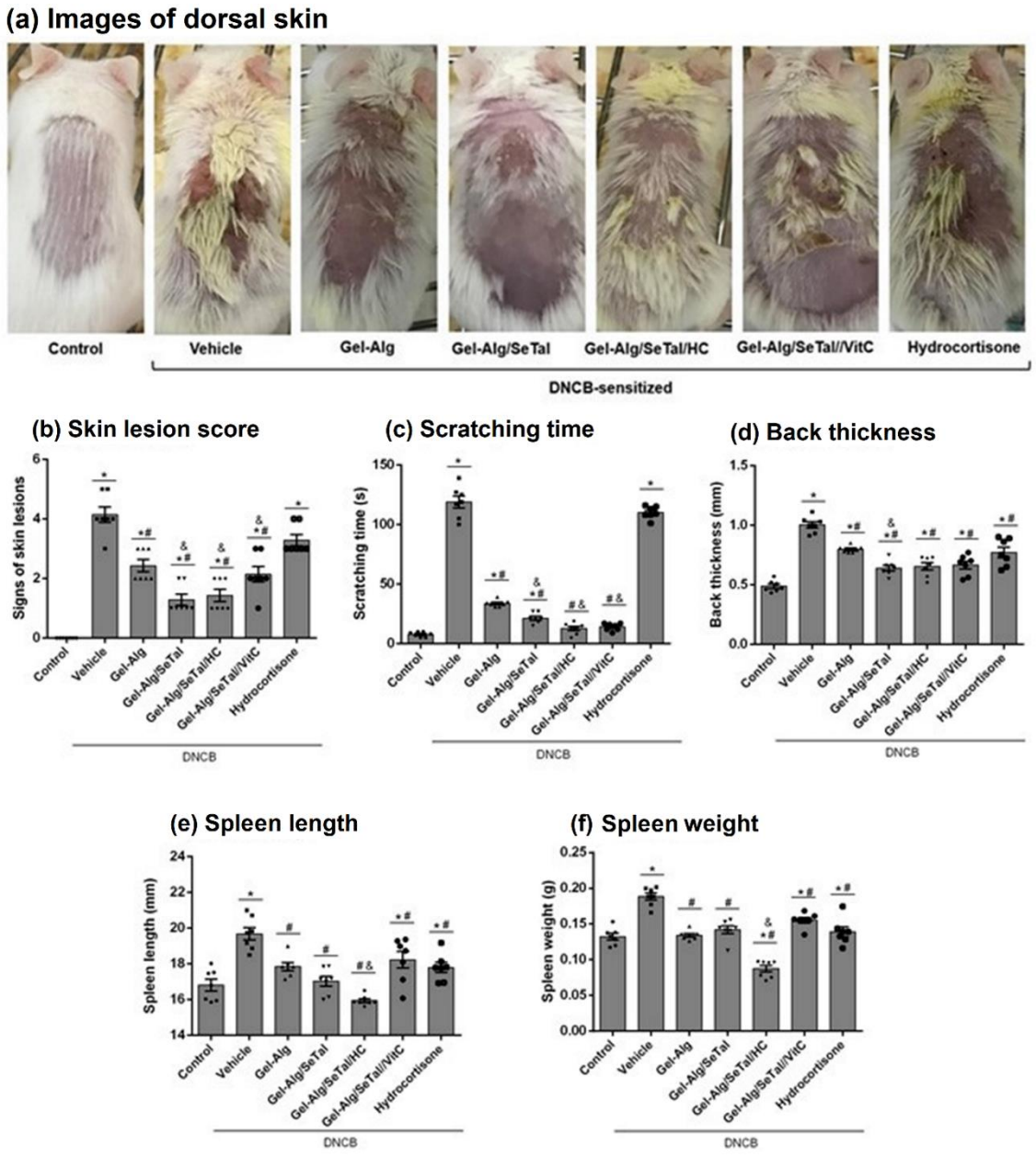

Figure 6. Effects of topical treatment with various films (Gel-Alg, Gel-Alg/SeTal, Gel-Alg/SeTal/HC, and Gel-Alg/SeTal/VitC), as well as hydrocortisone cream on atopic-dermatitis-like (AD-like) symptoms in mice induced by DNCB. (a) Photographic images of dorsal skin, (b) skin lesion scores, (c) scratching times, (d) back thicknesses, (e) Spleen lengths, and (f) Spleen mass after DNCB sensitization. Data are means ± SEMs (one-way ANOVA followed by Tukey's test). ***** $p < 0.05$ compared with the control group, **#** $p < 0.05$ compared with the DNCB treatment group, and *&* $p < 0.05$ compared with the hydrocortisone (HC) group.

3.3.2 Effects of the prepared films on the inflammatory responses of AD-like skin lesions in mice

AD is a complex disease involving both abnormal immunological and inflammatory pathways. Chronically, it is characterized by lesions resulting from inflammatory processes which trigger skin edema [20]. Current treatments for AD work by reducing major physical symptoms, such as excessive scratching and damage caused by skin inflammation [44]. However, these treatments have side effects that reduce treatment compliance [45]. Inflammation severity was gauged by ear swelling, with the effects of the various treatments shown in Figure 7. One-way ANOVA followed by Tukey's post-hoc test demonstrated that DNCB increases ear swelling compared to the control group [$F_{6,42} = 415.40$, $p < 0.0001$] (Figure 7a). Treatment with Gel-Alg ($p < 0.0001$), Gel-Alg/SeTal ($p < 0.0001$), Gel-Alg/SeTal/HC ($p < 0.0001$), and Gel-Alg/SeTal/VitC ($p < 0.0001$) films, and HC cream ($p < 0.0001$) reduced DNCB-induced ear edema, with Gel-Alg/SeTal/HC and Gel-Alg/SeTal/VitC showing superior effects when compared to HC. The combination of SeTal and HC in the Gel-Alg/SeTal/HC film provided a superior effect compared to Gel-Alg/SeTal alone.

Topical sensitization with DNCB triggers an inflammatory process that can be detected as increased ear edema, with this process related to the accumulation of

polymorphonuclear leukocytes (PMNs) including neutrophils. The number of PMNs can be quantified by the activity of MPO, a oxidant-generating heme enzyme released primarily by neutrophils [46]. Figures 7b and 7c show the effect of topical film treatment (Gel-Alg, Gel-Alg/SeTal, Gel-Alg/Setal, Gel-Alg/SeTal/HC or Gel-Alg/SeTal/VitC) on MPO activity in the ear and back skin of mice, respectively. One-way ANOVA followed by Tukey's post-hoc test revealed that DNCB significantly increased MPO activity in mouse ears [$F_{6,42} = 355.10$, $p < 0.0001$] and dorsal skin [$F_{6,42} = 415.50$, $p < 0.0001$] compared to the control group as expected. The Gel-Alg ($p < 0.0001$), Gel-Alg/SeTal ($p < 0.0001$), Gel-Alg/SeTal/HC ($p < 0.0001$), Gel-Alg/SeTal/VitC ($p < 0.0001$) films and the HC cream ($p < 0.0001$) decreased MPO activity in the ear (Figure 7b) and dorsal skin (Figure 7c) compared to mice sensitized with DNCB but otherwise left untreated. The Gel-Alg/SeTal, Gel-Alg/SeTal/HC, Gel-Alg/SeTal/VitC films were more effective than HC cream (positive control) in reducing the MPO activity in the analyzed tissue. Furthermore, the Gel-Alg/SeTal/HC film exhibited superior performance for reducing MPO activity in the dorsal skin of mice sensitized with DNCB than Gel-Alg/SeTal.

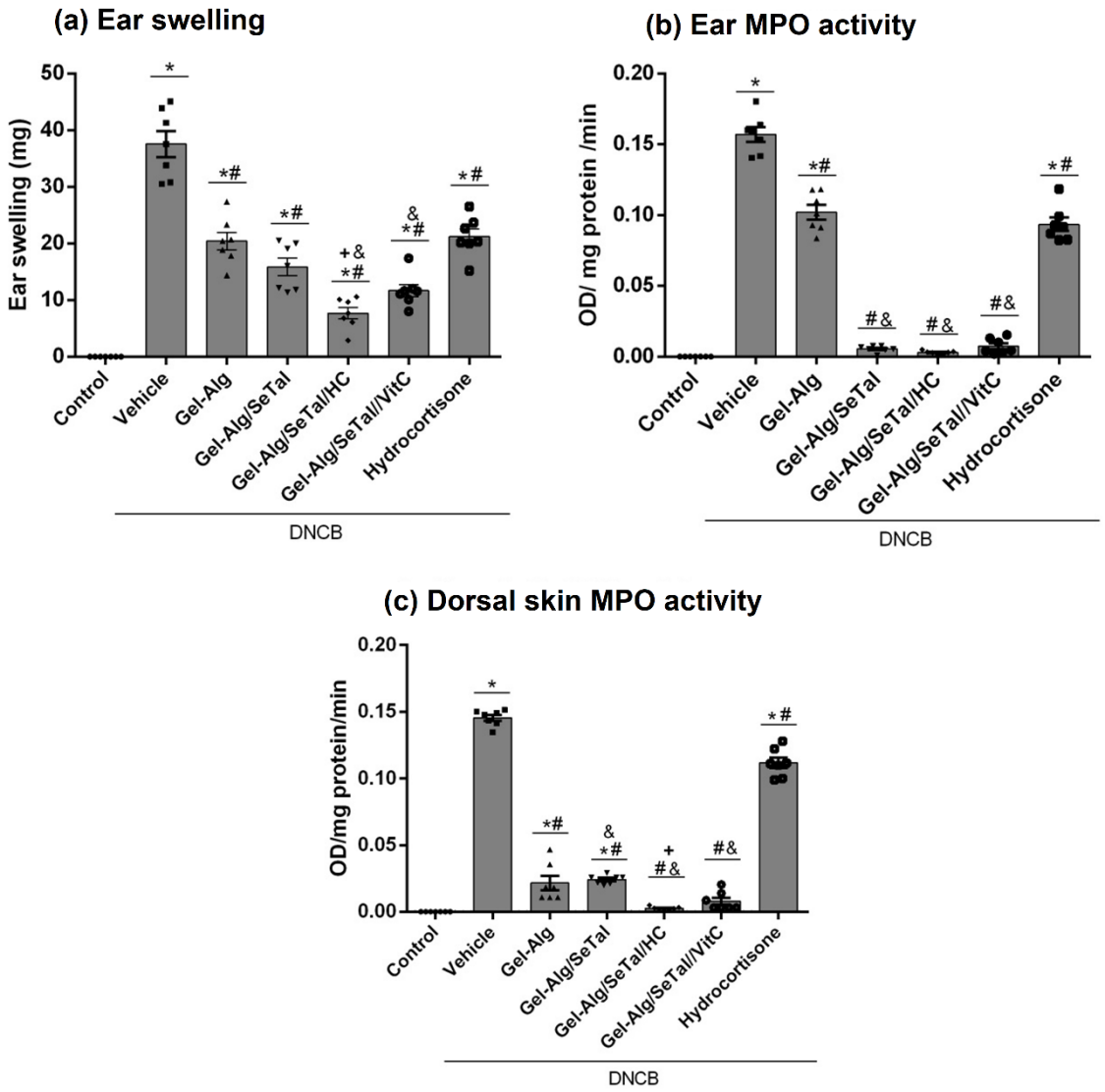

Figure 7. Effect of topical treatment with films (Gel-Alg, Gel-Alg/SeTal, Gel-Alg/SeTal/HC and Gel-Alg/SeTal/VitC) and hydrocortisone (HC) cream on (a) ear swelling, (b) ear MPO activity and (c) dorsal skin MPO activity Data are means ± SEMs (one-way ANOVA followed by Tukey's test). * $p < 0.05$ compared with the control group, # $p < 0.05$ compared with the vehicle-DNCB group, + $p < 0.05$ compared with the Gel-Alg/SeTal group, and & $p < 0.05$ compared with the hydrocortisone group.

3.3.3 Effect of prepared films on NOx levels, as an oxidative parameter in AD-like skin lesions in mice

Skin inflammation in AD patients plays an important role in the pathogenesis of this disease through the overproduction of oxidants, with consequent decreases in

antioxidant defense capacity [47]. Multiple endogenous and exogenous factors can increase oxidant production including the inflammatory responses of leukocytes, with this resulting in altered NOx levels [48]. Elevated oxidant levels can induce damage to cellular and extracellular macromolecules, including lipids, proteins, and nucleic acids, with this resulting in disruption to biochemical processes [49]. Consequently, oxidative stress is often studied in AD-like models, given that an imbalanced redox system appears to predispose to AD pathogenesis [50].

Figure 8 shows how Gel-Alg, Gel-Alg/SeTal, Gel-Alg/Setal, Gel-Alg/SeTal/HC, Gel-Alg/SeTal/VitC, and HC cream treatment affect NOx levels in the dorsal skin of mice. One-way ANOVA followed by Tukey's post-hoc test revealed that animals sensitized with DNCB show higher NOx levels compared to the control group [$F_{6,42}$ = 72.86, $p < 0.0001$]. Treatment with Gel-Alg ($p < 0.0001$), Gel-Alg/SeTal ($p < 0.0001$), Gel-Alg/SeTal/HC ($p < 0.0001$), Gel-Alg/SeTal/VitC ($p < 0.0001$), or HC cream ($p < 0.0001$) ameliorated the higher NOx levels induced by DNCB. The Gel-Alg/SeTal/VitC film provided a superior effect in reducing NOx levels caused by DNCB in the dorsal skins of mice than Gel-Alg/SeTal or HC cream. This was as expected, as VitC is a potent natural antioxidant and anti-inflammatory agent [51,52], and can also modulate the immune system [53]. SeTal has also been shown to have potent antioxidant activity, acting at different points in the general mechanism of antioxidant defense [54]. Thus, SeTal may contribute to suppressing AD-like skin lesions via an antioxidant activity, though other mechanisms cannot be excluded. Therefore, the combined antioxidant and anti-inflammatory effects of SeTal may provide an effective therapy for AD-like lesions.

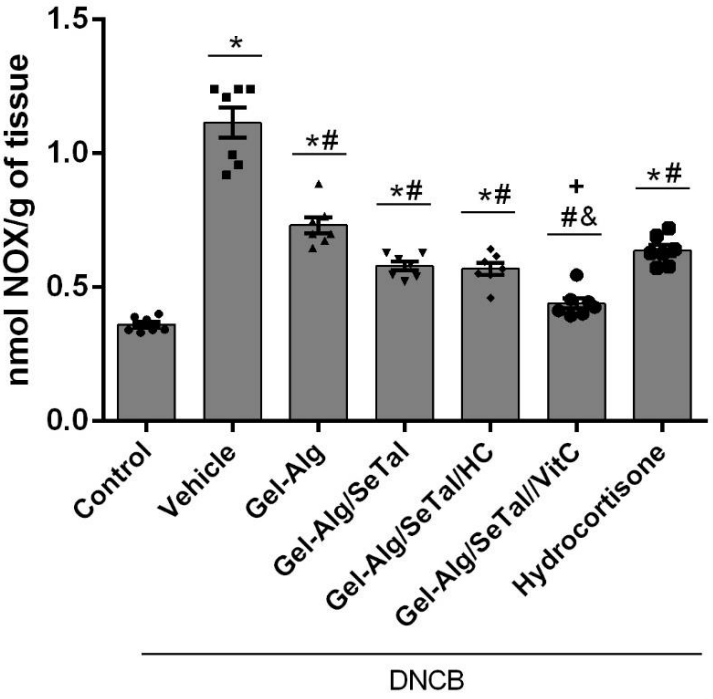

Figure 8. Effects of topical treatments with films (Gel-Alg, Gel-Alg/SeTal, Gel-Alg/SeTal/HC, Gel-Alg/SeTal/VitC) and hydrocortisone (cream) on nitric oxide level in mouse dorsal skin. Data are means ± SEMs (one-way ANOVA followed by Tukey's test). * $p < 0.05$ compared with the control group, # $p < 0.05$ compared with the vehicle-DNCB group, + $p < 0.05$ compared with the Gel-Alg/SeTal group, and & $p < 0.05$ compared with the hydrocortisone group.

3.3.4. Effects of the prepared films on AD-type skin lesions in mice as determined by morphological analysis

Histological scores were evaluated using H.E. to identify the effects of DNCB sensitization and film treatment on AD-like skin lesions. The severities of the morphological alterations to the dorsal skin caused by exposure to the various treatments are shown in Figure 9. The dorsal skin of control animals exhibited normal histological architecture (Figures 9a and 9b), while dorsal skin sections of animals sensitized by DNCB exhibited intraepidermal pustules along with thick crusts (Figure 9c) and marked inflammatory eosinophil, macrophage, and lymphocyte infiltrates in the superficial, deep,

and subcutaneous dermises (Figure 9d). The animals that received HC cream had a thinner dermis and exhibited low dermal inflammatory responses (Figure 9e) with few inflammatory cells present in the dermis and subcutaneous regions (Figure 9f). While crusts were observed to a limited extent, no intraepidermal pustules were present. The dorsal skins of animals that received the Gel-Alg film exhibited marked crusts covering the epidermis with intraepidermal pustules (Figure 9g), in addition to moderate inflammatory polymorphonuclear, macrophage, and lymphocyte infiltrates in their superficial, deep, and subcutaneous dermises (Figure 9h).

The animals treated with Gel-Alg/SeTal film presented large intraepidermal pustules and multiple crust layers (Figure 9i), in addition to a marked inflammatory response in the superficial and deep dermis along with eosinophil, macrophage, and lymphocyte infiltration (Figure 9j). However, fewer infiltrates were observed in subcutaneous tissue. In contrast, the animals treated with the Gel-Alg/SeTal/HC film exhibited fewer intraepidermal pustules, while multiple crust layers were retained between keratin layers (Figure 9k). More discrete inflammatory responses were detected in the superficial and deep dermises (Figure 9l). The subcutaneous region showed abundant inflammatory eosinophil infiltrates, along with edema and dilated lymphatic vessels. The dorsal skin of mice treated with Gel-Alg/SeTal/VitC film showed few intraepidermal pustules. Crusting was also observed but without the formation of multiple layers (Figure 9m). The eosinophil inflammatory response was more marked than those of mononuclear cells and extended almost homogeneously through the dermis and subcutaneous tissue (Figure 9n).

These data demonstrate that DNCB induces a significant increase in immune cell (eosinophils, macrophages, and lymphocytes) infiltration into the dermis compared to the control group (Figures 9c and 9d). Eosinophils act as immune modulators, secreting

multiple chemical mediators and cytokines that recruit more immune cells to the affected region, thereby exacerbating the inflammatory process [55]. Treatment with HC resulted in a thinning of the skin, a known side effect associated with the use of corticosteroid-class drugs [56]. Thus, corticosteroids delay tissue healing as they inhibit the regulation of immune and inflammatory reactions by reducing the expression of interleukins and growth factors responsible for neovascularization and fibroblast migration [56]. Our histological analyses also demonstrated that the combination of SeTal and HC (Gel-Alg/SeTal/HC) provides advantages over HC treatment alone in this regard, in addition to improving wound healing through the formation of fewer intradermal pustules and more-discrete inflammatory responses in the superficial and deep dermises.

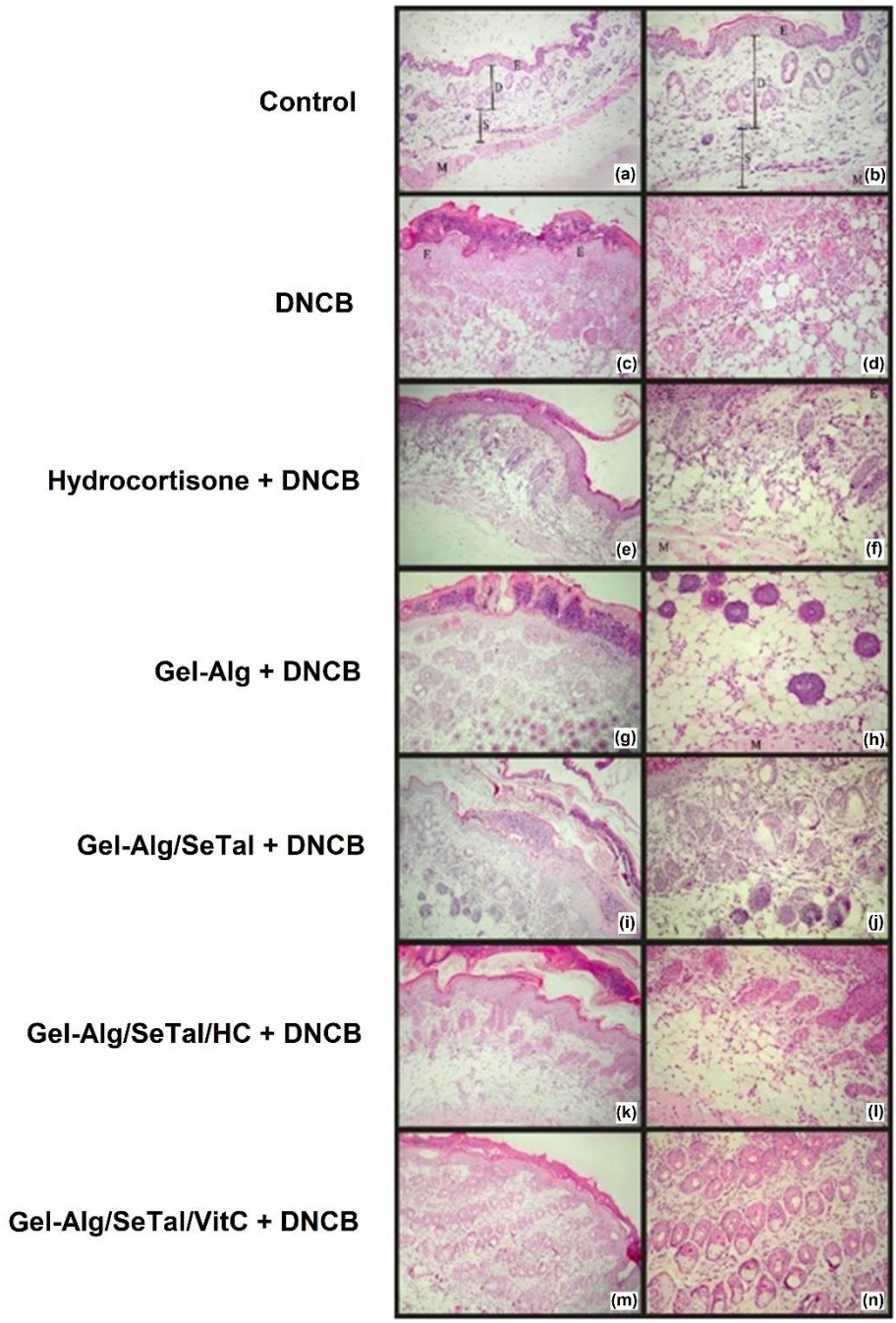

Figure 9. Photomicrographs (100×, left; 200×, right) showing the severity of dorsal-skin morphological alterations caused by sensitization with DNCB and various treatments. (a) and (b) correspond to control animals, (c) and (d) represent animals sensitized with DNCB, (e) and (f) represent the HC cream group, (g) and (h) represent the Gel-Alg group, (i) and (j) represent the Gel-Alg/SeTal group, (k) and (l) represent the Gel-Alg/SeTal/HC group, and (m) and (n) correspond to the Gel-Alg/SeTal/VitC group. Labels: Epidermis (E), dermis (D), subcutaneous (S), and nuscle layer (M). All sections were H.E. stained.

Conclusion

Biopolymeric films of Gel and Alg were prepared and loaded with different compounds (SeTal, HC, and/or VitC) to serve as biomaterials for treating and attenuating symptoms of AD. Characterization analyses confirmed the presence of the compounds in the film matrices and demonstrated that these compounds affect different properties (thermal, mechanical, and swelling). The interactions among the encapsulated compounds and the Gel-Alg matrix caused these changes and affected their release behavior as assessed. Release experiments performed in simulated wound fluid (pH 7.4) revealed that only SeTal, which has a lower affinity with the film matrix, is released. SeTal was controlled-released, and this process occurs due to a combined mechanism involving polymer-chain relaxation, diffusion, and erosion. A series of in-vivo and ex-vivo studies showed that films loaded with SeTal, HC, and/or VitC have beneficial effects on multiple parameters used to evaluate AD in a DNCB-induced model. These films were more efficient at treating or attenuating key disease parameters compared to the positive control (HC cream). Therefore, encapsulating SeTal with HC and/or VitC in a biopolymer film of Gel-Alg appears to be a promising alternative therapy for long-term treatment of AD. Furthermore, these biopolymer films also reduced adverse effects associated with corticosteroids, such as HC. These films may also provide beneficial effects on other skin diseases.

Author statement

The manuscript and the data reported here have not been published previously and are not under consideration for publication elsewhere. All listed authors have contributed significantly to the research and manuscript preparation. They consent to their names being on the manuscript and have approved the final article. All authors have read the

manuscript and have agreed to submit it in its current form for consideration for publication.

Author contributions

G.T.V., R.L.O, C.L. and E.A.W. conceived and designed the study. M.P.S performed the histological analysis. A.B.N. and V.R.S. Methodology, Formal analysis, Investigation. A.R.F., A.B.N., G.T.V., R.L.O., M.J.D., C.H.S. and E.A.W. wrote and revised the manuscript. A.R.F., E.A.W and C.L. supervised the study. All authors approved the final version of the manuscript.

Declaration of Competing Interest

The authors declare that they have no conflicts of interest, except for M.J.D. and C.H.S. who are major shareholders and Directors of Seleno Therapeutics Pty. Ltd., which holds patents on the development and use of SeTal.

Acknowledgments

We are grateful for financial support from Seleno Therapeutics Pty. Ltd., and grants and scholarships from the following agencies: CNPq (429859/2018-0, 312747/2020-9), FAPERGS (PqG 21/2551-0001943-3 and 21/2551-0002162-4), CAPES, the Independent Research Fund Denmark (Danmarks Frie Forskningsfond; DFF-7014-00047) and the Novo Nordisk Foundation (NNF13OC0004294 and NNF20SA0064214). CNPq is also acknowledged for fellowships to A.R.F., E.A.W. and C.L. This study was financed in part by the Coordenação de Aperfeiçoamento de Pessoal de Nível Superior - Brasil (CAPES) - Finance Code 001, and forms part of the activities of the International SeS Redox and Catalysis Network.

References

[1] S. Weidinger, N. Novak, Atopic dermatitis, Lancet. 387 (2016) 1109–1122. https://doi.org/10.1016/S0140-6736(15)00149-X.

[2] E. Axon, J.R. Chalmers, M. Santer, M.J. Ridd, S. Lawton, S.M. Langan, D.J.C. Grindlay, I. Muller, A. Roberts, A. Ahmed, H.C. Williams, K.S. Thomas, Safety of topical corticosteroids in atopic eczema: an umbrella review, BMJ Open. 11 (2021) e046476. https://doi.org/10.1136/bmjopen-2020-046476.

[3] G.T. Voss, R.L. de Oliveira, M.J. Davies, W.B. Domingues, V.F. Campos, M.P. Soares, C. Luchese, C.H. Schiesser, E.A. Wilhelm, Suppressive effect of 1,4-anhydro-4-seleno-D-talitol (SeTal) on atopic dermatitis-like skin lesions in mice through regulation of inflammatory mediators, J. Trace Elem. Med. Biol. 67 (2021) 126795. https://doi.org/10.1016/j.jtemb.2021.126795.

[4] C. Storkey, D.I. Pattison, J.M. White, C.H. Schiesser, M.J. Davies, Preventing Protein Oxidation with Sugars: Scavenging of Hypohalous Acids by 5-Selenopyranose and 4-Selenofuranose Derivatives, Chem. Res. Toxicol. 25 (2012) 2589–2599. https://doi.org/10.1021/tx3003593.

[5] S. Adepu, S. Ramakrishna, Controlled Drug Delivery Systems: Current Status and Future Directions, Molecules. 26 (2021) 5905. https://doi.org/10.3390/molecules26195905.

[6] M.J. Davies, C.H. Schiesser, 1,4-Anhydro-4-seleno- <scp>d</scp> -talitol (SeTal): a remarkable selenium-containing therapeutic molecule, New J. Chem. 43 (2019) 9759–9765. https://doi.org/10.1039/C9NJ02185J.

[7] R. Naomi, H. Bahari, P.M. Ridzuan, F. Othman, Natural-Based Biomaterial for Skin Wound Healing (Gelatin vs. Collagen): Expert Review, Polymers (Basel). 13 (2021) 2319. https://doi.org/10.3390/polym13142319.

[8] A. Ahmady, N.H. Abu Samah, A review: Gelatine as a bioadhesive material for medical and pharmaceutical applications, Int. J. Pharm. 608 (2021) 121037. https://doi.org/10.1016/j.ijpharm.2021.121037.

[9] B. Cohen, O. Pinkas, M. Foox, M. Zilberman, Gelatin–alginate novel tissue adhesives and their formulation–strength effects, Acta Biomater. 9 (2013) 9004–

9011. https://doi.org/10.1016/j.actbio.2013.07.002.

[10] J. Sun, H. Tan, Alginate-Based Biomaterials for Regenerative Medicine Applications, Materials (Basel). 6 (2013) 1285–1309. https://doi.org/10.3390/ma6041285.

[11] A. Dodero, S. Alberti, G. Gaggero, M. Ferretti, R. Botter, S. Vicini, M. Castellano, An Up-to-Date Review on Alginate Nanoparticles and Nanofibers for Biomedical and Pharmaceutical Applications, Adv. Mater. Interfaces. 8 (2021) 2100809. https://doi.org/10.1002/admi.202100809.

[12] A. Das, S. Panda, Use of topical corticosteroids in dermatology: An evidence-based approach, Indian J. Dermatol. 62 (2017). https://doi.org/10.4103/ijd.IJD_169_17.

[13] G.T. Voss, M.S. Gularte, R.L. de Oliveira, C. Luchese, A.R. Fajardo, E.A. Wilhelm, Biopolymeric films as delivery vehicles for controlled release of hydrocortisone: Promising devices to treat chronic skin diseases, Mater. Sci. Eng. C. 114 (2020) 111074. https://doi.org/10.1016/j.msec.2020.111074.

[14] J. Moores, Vitamin C: a wound healing perspective, Br. J. Community Nurs. 18 (2013) S6–S11. https://doi.org/10.12968/bjcn.2013.18.Sup12.S6.

[15] K. Wang, H. Jiang, W. Li, M. Qiang, T. Dong, H. Li, Role of Vitamin C in Skin Diseases, Front. Physiol. 9 (2018). https://doi.org/10.3389/fphys.2018.00819.

[16] H. Assier, P. Wolkenstein, C. Grille, O. Chosidow, Contact dermatitis caused by ascorbyl tetraisopalmitate in a cream used for the management of atopic dermatitis, Contact Dermatitis. 71 (2014) 60–61. https://doi.org/10.1111/cod.12193.

[17] C. Pena Serna, J.F. Lopes Filho, Biodegradable Zein-Based Blend Films: Structural, Mechanical and Barrier Properties, Food Technol. Biotechnol. 53 (2015). https://doi.org/10.17113/ftb.53.03.15.3725.

[18] C.-C. Chan, C.-J. Liou, P.-Y. Xu, J.-J. Shen, M.-L. Kuo, W.-B. Len, L.-E. Chang, W.-C. Huang, Effect of dehydroepiandrosterone on atopic dermatitis-like skin lesions induced by 1-chloro-2,4-dinitrobenzene in mouse, J. Dermatol. Sci. 72 (2013) 149–157. https://doi.org/10.1016/j.jdermsci.2013.06.015.

[19] G. Park, H.G. Kim, S. Lim, W. Lee, Y. Sim, M.S. Oh, Coriander Alleviates 2,4-

Dinitrochlorobenzene-Induced Contact Dermatitis-Like Skin Lesions in Mice, J. Med. Food. 17 (2014) 862–868. https://doi.org/10.1089/jmf.2013.2910.

[20] H. Kim, J.R. Kim, H. Kang, J. Choi, H. Yang, P. Lee, J. Kim, K.W. Lee, 7,8,4′-Trihydroxyisoflavone Attenuates DNCB-Induced Atopic Dermatitis-Like Symptoms in NC/Nga Mice, PLoS One. 9 (2014) e104938. https://doi.org/10.1371/journal.pone.0104938.

[21] K. Suzuki, H. Ota, S. Sasagawa, T. Sakatani, T. Fujikura, Assay method for myeloperoxidase in human polymorphonuclear leukocytes, Anal. Biochem. 132 (1983) 345–352. https://doi.org/10.1016/0003-2697(83)90019-2.

[22] M.M. Bradford, A rapid and sensitive method for the quantitation of microgram quantities of protein utilizing the principle of protein-dye binding, Anal. Biochem. 72 (1976) 248–254. https://doi.org/10.1016/0003-2697(76)90527-3.

[23] K.M. Miranda, M.G. Espey, D.A. Wink, A Rapid, Simple Spectrophotometric Method for Simultaneous Detection of Nitrate and Nitrite, Nitric Oxide. 5 (2001) 62–71. https://doi.org/10.1006/niox.2000.0319.

[24] H. Staroszczyk, K. Sztuka, J. Wolska, A. Wojtasz-Pająk, I. Kołodziejska, Interactions of fish gelatin and chitosan in uncrosslinked and crosslinked with EDC films: FT-IR study, Spectrochim. Acta Part A Mol. Biomol. Spectrosc. 117 (2014) 707–712. https://doi.org/10.1016/j.saa.2013.09.044.

[25] Z. Hussain, H. Katas, M.C.I. Mohd Amin, E. Kumolosasi, F. Buang, S. Sahudin, Self-assembled polymeric nanoparticles for percutaneous co-delivery of hydrocortisone/hydroxytyrosol: An ex vivo and in vivo study using an NC/Nga mouse model, Int. J. Pharm. 444 (2013) 109–119. https://doi.org/10.1016/j.ijpharm.2013.01.024.

[26] G.T. Voss, M.S. Gularte, A.G. Vogt, J.L. Giongo, R.A. Vaucher, J.V.Z. Echenique, M.P. Soares, C. Luchese, E.A. Wilhelm, A.R. Fajardo, Polysaccharide-based film loaded with vitamin C and propolis: A promising device to accelerate diabetic wound healing, Int. J. Pharm. 552 (2018) 340–351. https://doi.org/10.1016/j.ijpharm.2018.10.009.

[27] M. Moghadam, M.S. Seyed Dorraji, F. Dodangeh, H.R. Ashjari, S.N. Mousavi, M.H. Rasoulifard, Design of a new light curable starch-based hydrogel drug

delivery system to improve the release rate of quercetin as a poorly water-soluble drug, Eur. J. Pharm. Sci. 174 (2022) 106191. https://doi.org/10.1016/j.ejps.2022.106191.

[28] A. Abruzzo, F. Bigucci, T. Cerchiara, F. Cruciani, B. Vitali, B. Luppi, Mucoadhesive chitosan/gelatin films for buccal delivery of propranolol hydrochloride, Carbohydr. Polym. 87 (2012) 581–588. https://doi.org/10.1016/j.carbpol.2011.08.024.

[29] J. Tarique, S.M. Sapuan, A. Khalina, Effect of glycerol plasticizer loading on the physical, mechanical, thermal, and barrier properties of arrowroot (Maranta arundinacea) starch biopolymers, Sci. Rep. 11 (2021) 13900. https://doi.org/10.1038/s41598-021-93094-y.

[30] G. Dabiri, E. Damstetter, T. Phillips, Choosing a Wound Dressing Based on Common Wound Characteristics, Adv. Wound Care. 5 (2016) 32–41. https://doi.org/10.1089/wound.2014.0586.

[31] N. Peppas, Hydrogels in pharmaceutical formulations, Eur. J. Pharm. Biopharm. 50 (2000) 27–46. https://doi.org/10.1016/S0939-6411(00)00090-4.

[32] M. Nagarsenker, U. Shinde, Characterization of gelatin-sodium alginate complex coacervation system, Indian J. Pharm. Sci. 71 (2009) 313. https://doi.org/10.4103/0250-474X.56033.

[33] A. Celebioglu, T. Uyar, Hydrocortisone/cyclodextrin complex electrospun nanofibers for a fast-dissolving oral drug delivery system, RSC Med. Chem. 11 (2020) 245–258. https://doi.org/10.1039/C9MD00390H.

[34] R.W. Korsmeyer, R. Gurny, E. Doelker, P. Buri, N.A. Peppas, Mechanisms of solute release from porous hydrophilic polymers, Int. J. Pharm. 15 (1983) 25–35. https://doi.org/10.1016/0378-5173(83)90064-9.

[35] S.T. Lopina, D.G. Kanjickal, Modeling of Drug Release from Polymeric Delivery Systems?A Review;, Crit. Rev. Ther. Drug Carrier Syst. 21 (2004) 345–386. https://doi.org/10.1615/CritRevTherDrugCarrierSyst.v21.i5.10.

[36] D.L.A. Sitta, M.R. Guilherme, E.P. da Silva, A.J.M. Valente, E.C. Muniz, A.F. Rubira, Drug release mechanisms of chemically cross-linked albumin

microparticles: Effect of the matrix erosion, Colloids Surfaces B Biointerfaces. 122 (2014) 404–413. https://doi.org/10.1016/j.colsurfb.2014.07.014.

[37] P. Bassi, G. Kaur, Polymeric films as a promising carrier for bioadhesive drug delivery: Development, characterization and optimization, Saudi Pharm. J. 25 (2017) 32–43. https://doi.org/10.1016/j.jsps.2015.06.003.

[38] K. Saito, O. Takenouchi, Y. Nukada, M. Miyazawa, H. Sakaguchi, An in vitro skin sensitization assay termed EpiSensA for broad sets of chemicals including lipophilic chemicals and pre/pro-haptens, Toxicol. Vitr. 40 (2017) 11–25. https://doi.org/10.1016/j.tiv.2016.12.005.

[39] G. Lin, S. Gao, J. Cheng, Y. Li, L. Shan, Z. Hu, 1 **β** -Hydroxyalantolactone, a sesquiterpene lactone from *Inula japonica* , attenuates atopic dermatitis-like skin lesions induced by 2,4-dinitrochlorobenzene in the mouse, Pharm. Biol. 54 (2016) 516–522. https://doi.org/10.3109/13880209.2015.1050745.

[40] G.-H. Moon, Y. Lee, E.-K. Kim, K.-H. Chung, K.-J. Lee, J.-H. An, Immunomodulatory and Anti-inflammatory Effects of Asiatic Acid in a DNCB-Induced Atopic Dermatitis Animal Model, Nutrients. 13 (2021) 2448. https://doi.org/10.3390/nu13072448.

[41] S.-C. Han, G.-J. Kang, Y.-J. Ko, H.-K. Kang, S.-W. Moon, Y.-S. Ann, E.-S. Yoo, Fermented fish oil suppresses T helper 1/2 cell response in a mouse model of atopic dermatitis via generation of CD4+CD25+Foxp3+ T cells, BMC Immunol. 13 (2012) 44. https://doi.org/10.1186/1471-2172-13-44.

[42] T.-K. Lin, L. Zhong, J. Santiago, Association between Stress and the HPA Axis in the Atopic Dermatitis, Int. J. Mol. Sci. 18 (2017) 2131. https://doi.org/10.3390/ijms18102131.

[43] E. Kasahara, M. Inoue, Cross-talk between HPA-axis-increased glucocorticoids and mitochondrial stress determines immune responses and clinical manifestations of patients with sepsis, Redox Rep. 20 (2015) 1–10. https://doi.org/10.1179/1351000214Y.0000000107.

[44] W. Frazier, N. Bhardwaj, Atopic Dermatitis: Diagnosis and Treatment, Am. Fam. Physician. 101 (2020).

[45] L.F. Eichenfield, W.L. Tom, T.G. Berger, A. Krol, A.S. Paller, K. Schwarzenberger, J.N. Bergman, S.L. Chamlin, D.E. Cohen, K.D. Cooper, K.M. Cordoro, D.M. Davis, S.R. Feldman, J.M. Hanifin, D.J. Margolis, R.A. Silverman, E.L. Simpson, H.C. Williams, C.A. Elmets, J. Block, C.G. Harrod, W.S. Begolka, R. Sidbury, Guidelines of care for the management of atopic dermatitis, J. Am. Acad. Dermatol. 71 (2014) 116–132. https://doi.org/10.1016/j.jaad.2014.03.023.

[46] D. Odobasic, A.R. Kitching, S.R. Holdsworth, Neutrophil-Mediated Regulation of Innate and Adaptive Immunity: The Role of Myeloperoxidase, J. Immunol. Res. 2016 (2016) 1–11. https://doi.org/10.1155/2016/2349817.

[47] L. Bertino, F. Guarneri, S.P. Cannavò, M. Casciaro, G. Pioggia, S. Gangemi, Oxidative Stress and Atopic Dermatitis, Antioxidants. 9 (2020) 196. https://doi.org/10.3390/antiox9030196.

[48] S. Dong, X. Lyu, S. Yuan, S. Wang, W. Li, Z. Chen, H. Yu, fengsheng Li, Q. Jiang, Oxidative stress: A critical hint in ionizing radiation induced pyroptosis, Radiat. Med. Prot. 1 (2020) 179–185. https://doi.org/10.1016/j.radmp.2020.10.001.

[49] C.A. Juan, J.M. Pérez de la Lastra, F.J. Plou, E. Pérez-Lebeña, The Chemistry of Reactive Oxygen Species (ROS) Revisited: Outlining Their Role in Biological Macromolecules (DNA, Lipids and Proteins) and Induced Pathologies, Int. J. Mol. Sci. 22 (2021) 4642. https://doi.org/10.3390/ijms22094642.

[50] O. Simonetti, T. Bacchetti, G. Ferretti, E. Molinelli, G. Rizzetto, L. Bellachioma, A. Offidani, Oxidative Stress and Alterations of Paraoxonases in Atopic Dermatitis, Antioxidants. 10 (2021) 697. https://doi.org/10.3390/antiox10050697.

[51] K. Blaschke, K.T. Ebata, M.M. Karimi, J.A. Zepeda-Martínez, P. Goyal, S. Mahapatra, A. Tam, D.J. Laird, M. Hirst, A. Rao, M.C. Lorincz, M. Ramalho-Santos, Vitamin C induces Tet-dependent DNA demethylation and a blastocyst-like state in ES cells, Nature. 500 (2013) 222–226. https://doi.org/10.1038/nature12362.

[52] H. Sies, Role of Metabolic H2O2 Generation, J. Biol. Chem. 289 (2014) 8735–8741. https://doi.org/10.1074/jbc.R113.544635.

[53] J. Manning, B. Mitchell, D.A. Appadurai, A. Shakya, L.J. Pierce, H. Wang, V.

Nganga, P.C. Swanson, J.M. May, D. Tantin, G.J. Spangrude, Vitamin C Promotes Maturation of T-Cells, Antioxid. Redox Signal. 19 (2013) 2054–2067. https://doi.org/10.1089/ars.2012.4988.

[54] H.H. Ng, C.H. Leo, K. O'Sullivan, S.-A. Alexander, M.J. Davies, C.H. Schiesser, L.J. Parry, 1,4-Anhydro-4-seleno-d-talitol (SeTal) protects endothelial function in the mouse aorta by scavenging superoxide radicals under conditions of acute oxidative stress, Biochem. Pharmacol. 128 (2017) 34–45. https://doi.org/10.1016/j.bcp.2016.12.019.

[55] B. Homey, M. Steinhoff, T. Ruzicka, D.Y.M. Leung, Cytokines and chemokines orchestrate atopic skin inflammation, J. Allergy Clin. Immunol. 118 (2006) 178–189. https://doi.org/10.1016/j.jaci.2006.03.047.

[56] L.M. Howe, Treatment of Endotoxic Shock: Glucocorticoids, Lazaroids, Nonsteroidals, Others, Vet. Clin. North Am. Small Anim. Pract. 28 (1998) 249–267. https://doi.org/10.1016/S0195-5616(98)82004-4.

Supporting information for

Evaluation of gelatin-alginate films containing 1,4-anhydro-4-seleno-*D*-talitol (SeTal) in the treatment of atopic dermatitis-like skin lesions in mice

Guilherme T. Voss[a], Michael J. Davies [c,d], Carl H. Schiesser[d], Renata L. De Oliveira[a], Andresa B. Nornberg[b], Victória Ross[b], Cristiane Luchese[a], André R. Fajardo[b*], and Ethel A. Wilhelm[a*]

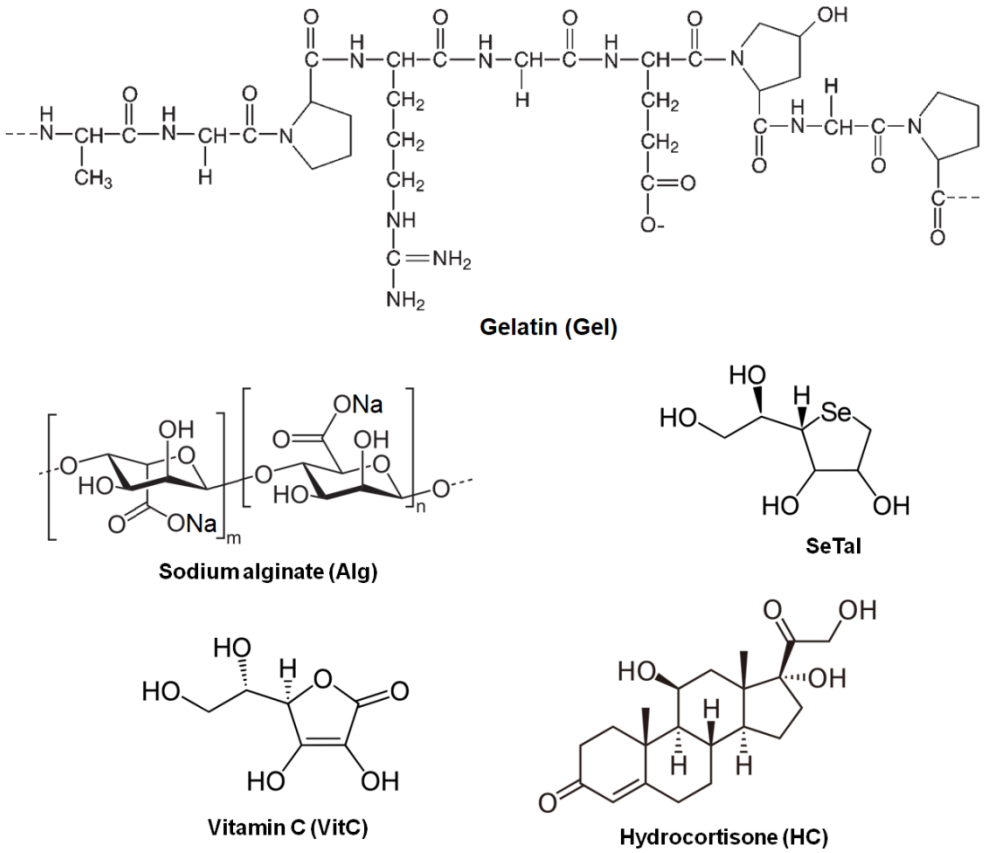

Figure S1. Compounds used in this study.

FTIR analysis

The spectrum of Alg exhibited a broad band centered at 3428 cm^{-1} related to the O–H stretching (hydroxyl groups) and bands in the range of 2970–2810 cm^{-1} attributed to C–H stretching (Figure S2). Characteristic bands of carboxylate groups stretching were observed at 1620 cm^{-1} (C=O asymmetric) and 1413 cm^{-1} (C=O symmetric), respectively. Bands in the range of 1150–950 cm^{-1} are attributed to the C–O stretching of the pyranose ring with contributions from C–C–H and C–OH deformations [1]. The bands noticed at 942, 887, and 815 cm^{-1} are assigned to the C–O stretching of uronic acid residues, β-C_1–H deformation, and mannuronic acid residues [2]. For Gel, the band centered at 3450 cm^{-1} is due to the O–H stretching (hydroxyl group) overlapping the band associated with the N–H stretching (primary amine and amide groups). Bands related to the C–H stretching (CH_2 and CH_3 groups) are observed in the range of 2990–2820 cm^{-1}, while the amide I band is at 1641 cm^{-1} [3]. This band overlapped the amide II band typically observed around 1540 cm^{-1}. Amide III band is noticed at 1235 cm^{-1}, respectively. The spectrum of SeTal exhibited a broad band centered around 3350 cm^{-1} related to O–H stretching (hydroxyl groups), bands in the range of 3000–2800 cm^{-1} are due to C-H stretching (CH_x groups), and the band at 1437 cm^{-1} is due to C–H bending (CH_2 groups). The band at 1353 cm^{-1} is due to the C–OH bending and bands in the range of 1200–950 cm^{-1} are attributed to C–O and C–C stretching. The band at 862 cm^{-1} is assigned to C–C ring stretching and the shoulder-type band at around 540 cm^{-1} refers to C–Se stretching [4]. For VitC, bands in the range of 3650–3150 cm^{-1} are related to the O-H stretching (free and H-bonded hydroxyl groups), while the bands in the range of 3050–2900 cm^{-1} are due to C–H stretching (CH and CH_2 groups). Bands at 1755 and 1652 cm^{-1} are attributed to the C=O and C=C stretching in the five-membered lactone ring. The band at 1322 cm^{-1} is due to the C–H wagging (CH_2 groups) and the bands in the range of 1200–950 cm^{-1} can be associated with C–O–C stretching, C–OH and C–H bending, and deformation of the lactone ring [5]. Finally, the band at 863 cm^{-1} is assigned to the C–C stretching in the lactone ring. The spectrum of HC exhibited bands in the range of 3600–3200 cm^{-1}due to the O–H stretching (hydroxyl groups), a band at 3016 cm^{-1} assigned to aromatic C–H stretching, and bands in the range of 2900–2800 cm^{-1} due to aliphatic C–H stretching (CH_2 and CH_3 groups). Two bands at 1743 cm^{-1} and 1725 cm^{-1} are due to C=O stretching (carbonyl groups) and the band at 1625 cm^{-1} is due to C=C stretching. Bands at 1326, 1272, and 1231 cm^{-1} are associated with C–C and C–O stretching. The bands associated

with the C–H in-plane and out-of-plane bending modes are observed in the range of 1150–850 cm^{-1} [6].

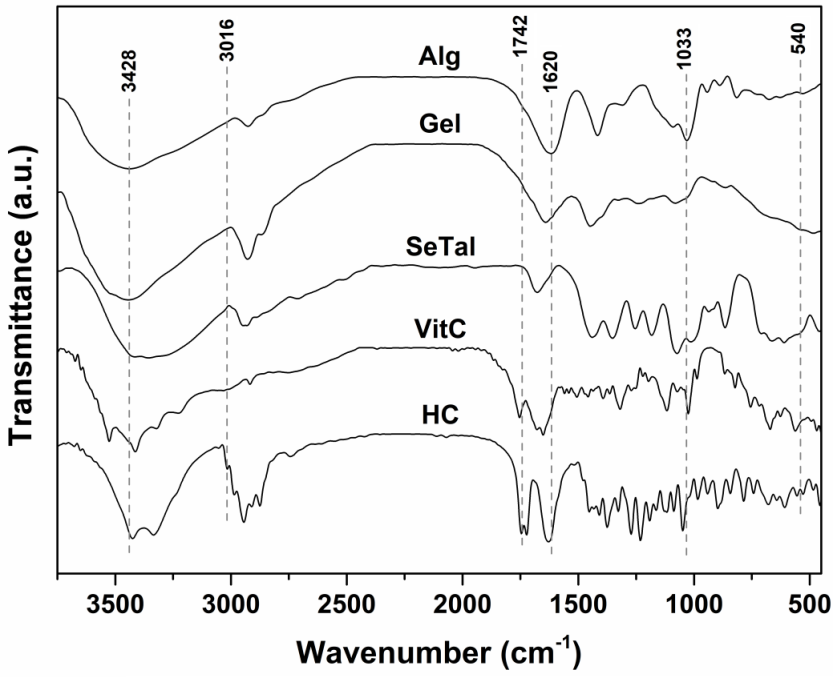

Figure S2. FTIR spectra of Alg, Gel, SeTal, VitC, and HC.

XRD analysis

As observed in Figure S3, the XRD patterns of SA and Gel exhibited broad-halo peaks at around 2θ ≈ 13.1º and 21.3º (for SA) and 7.9º and 20.3º (for Gel) denoting that both have a predominant amorphous nature, corroborating previous reports [7,8]. On the other hand, the encapsulated compounds (SeTal, VitC, and HC) exhibited several well-defined XRD peaks in the 2θ range analyzed. Overall, such diffraction patterns denote that all compounds have a highly crystalline nature with crystallites of different sizes. For SeTal, the main diffraction peaks were noticed at 2θ ≈ 11.0º, 14.2º, 17.3º, 19.6º, 21.8º, 22.9º, 24.8º, and 33.2º. Probably, the ordering of the SeTal structure is due to the intermolecular forces among their molecules (H-bonds, van de Waals, etc.). The main diffraction peaks for VitC were observed at 2θ ≈ 10.4º, 19.8º, 25.2º, 27.1º, and 35.5º [9], while HC diffraction peaks were observed at 2θ ≈ 12.0º, 15.7º, 16.5º, 16.9º, and 21.4º [10].

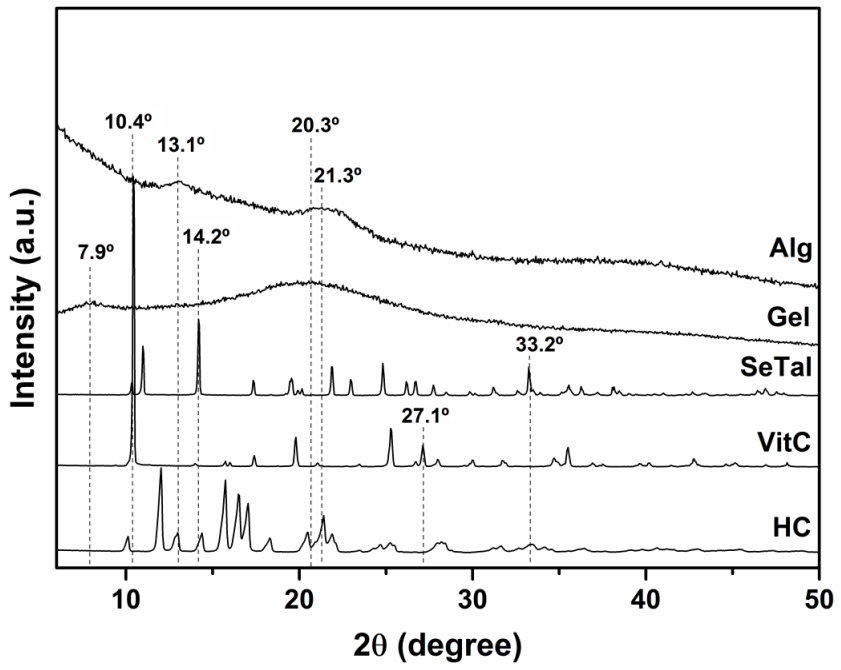

Figure S3. XRD pattern of Alg, Gel, SeTal, VitC, and HC.

Thermal analysis

TGA curve for Alg exhibited two main weight-loss stages, where the first (temperature range of 30–120 ºC) is due to the water evaporation and the second (range of 200–300 ºC) refers to its thermal decomposition [11] (Figure S4). For Gel, again two main weight-loss stages were noticed from its TGA curve. The first stage (range of 30–140 ºC) corresponds to dehydration and the second stage (range of 240–420 ºC) is attributable to the protein chain breakage and peptide chain rupture of Gel [12]. TGA curves of the encapsulated compounds (SeTal, VitC, or HC) did not exhibit the weight-loss stages associated with water evaporation. Indeed, it can be seen from Figure S4 that these three compounds have high thermal stability since they did not show weight loss at temperatures below 190 ºC. The thermal decomposition of SeTal occurs in two stages. The first (range of 220–315 ºC) is likely due to decarboxylation and dehydration reactions, while the second stage (temperature range of 320–400 ºC) encompasses decarboxylation and carbonization reactions. The TGA curve of VitC exhibited three-weight loss stages, which refers to their thermal decomposition. The first stage (range of 190–280 ºC) is due to the decarboxylation and dehydration reactions [13]. The second and third weight-loss stages (temperature ranges of 245–380 ºC and 390–500 ºC) are due to decarboxylation and decarbonylation reactions and a slow carbonization process [13]. The TGA curve of HC exhibited two main weight-loss stages associated with its thermal degradation. The first stage (range of 240–390 ºC) can be correlated to the decarboxylation and dehydration reactions, while the second stage (range of 240–500 ºC) refers to the carbonization of this compound [14].

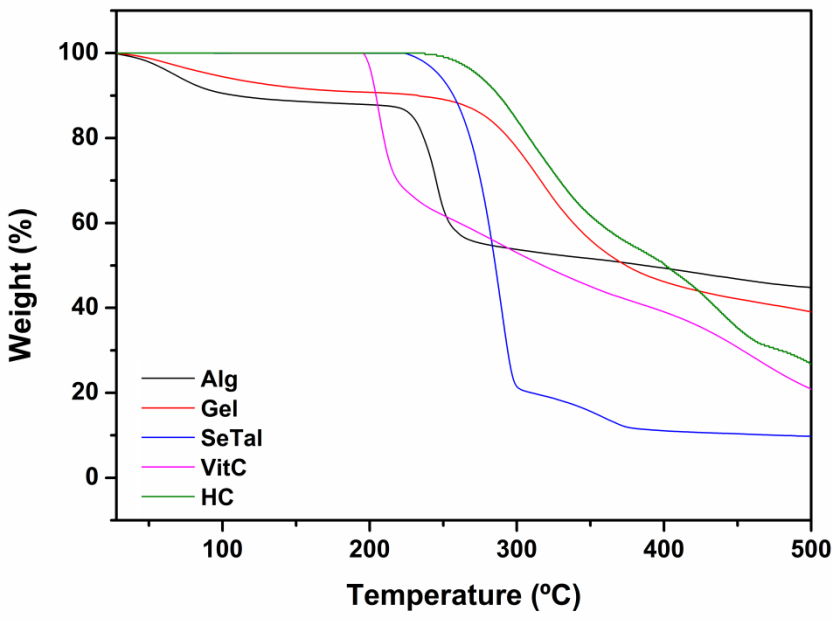

Figure S4. TGA curves of Alg, Gel, SeTal, VitC, and HC.

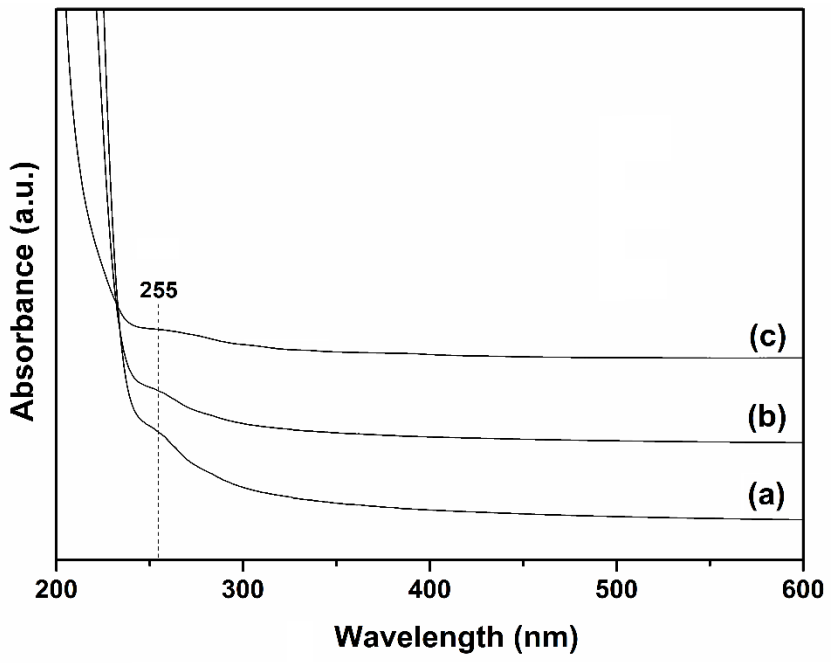

Figure S5. UV-Vis spectra of the release medium collected after 24 h from the acceptor compartment of the Franz cells for the experiments performed with (a) Gel-Alg/SeTal, (b) Gel-Alg/SeTal/HC, and (c) Gel-Alg/SeTal/VitC.

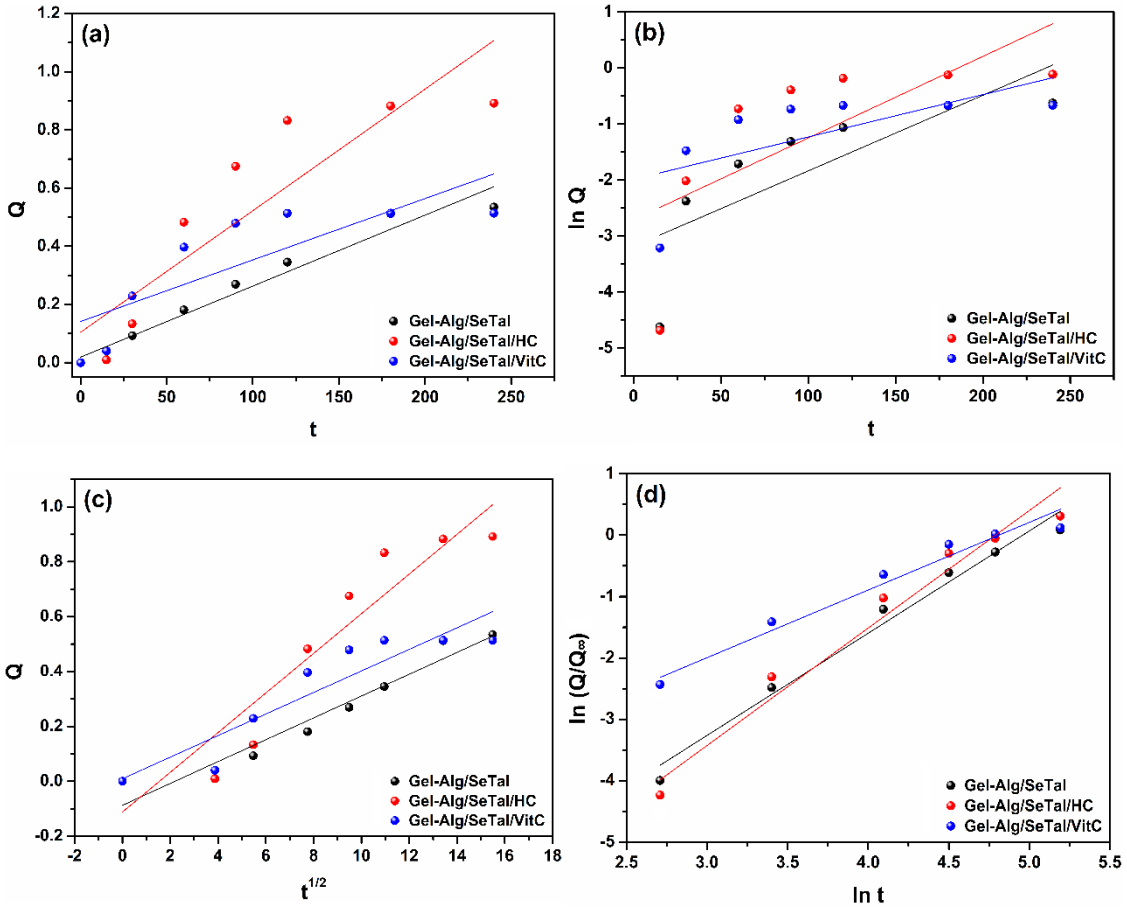

Figure S6. (a) Zero-order, (b) first-order, (c) Higuchi, and (d) Korsmeyer-Peppas plots for the release of SeTal from the prepared films.

References

[1] H. Daemi, M. Barikani, Synthesis and characterization of calcium alginate nanoparticles, sodium homopolymannuronate salt and its calcium nanoparticles, Sci. Iran. 19 (2012) 2023–2028. https://doi.org/10.1016/j.scient.2012.10.005.

[2] Z. Belattmania, S. Kaidi, S. El Atouani, C. Katif, F. Bentiss, C. Jama, A. Reani, B. Sabour, V. Vasconcelos, Isolation and FTIR-ATR and 1H NMR Characterization of Alginates from the Main Alginophyte Species of the Atlantic Coast of Morocco, Molecules. 25 (2020) 4335. https://doi.org/10.3390/molecules25184335.

[3] D.A. Prystupa, A.M. Donald, Infrared study of gelatin conformations in the gel and sol states, Polym. Gels Networks. 4 (1996) 87–110. https://doi.org/10.1016/0966-7822(96)00003-2.

[4] F.A. Devillanova, G. Verani, D.N. Sathyanarayana, An infrared spectroscopic investigation on *N* -methyl-1,3-thiazolidine-2-thione and -2-selone, J. Heterocycl. Chem. 15 (1978) 945–947. https://doi.org/10.1002/jhet.5570150609.

[5] C. Yohannan Panicker, H. Tresa Varghese, D. Philip, FT-IR, FT-Raman and SERS spectra of Vitamin C, Spectrochim. Acta Part A Mol. Biomol. Spectrosc. 65 (2006) 802–804. https://doi.org/10.1016/j.saa.2005.12.044.

[6] P. Manivannan, R.T. Kumar, V. Periyanayagasamy, Spectral analysis of hydrocortisone, J. Chem. Pharm. Sci. 5 (2009) 1–5.

[7] S. Bhagyaraj, I. Krupa, Alginate-Mediated Synthesis of Hetero-Shaped Silver Nanoparticles and Their Hydrogen Peroxide Sensing Ability, Molecules. 25 (2020) 435. https://doi.org/10.3390/molecules25030435.

[8] J. Peng, X. Wang, T. Lou, Preparation of chitosan/gelatin composite foam with ternary solvents of dioxane/acetic acid/water and its water absorption capacity, Polym. Bull. 77 (2020) 5227–5244. https://doi.org/10.1007/s00289-019-03016-2.

[9] R. Najafi-Taher, M.A. Derakhshan, R. Faridi-Majidi, A. Amani, Preparation of an ascorbic acid/PVA–chitosan electrospun mat: a core/shell transdermal delivery system, RSC Adv. 5 (2015) 50462–50469. https://doi.org/10.1039/C5RA03813H.

[10] H.S. Ali, S. Khan, P. York, S.M. Shah, J. Khan, Z. Hussain, B.A. Khan, A stable hydrocortisone nanosuspension for improved dissolution: Preparation, characterization and in vitro evaluation., Pak. J. Pharm. Sci. 30 (2017) 1635–1643.

[11] A.R. Fajardo, M.B. Silva, L.C. Lopes, J.F. Piai, A.F. Rubira, E.C. Muniz, Hydrogel based on an alginate–Ca2+/chondroitin sulfate matrix as a potential colon-specific drug delivery system, RSC Adv. 2 (2012) 11095.

https://doi.org/10.1039/c2ra20785k.

[12] N.C. Homem, T.D. Tavares, C.S. Miranda, J.C. Antunes, M.T.P. Amorim, H.P. Felgueiras, Functionalization of Crosslinked Sodium Alginate/Gelatin Wet-Spun Porous Fibers with Nisin Z for the Inhibition of Staphylococcus aureus-Induced Infections, Int. J. Mol. Sci. 22 (2021) 1930. https://doi.org/10.3390/ijms22041930.

[13] S. Jingyan, L. Yuwen, W. Zhiyong, W. Cunxin, Investigation of thermal decomposition of ascorbic acid by TG-FTIR and thermal kinetics analysis, J. Pharm. Biomed. Anal. 77 (2013) 116–119. https://doi.org/10.1016/j.jpba.2013.01.018.

[14] A. Celebioglu, T. Uyar, Hydrocortisone/cyclodextrin complex electrospun nanofibers for a fast-dissolving oral drug delivery system, RSC Med. Chem. 11 (2020) 245–258. https://doi.org/10.1039/C9MD00390H.

5. DISCUSSÃO

Os resultados dessa tese demonstram, pela primeira vez, *(i)* o efeito do SeTal nas lesões semelhates a DA em camundongos, *(ii)* a utilização de um filme de base biológica feito de gelatina e/ou amido para atuar como veículo para encapsulamento e liberação controlada de HC e *(iii)* o uso de filmes biopoliméricos constituídos de gelatina e alginato de sódio carregados com SeTal, SeTal + HC e SeTal + vitamina C, como uma abordagem para tratar lesões semelhantes a DA. Os resultados apresentados no primeiro estudo, revelam um efeito supressor do SeTal em lesões de pele, comportamento de coçar e edema da orelha induzido pela exposição ao DNCB, provavelmente por meio de uma redução dos processos inflamatórios locais.

Através dos resultados obtidos nessa tese, destaca-se a possibilidade da implementação de um futuro tratamento capaz de ser disponibilizado no Sistema Único de Saúde (SUS), que é um dos maiores e mais complexos sistemas de saúde pública do mundo. A possibilidade supracitada seria possível, devido aos resultados promissores do composto SeTal, aliados com a facilidade na produção dos filmes poliméricos utilizados. Torna-se importante salientar que o composto SeTal possui vantagens terapêuticas sobre outros compostos orgânicos de selênio, devido à sua alta solubilidade em água (permitindo depuração rápida e evitando qualquer bioacumulação aparente da droga em depósitos de gordura, que é um fator limitante de outros compostos dessa classe), baixa degradabilidade (permanece intacto durante armazenamento prolongado), pouca biotransformação e disponibilidade por via oral (Zacharias et al., 2020). A hipótese do mecanismo de ação do SeTal está relacionada com a normalização da atividade dos linfócitos Th2 e da redução da expressão de citocinas envolvidas na fisiopatologia da doença. Outro ponto importante que corroborou com a escolha do SeTal como possível tratamento para DA, é que possivelmente este composto reduz o estresse oxidativo principalmente pelo mecanismo de eliminação do radical superóxido (Zacharias et al., 2020).

O curso primário de tratamento para indivíduos com lesões de DA envolve o uso de corticosteroides tópicos devido a sua ação anti-inflamatória (Tan & Gonzalez, 2012). Porém, no primeiro estudo, foi observado um alto indice de mortalidade em animais sensibilizado pelo DNCB e submetido a HC durante o período de tratamento. A taxa de mortalidade observada nesse estudo, atrelada

aos efeitos adversos conhecidos da classe dos corticosteroides, impulsionaram a realização do segundo estudo utilizando o biomatrial para encapsulamento da HC.

Nesse contexto, os resultados obtidos no segundo estudo revelaram que a HC encapsulada não interagiu com as matrizes poliméricas, embora sua presença cause mudanças na mecânica e intumescimento dos filmes preparados. Experimentos de liberação *in vitro* mostraram que o mecanismo de liberação de HC é impulsionado por difusão para ambos os tipos de filme. Experimentos *in vivo* e *ex vivo* indicaram que todos filmes preparados (carregados ou não com HC) exercem efeitos positivos sobre os parâmetros avaliados no modelo de DA induzida por DNCB. No geral, os filmes carregados com HC foram mais efetivos no tratamento e atenuação de sintomas semelhantes aos da DA em comparação com o creme de HC comercial (1%) (utilizado como referência). Além disso, foi demonstrado que ambos os filmes carregados com HC exerceram menor toxicidade nos animais tratados do que o creme HC comercial (Voss et al., 2020).

Na fase de caracterização dos filmes, os materiais de partida utilizados foram caracterizados por análise de espectroscopia no infravermelho por transformada de Fourier (FTIR). Resumidamente, os espectros de gelatina e amido exibiram as principais bandas características de tais compostos corroborando com estudos anteriores (Ullah et al., 2019). O filme de gelatina exibiu as principais bandas provenientes da gelatina com algumas discrepâncias, provavelmente devido a presença de glicerol (plastificante). Com a adição do amido, nenhuma mudança aparente foi observada comparando com o filme de gelatina, resultados semelhantes foram relatados por Wang e colaboradores (2017). Os espectros de FTIR dos filmes carregados com HC foram semelhantes aos demais filmes, indicando que a HC não exerce um efeito perceptível na natureza química dos filmes. Os espectros dos filmes carregados com HC exibiram uma banda em 1742 cm^{-1}, atribuído ao alongamento C=O proveniente do HC. A presença de outras bandas de baixa intensidade na região de 1500-1200 cm^{-1} dos espectros destes filmes também podem ser associados a HC (Hussain et al., 2013). A partir desses dados, pode-se inferir que a HC foi eficientemente encapsulada em ambos os filmes; no entanto, nenhuma interação covalente aparente ocorre entre HC e as matrizes dos filmes.

No teste de análise termogravimétrica (TGA/DTG), a HC pura exibiu três perdas de pesos, estágios que começam em 218 °C e terminam em 635 °C, e seu principal estágio de decomposição tem uma temperatura máxima de 306 °C (Celebioglu & Uyar, 2020). No final da análise o resíduo de HC correspondia a 5% do seu peso inicial. O filme de gel exibiu dois estágios de perda de peso, o primeiro estágio (de 30 °C a 120 °C) é atribuído à perda de compostos voláteis e água, enquanto a segunda fase (de 120 °C a 520 °C) está associada à quebra da cadeia proteica e à ruptura da cadeia peptídica da gelatina (Soliman & Furuta, 2014). Além disso, a decomposição térmica do glicerol (o plastificante) ocorre entre 160 e 270 °C (Hoque et al., 2011). A estabilidade térmica do filme de gelatina foi significativamente alterada após a adição de HC na formulação do filme. A temperatura associada com a decomposição térmica da gelatina mudou de 332 °C para 257 °C para o filme de gelatina carregado com HC, o que pode sugerir que a droga afeta as interações inter e intramoleculares entre as correntes de gelatina. Além disso, as curvas TGA/DTG obtidas para o filme carregado com HC, não exibiram os estágios de degradação da HC, sugerindo que a droga está no estado amorfo dentro da matriz do filme, que é desejável, levando em consideração a dispersão de HC e a liberação subsequente (Celebioglu & Uyar, 2020).

Além disso, as curvas TGA/DTG do filme de gelatina+amido mostraram dois estágios de perda de peso, o primeiro é devido à perda de compostos voláteis e água (de 30 °C a 130 °C) enquanto a segunda (de 130 °C a 500 °C) refere-se à decomposição térmica de gelatina e amido (Quadrado & Fajardo, 2020; Podshivalov et al., 2017). A ausência de um novo estágio de perda de peso indica alta compatibilidade entre os polímeros, atribuindo esta compatibilidade com as inúmeras interações que ocorrem entre gelatina e amido. Provavelmente devido a essas interações, o carregamento de HC não afetou a estabilidade térmica do filme de gelatina+amido+HC (Soliman & Furuta, 2014). Através da Microscopia eletrônica de varredura (SEM), todos os filmes preparados foram uniformes, não porosos e apresentaram superfícies homogêneas, o que sugere boa compatibilidade entre materiais de partida (gelatina, amido e glicerol). De acordo com alguns autores, o glicerol pode atuar como plastificante e compatibilizante da mistura de gelatina/amido (Podshivalov et al., 2017). Estes resultados aliados ao teste de tração e intumescimento demonstram que os

filmes apresentaram características ideais para carrear a HC. Ambos os filmes carregados com HC têm capacidade de absorção de líquido, o que é desejável para tratar doenças de pele crônicas, como a DA. Tendo em vista que materiais expansíveis podem absorver exsudatos e fornecer um ambiente úmido, o que reduz o risco de escamação da pele e contaminação por microorganismos (Negut et al., 2018).

Os resultados promissores do SeTal no primeiro estudo e dos biofilmes no segudo estudo, impulsionaram a realização do terceiro projeto. Sendo assim, foi realizada a incorporação de SeTal, SeTal + HC e SeTal + vitamina C em biomateriais de gelatina e alginato de sódio. Os constituintes gelatina e alginato foram escolhidos considerando seus aspectos atrativos para a preparação de biomateriais para liberação tópica de fármacos na pele (Bhutani et al., 2016). A gelatina é um biopolímero solúvel em água derivado do colágeno amplamente utilizado para adesivos cutâneos devido às suas propriedades naturais atrativas (Xu et al., 2021). Por outro lado, o alginato é um polissacarídeo linear natural composto por unidades dos ácidos 1,4-β-D-manurônico e α-L-gulurônico, extraído comercialmente de algas marrons, com reconhecidas propriedades biológicas (Zdiri et al., 2022). Ademais, a utilização de vitamina C se deu por sua poderosa ação antioxidante natural que possui um papel fundamental em vários processos estruturais e funcionais da pele (Nielsen et al., 2021). Está bem estabelecido que a deficiência de vitamina C desencadeia ou agrava a ocorrência e o desenvolvimento de algumas doenças de pele, incluindo a DA (Chang et al., 2020). Além disso, a vitamina C atua na síntese de colágeno como um cofator importante para as enzimas lisil e prolil hidroxilases, auxiliando na formação dessa proteína que é de suma importancia na cicatrização (DePhillipo et al., 2018).

Várias formas de dermatose como a DA apresentam prurido intenso, dessa forma este parâmetro é um importante critério de diagnóstico. Frente a isso, o comportamento de coçar é uma possível abordagem para avaliar o efeito anti-pruriginoso dos tratamentos (G. Park & Oh, 2014). No primeiro estudo, o Setal foi capaz de reduzir o comportamento de coçar induzido pelo DNCB. Da mesma forma os biomateriais carragados com HC (segundo estudo) e SeTal, SeTal + HC ou SeTal + vitamina C (terceiro estudo), reduziram este comportamento nos camundongos. Estes resultados são importantes pois o prurido intenso e lesões

eczematosas são características da DA, e esses fatores causam estresse psicológico severo e afetam a qualidade de vida de pacientes com a doença (Bruno et al., 2016). Além disso, a pele afetada pela DA apresenta vermelhidão e coceira excessiva, podendo causar feridas na pele e vazamento de fluidos (Tokura, 2010).

Respostas alérgicas e inflamatórias repetidas em pacientes com DA, ao longo do tempo resultam em um endurecimento e espessamento da superfície da pele (Yarbrough et al., 2013). No primeiro estudo, o SeTal nas duas concentrações testadas (1% e 2%), atenuou a gravidade das lesões cutâneas induzidas por DNCB. Surpreendentemente, HC (1%, creme comercial) não alterou a gravidade das lesões induzidas por este hapteno. Os dados do SeTal são consistentes com os observados no comportamento de coçar, e isso destaca o possível efeito supressor desse composto contra as lesões cutâneas semelhantes a DA. Além disso, tratamento tópico com SeTal ou HC reduziu o edema de orelha dos animais expostos ao DNCB. Em paralelo, no segundo estudo o tratamento tópico com filmes carregados ou não com HC, foi capaz de reduzir a gravidade das lesões cutâneas induzidas por DNCB. Porém, os filmes carregados com HC tiveram uma melhora significativa em comparação com HC creme (1%) (medicamento de referência), tendo em vista que, nenhuma diferença significativa foi detectada após o tratamento com HC (1%) na gravidade das lesões cutâneas, quando comparado com o grupo induzido por DNCB. De acordo com os resultados obtidos, o presente estudo demonstra pela primeira vez, que os biomateriais reduziram os sinais de toxicidade causada por HC (creme comercial) durante o tratamento por um longo período e a gravidade das lesões em sintomas semelhantes aos da DA em camundongos. No terceiro estudo, o efeito do tratamento tópico com os biomateriais incorporados com SeTal, SeTal + HC e SeTal + vitamina C, foi realizado afim de avaliar o efeito sinérgico do SeTal com a HC e a vitamina C, bem como se a HC apresentaria efeito adversos após ser incorporada no filme biopolimérico e associada com o SeTal. Sendo assim, foi avaliada a gravidade da lesão da pele, comportamento de coçar e espessura da pele dorsal. O DNCB aumentou significativamente os escores de gravidade da pele, comportamento de coçar e espessamento da pele dorsal, quando comparado ao grupo controle. O tratamento tópico com os biomateriais carregados com SeTal, SeTal + HC ou SeTal + vitamina C,

reduziram a gravidade das lesões cutâneas induzidas pelo DNCB, comportamento de coçar e espessamento da pele dorsal. Os biomateriais carregados com SeTal, SeTal + HC ou SeTal + vitamina C, tiveram melhora significativa em relação ao HC creme.

A causa da DA é multifatorial e apresenta interação entre predisposição genética e fatores ambientais que iniciam a inflamação (Udompataikul & Limpa-o-vart, 2012). A pele afetada pelas lesões da DA apresenta vermelhidão, edema, pápulas eritematosas, que são características de processos inflamatórios (Tokura, 2010). A gravidade da inflamação pode ser facilmente avaliada pelo edema da orelha em modelos animais utilizando camundongos. Nos três estudos realizados, os tratamentos foram efetivos em reduzir o edema de orelha dos camundongos após a indução com DNCB. O edema de orelha observado nos camundongos ocorre devido ao processo inflamatório desencadeado pela aplicação tópica de DNCB, que também está relacionada à migração de células de defesa (leucócitos polimorfonucleares). Estes leucócitos polimorfonucleares podem ser estimados pela determinação da atividade da enzima MPO, a qual está bem estabelecida como um marcador de influxo de neutrófilos para o tecido (Odobasic et al., 2016). Dessa forma, em uma tentativa de vincular os efeitos supressores observados nos experimentos, com a modulação da inflamação, a atividade de MPO foi avaliada. A MPO é uma enzima presentes nos grânulos intracelulares de neutrófilos ativados, monócitos e alguns macrófagos (Davies et al., 2008). Portanto, devido a importância dos neutrófilos na patogênese de várias doenças, e a falta de estratégias eficazes para mensurá-los, tornam a MPO um potencial alvo terapêutico (Odobasic et al., 2016).

No primeiro estudo, o tratamento com SeTal foi capaz de reduzir a atividade da MPO tanto na pele dorsal quanto na pele da orelha, caracterizando assim uma atividade sistêmica deste composto. O SeTal 2% provou ser menos eficiente do que o 1% na normalização da atividade da MPO na pele dorsal. Uma explicação para esse resultado ainda não foi obtida. No entanto, com base em nosso conjunto de resultados, o SeTal é promissor para o tratamento de lesões associadas a DA; no entanto, este é um estudo preliminar. Por outro lado, a HC (creme comercial) foi eficaz apenas na redução da atividade da MPO na pele da orelha. Desta maneira, a aplicação tópica de SeTal foi capaz de reverter o quadro inflamatório induzido por DNCB e potencialmente aliviar os sintomas e lesões

cutâneas. Os biomateriais (segundo e terceiro estudo), de forma geral foram capazes de diminuir a atividade da MPO tanto na orelha como no dorso, quando comparado com camundongos expostos ao DNCB. Esses resultados corroboram com os do edema de orelha. Além disso, os biomateriais (HC, SeTal, SeTal + HC e SeTal + vitamina C), reduziram a atividade da MPO da orelha quando comparado ao creme HC (medicamento de referência). Ademais, o tratamento com os biomateriais carregados com HC no segundo estudo reduziram a sua atividade sistêmica, evitando a morte dos animais durante o experimento.

Os pacientes com DA possuem um subconjunto de linfócitos T e citocinas que podem ser usadas como biomarcadores para o diagnóstico de DA (Brandt & Sivaprasad, 2011). No primeiro estudo, o SeTal diminui a expressão de mRNA de citocinas envolvidas na fisiopatologia da DA, assim reduzindo a condição inflamatória e as respostas alérgicas desencadeadas por esses mediadores. No entanto, nenhuma alteração na expressão de TNF-α e IL-33 foi observada em animais tratados com HC (creme comercial). O TNF-α é uma potente citocina inflamatória bem conhecida que está envolvida na transdução do sinal da inflamação induzindo a migração do fator nuclear kappa B (NF-kB) para os núcleos dos queratinócitos e é um fator importante no controle da diferenciação celular e das respostas imunes, o que torna essa citocina um importante marcador da inflamação na DA (Jung et al., 2015). Acredita-se que IL-18 e IL-33 estejam envolvidas na patologia da DA, uma vez que essas citocinas pertencem a família IL-1, que é responsável por regular as respostas inflamatórias (Paller et al., 2017). Na verdade, a IL-18 pode estimular a resposta dos linfócitos T, visto que células epidérmicas dendríticas inflamatórias liberam IL-18 (Peng & Novak, 2015). Além disso, em um estudo anterior, um aumento nos níveis séricos de IL-18 foi observado em crianças, adultos e em um modelo experimental usando camundongos (Tanaka et al., 2001). A DA é mediada por uma resposta exacerbada do sistema imunológico. O baço é o maior órgão do sistema linfático e é responsável pela produção de células do sistema imunológico que combatem infecções (Moon et al., 2021). Assim, no terceiro estudo foi realizado as medidas de comprimento e o peso do baço para avaliar a esplenomegalia, o que indica uma anormalidade imunológica (Han et al., 2012). O tratamento com os filmes SeTal, SeTal + HC e SeTal + vitamina C, foram capazes de controlar alterações

no baço de animais expostos ao DNCB. Comparado ao grupo tratado com HC (creme comercial), o efeito do tratamento tópico com SeTal + HC foi mais eficaz no controle das alterações esplênicas. A HC é um análogo sintético do cortisol e sua administração a longo prazo é conhecida por resultar na supressão do eixo hipotálamo-hipófise-adrenal (HPA) e do hormônio adrenocorticotrófico (ACTH), o que leva a efeitos adversos como atrofia adrenal (Schäcke et al., 2002). Por sua vez, alterações no eixo HPA resultam em alterações no sistema imunológico e nas vias inflamatórias, conforme observado nesse estudo, através de alterações no baço de animais expostos ao DNCB. Assim, a encapsulação de HC em filmes biopoliméricos proporcionou redução dos efeitos adversos do HC tópico, bem como a sua incorporação com SeTal melhorou seus efeitos (Eyerich et al., 2013).

Os estudos histológicos revelam que os animais tratados com SeTal apresentam fibras de colágeno nas camadas superficiais e profundas da derme intercaladas com grande quantidade de fibroblastos jovens. Como esperado, o uso de HC (creme comercial) resultou na redução de fibras de colágeno que formaram bandas densas principalmente na derme superficial, que é um conhecido efeito colateral associado ao uso de corticosteroides (Howe, 1998). Os corticosteroides retardam a cicatrização porque inibem a expressão de interleucinas e fatores de crescimento responsáveis pela neovascularização e migração fibroblástica (Howe, 1998). Claramente, o SeTal fornece uma vantagem sobre o HC creme a este respeito, e foi relatado que melhora a cicatrização de feridas (Davies & Schiesser, 2019).

Quando o eixo HPA é estimulado, um aumento substancial na concentração plasmática de glicocorticóides pode ser observado, portanto, este é considerado um parâmetro adequado para avaliar níveis de estresse dos animais (Touma et al., 2003). No segundo estudo os níveis de corticosterona foram avaliados como marcador de estresse nos animais (Brown & Grunberg, 1995; Arndt et al., 2009). O tratamento com dois dos filmes testados (gelatina e gelatina+HC), reduziram os níveis de corticosterona plasmática quando comparado com o grupo induzido por DNCB e HC. Por outro lado, o tratamento com filme contendo apenas amido não reduziu os níveis de corticosterona quando comparado ao grupo induzido com DNCB. Como mencionado, a determinação da corticosterona plasmática é a maneira mais comum de analisar o nível de estresse de animais de laboratório.

No entanto, a corticosterona plasmática responde com sensibilidade a estressores, especialmente para pequenos animais (Touma et al., 2003). Assim, esse fator pode ter influenciado os resultados. Outra hipótese é que a corticosterona, sendo um análogo sintético de corticosterona, poderia ser detectada por meio de uma maior absorção sistêmica em alguns tratamentos, como o tratamento com o filme de gelatina+amido+HC. No entanto, os efeitos tóxicos observados quando existe uma maior absorção de HC não foram observados em nenhum dos tratamentos com os filmes. De acordo com isto, ao avaliar os marcadores de dano hepático foi demonstrado que o tratamento com a HC incorporado ao filme biopolimerico não apresentou toxicidade hepática.

Outro mecanismo importante estudado é o estresse oxidativo, que parece ser um fator que predispõe o patogênese da DA (Bertino et al., 2020). A inflamação da pele em pacientes com esta doença desempenha um papel importante na patogênese da doença, através da superprodução de agentes oxidantes como radicais livres e baixa capacidade de defesa antioxidante (Ji & Li, 2016). Existem diversos fatores endógenos e exógenos pelos quais ocorre o aumento da produção de espécies reativas, dentre eles está as respostas inflamatórias dos leucócitos envolvendo um desequilíbrio nos níveis de nitrito e nitrato (NOx) (Lambeth, 2007).

No terceiro estudo,foram avaliados os níveis de Nox na pele dorsal dos camundongos após o tratamento com os filmes biopoliméricos. Dessa forma, nesse estudo todos bioamateriais protegeram contra o aumento dos níveis de NOx induzido pela exposição ao DNCB. Além disso, vale ressaltar que a associação de SeTal a vitamina C, proporcionou efeito superior aos demais tratamentos utilizados. Esse resultado já era esperado, considerando que a vitamina C atua como um potente antioxidante natural, além de possuir propriedades anti-inflamatórias (Blaschke et al., 2013). O efeito antioxidante da vitamina C, desempenha um papel importante no metabolismo celular através da proteção contra as espécies reativas derivadas da atividade metabólica, protegendo assim os componentes biológicos dos danos oxidativos (Sies, 2014). Além disso, corroborando com as informações supracitadas, resultados encontrados em um estudo anterior, demonstraram que o SeTal foi capaz de modular a atividade antioxidante em camundongos, suprimindo os níveis de radicais superóxidos (Ng et al., 2017). Assim, acreditamos que o efeito

antioxidante do SeTal pode estar envolvido na redução de lesões cutâneas semelhantes a DA. Portanto, a combinação do efeito antioxidante e anti-inflamatório desse composto pode proporcionar uma terapia mais eficaz para o tratamento de lesões dessa patologia.

Em conjunto, os resultados apresentados nessa tese sugerem que os tratamentos utilizados *(i)* reduziram as lesões semelhantes a DA; *(ii)* reduziram o prurido; *(iii)* atenuaram a inflamação; *(iv)* modularam parâmetros imunológicos; *(v)* reduziram os níveis de um marcador de estresse oxidativo; *(vi)* aumentaram a síntese de colágeno e *(vii)* reduziram os efeitos adversos quando comparado ao medicamento de referência (HC creme), no modelo utilizando camundongos. Nesse sentido, os tratamentos testados podem ser uma abordagem multifuncional para a DA, uma condição multifatorial.

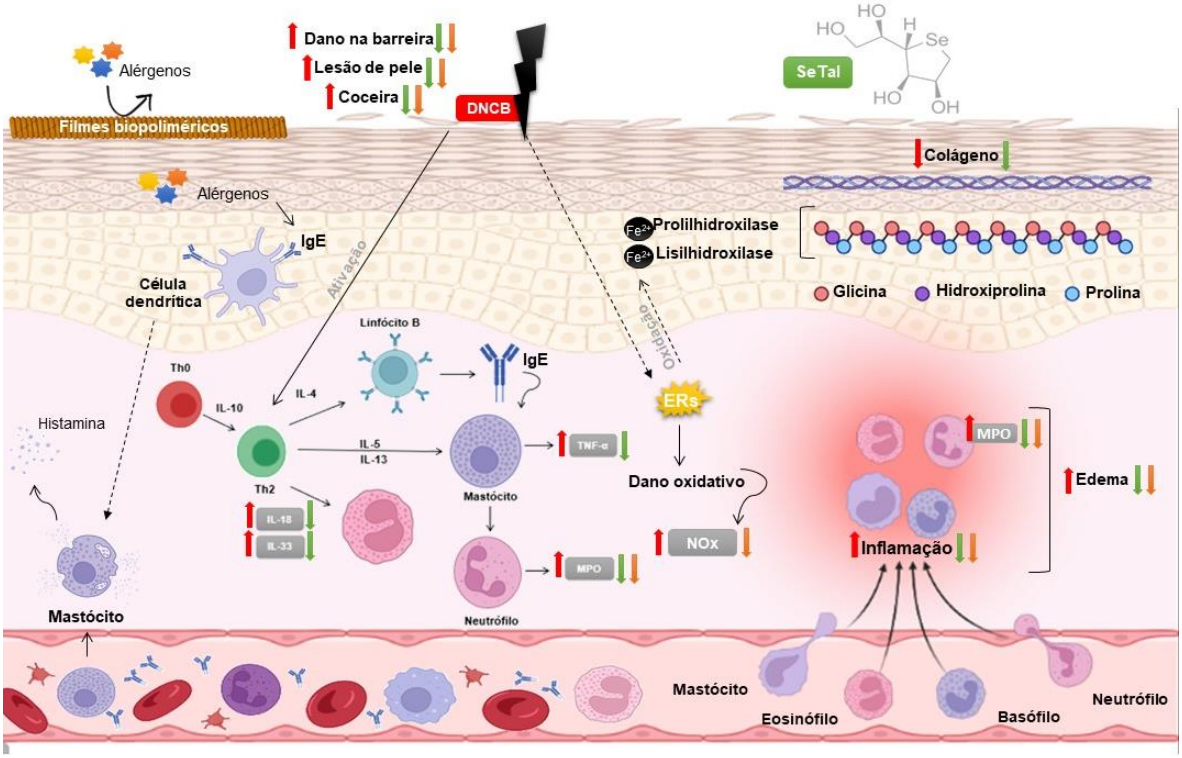

Figura 8. Resumo gráfico dos eventos ocasionados pelas induções com 2,4-dinitroclorobenzeno (DNCB), e dos mecanismos de ação do 1,4-anidro-4-seleno-D-talitol (SeTal) e filmes biopoliméricos em camunongos. Abreviações: 2,4-dinitroclorobenzeno (DNCB), Imunoglobulina E (IgE), Linfócito auxilar tipo 0 (Th0), Linfócito auxiliar tipo 2 (Th2), Interleucina (IL), Fator de necrose tumoral α (TNF-α), Mieloperoxidase (MPO), Espécies reativas (ERs). Fonte: Imagem do autor, 2022

6. CONCLUSÃO

Na presente tese o SeTal apresentou-se como uma alternativa de tratamento para as lesões semelhantes a DA. No geral, os tratamentos avaliados mostraram maior eficiência na atenuação dos sintomas e lesões semelhantes a DA e com efeitos adversos reduzidos em comparação com um dos tratamento utilizado para a DA, a HC creme. Ademais, cabe salientar que os biomateriais avaliados no segundo e terceiro estudo forneceram um curativo capaz de atuar como uma barreira física protegendo as lesões semelhantes à DA e prevenindo o contato da pele afetada com o meio externo, além de realizar a liberação controlada dos ativos, resultando em um menor número de aplicações e menores efeitos adversos. Dessa maneira, os biomaterias são classificados como veículos promissores para a liberação de ativos. Portanto, o SeTal pode ser uma importante alternativa terapêutica para o tratamento das lesões semelhantes a DA, além disso, quando incorporados juntamente nos filmes biopoliméricos o Setal, HC e a vitamina C tiveram resultados promissores e a HC (no filme biopolimérico) não apresentou efeito adverso.

7. PERPECTIVAS

Estudos adicionais também devem ser conduzidos no futuro para tratar de aspectos relacionados a concentração ótima de HC e SeTal nos filmes e penetração na pele após aplicação. Todas essas informações são obrigatórias para obter um dispositivo potencialmente aplicável no tratamento dessa patologia. Outro ponto importante que se deve destacar após a apresentação destes resultados é que a aplicação tanto do SeTal na sua forma livre como nos filme biopoliméricos pode ser estendida a outros estudos envolvendo doenças cutâneas/inflamatórias e até mesmo cicatrização de queimaduras.

8. REFERÊNCIAS

Arndt, S. S., Laarakker, M. C., van Lith, H. A., van der Staay, F. J., Gieling, E., Salomons, A. R., van't Klooster, J., & Ohl, F. (2009). Individual housing of mice--impact on behaviour and stress responses. *Physiology & Behavior*, *97*(3–4), 385–393. https://doi.org/10.1016/j.physbeh.2009.03.008

Azandaryani, A. H., Derakhshandeh, K., & Arkan, E. (2018). Electrospun nanobandage for hydrocortisone topical delivery as an antipsoriasis candidate. *International Journal of Polymeric Materials and Polymeric Biomaterials*, *67*(11), 677–685. https://doi.org/10.1080/00914037.2017.1375493

Ballaz, S. J., & Rebec, G. V. (2019). Neurobiology of vitamin C: Expanding the focus from antioxidant to endogenous neuromodulator. *Pharmacological Research*, *146*, 104321. https://doi.org/https://doi.org/10.1016/j.phrs.2019.104321

Basit, H. M., Cairul, M., Mohd, I., Ng, S., Katas, H., Shah, S. U., & Khan, N. R. (2020). Formulation and Evaluation of Microwave-Modified Chitosan-Curcumin Nanoparticles — A Promising Applications Following Burn Wounds. *Polymers*, *12*(2608), 1–20.

Berke, R., Singh, A., & Guralnick, M. (2012). Atopic dermatitis: an overview. *American Family Physician*, *86*(1), 35–42.

Bertino, L., Guarneri, F., Cannavò, S. P., Casciaro, M., Pioggia, G., & Gangemi, S. (2020). Oxidative stress and atopic dermatitis. *Antioxidants*, *9*(3), 1–15. https://doi.org/10.3390/antiox9030196

Bhutani, U., Laha, A., Mitra, K., & Majumdar, S. (2016). Sodium alginate and gelatin hydrogels: Viscosity effect on hydrophobic drug release. *Materials Letters*, *164*, 76–79. https://doi.org/https://doi.org/10.1016/j.matlet.2015.10.114

Bin, L., & Leung, D. Y. M. (2016). Genetic and epigenetic studies of atopic dermatitis. *Allergy, Asthma & Clinical Immunology*, *12*, 52. https://doi.org/10.1186/s13223-016-0158-5

Blaschke, K., Ebata, K. T., Karimi, M. M., Zepeda-Martínez, J. A., Goyal, P., Mahapatra, S., Tam, A., Laird, D. J., Hirst, M., Rao, A., Lorincz, M. C., & Ramalho-Santos, M. (2013). Vitamin C induces Tet-dependent DNA

demethylation and a blastocyst-like state in ES cells. *Nature*, *500*(7461), 222–226. https://doi.org/10.1038/nature12362

Brandt, E. B., & Sivaprasad, U. (2011). Th2 Cytokines and Atopic Dermatitis. *Journal of Clinical & Cellular Immunology*, *2*(3). https://doi.org/10.4172/2155-9899.1000110

Brown, K. J., & Grunberg, N. E. (1995). Effects of housing on male and female rats: crowding stresses male but calm females. *Physiology & Behavior*, *58*(6), 1085–1089. https://doi.org/10.1016/0031-9384(95)02043-8

Bruno, A., Habib, A., Zhang, Z., Li, Y., Chen, L., Du, Y., Huang, D., Han, H., & Dong, Z. (2016). *Fluoxetine Ameliorates Atopic Dermatitis-Like Skin Lesions in BALB/c Mice through Reducing Psychological Stress and Inflammatory Response*. https://doi.org/10.3389/fphar.2016.00318

Canevarolo, S. V. (2002). *CIÊNCIA DOS POLÍMEROS Um texto básico para tecnólogos e engenheiros 3ª edição-3ª reimpressão Revisada e ampliada*. *3 ed*, 53. www.artliber.com.br

Carl Herbert Schiesser, Corin Storkey, M. J. D. (2018). *Selenosugars for skin tissue repair*. https://patents.justia.com/patent/9895309

Cavalcanti, M. T., Silva, V. C., Costa, T. S., Florencio, I. M., & Florentino, E. R. (2011). Obtenção do amido do endocarpo da manga para diversificação produtiva na indústria de alimentos. *Revista Verde Agroecologia e Desenvolvimento Sustentável*, *6*, 80–83. http://www.gvaa.com.br/revista/index.php/RVADS/article/view/1135

Celebioglu, A., & Uyar, T. (2020). Hydrocortisone/cyclodextrin complex electrospun nanofibers for a fast-dissolving oral drug delivery system. *RSC Medicinal Chemistry*, *11*(2), 245–258. https://doi.org/10.1039/c9md00390h

Chabassol, A., & Green, P. (2012). Topical Corticosteroid Therapy : What You Need to Know. *Topical Corticosteroid Therapy: What You Need to Know*, *February*, 61–63.

Chang, C.-Y., Chen, J.-Y., Wu, M.-H., & Hu, M.-L. (2020). Therapeutic treatment with vitamin C reduces focal cerebral ischemia-induced brain infarction in rats by attenuating disruptions of blood brain barrier and cerebral neuronal apoptosis. *Free Radical Biology and Medicine*, *155*, 29–36. https://doi.org/https://doi.org/10.1016/j.freeradbiomed.2020.05.015

Chen, F.-M., & Liu, X. (2016). Advancing biomaterials of human origin for tissue

engineering. *Progress in Polymer Science*, *53*, 86–168. https://doi.org/10.1016/j.progpolymsci.2015.02.004

Cho, S.-M., Kim, M.-E., Kim, J.-Y., Park, J.-C., & Nahm, D.-H. (2014). Clinical Efficacy of Autologous Plasma Therapy for Atopic Dermatitis. *Dermatology*, *228*(1), 71–77. https://doi.org/10.1159/000356387

Cimmino, L., Neel, B. G., & Aifantis, I. (2018). Vitamin C in Stem Cell Reprogramming and Cancer. *Trends in Cell Biology*, *28*(9), 698–708. https://doi.org/https://doi.org/10.1016/j.tcb.2018.04.001

Comasseto, J. V. (1983). Vinylic selenides. *Journal of Organometallic Chemistry*, *253*(2), 131–181. https://doi.org/https://doi.org/10.1016/0022-328X(83)80118-1

Contardi, M., Heredia-Guerrero, J. A., Guzman-Puyol, S., Summa, M., Benítez, J. J., Goldoni, L., Caputo, G., Cusimano, G., Picone, P., Di Carlo, M., Bertorelli, R., Athanassiou, A., & Bayer, I. S. (2019). Combining dietary phenolic antioxidants with polyvinylpyrrolidone: transparent biopolymer films based on p-coumaric acid for controlled release. *J. Mater. Chem. B*, *7*(9), 1384–1396. https://doi.org/10.1039/C8TB03017K

Croft, L., Lu, J., Holmgren, A., & Khanna, K. (2007). From Selenium to Selenoproteins: Synthesis, Identity, and Their Role in Human Health. *Antioxidants & Redox Signaling*, *9*, 775–806. https://doi.org/10.1089/ars.2007.1528

Davies, M. J., Hawkins, C. L., Pattison, D. I., & Rees, M. D. (2008). Mammalian heme peroxidases: from molecular mechanisms to health implications. *Antioxidants & Redox Signaling*, *10*(7), 1199–1234. https://doi.org/10.1089/ars.2007.1927

Davies, M. J., & Schiesser, C. H. (2019). 1{,}4-Anhydro-4-seleno-d-talitol (SeTal): a remarkable selenium-containing therapeutic molecule. *New J. Chem.*, *43*(25), 9759–9765. https://doi.org/10.1039/C9NJ02185J

De Bezerril, B., & Sumário, A. (2014). Hipersensibilidade celular. *Imunologia Celular e Molecular*, 12. http://www.medicina.ufba.br/imuno/roteiros_imuno/hipersensibilidade_celular.pdf

de Bruin Weller, M. S., Knulst, A. C., Meijer, Y., Bruijnzeel-Koomen, C. A. F. M., & Pasmans, S. G. M. (2012). Evaluation of the child with atopic dermatitis.

Clinical and Experimental Allergy : Journal of the British Society for Allergy and Clinical Immunology, *42*(3), 352–362. https://doi.org/10.1111/j.1365-2222.2011.03899.x

de Oliveira, R. L., Voss, G. T., da C. Rodrigues, K., Pinz, M. P., Biondi, J. V., Becker, N. P., Blodorn, E., Domingues, W. B., Larroza, A., Campos, V. F., Alves, D., Wilhelm, E. A., & Luchese, C. (2022). Prospecting for a quinoline containing selenium for comorbidities depression and memory impairment induced by restriction stress in mice. *Psychopharmacology*, *239*(1), 59–81. https://doi.org/10.1007/s00213-021-06039-8

Dehghan Baniani, D., Bagheri, R., & Solouk, A. (2017). Preparation and characterization of a composite biomaterial including starch micro/nano particles loaded chitosan gel. *Carbohydrate Polymers*, *174*, 633–645. https://doi.org/https://doi.org/10.1016/j.carbpol.2017.06.095

Dehkharghani, R. A., Hosseinzadeh, M., Nezafatdoost, F., & Jahangiri, J. (2018). Application of Methodological Analysis for Hydrocortisone Nanocapsulation in Biodegradable Polyester and MTT Assay. *Polymer Science, Series A*, *60*(6), 770–776. https://doi.org/10.1134/S0965545X18070027

DePhillipo, N. N., Aman, Z. S., Kennedy, M. I., Begley, J. P., Moatshe, G., & LaPrade, R. F. (2018). Efficacy of Vitamin C Supplementation on Collagen Synthesis and Oxidative Stress After Musculoskeletal Injuries: A Systematic Review. *Orthopaedic Journal of Sports Medicine*, *6*(10), 2325967118804544. https://doi.org/10.1177/2325967118804544

Eichenfield, L. F., Tom, W. L., Berger, T. G., Krol, A., Paller, A. S., Schwarzenberger, K., Bergman, J. N., Chamlin, S. L., Cohen, D. E., Cooper, K. D., Cordoro, K. M., Davis, D. M., Feldman, S. R., Hanifin, J. M., Margolis, D. J., Silverman, R. A., Simpson, E. L., Williams, H. C., Elmets, C. A., … Sidbury, R. (2014). Guidelines of care for the management of atopic dermatitis: section 2. Management and treatment of atopic dermatitis with topical therapies. *Journal of the American Academy of Dermatology*, *71*(1), 116–132. https://doi.org/10.1016/j.jaad.2014.03.023

Eyerich, K., Novak, N., Eyerich, K., & Weidinger, S. (2013). *Immunology of atopic eczema: overcoming the Th1/Th2 paradigm*. https://doi.org/10.1111/all.12184

Fakhreddin Hosseini, S., Rezaei, M., Zandi, M., & Ghavi, F. F. (2013).

Preparation and functional properties of fish gelatin-chitosan blend edible films. *Food Chemistry*, *136*(3–4), 1490–1495. https://doi.org/10.1016/j.foodchem.2012.09.081

Forouzandehdel, S., Forouzandehdel, S., & Rezghi Rami, M. (2020). Synthesis of a novel magnetic starch-alginic acid-based biomaterial for drug delivery. *Carbohydrate Research*, *487*, 107889. https://doi.org/https://doi.org/10.1016/j.carres.2019.107889

Gómez-Guillén, M. C., Giménez, B., López-Caballero, M. E., & Montero, M. P. (2011). Functional and bioactive properties of collagen and gelatin from alternative sources: A review. *Food Hydrocolloids*, *25*(8), 1813–1827. https://doi.org/https://doi.org/10.1016/j.foodhyd.2011.02.007

Goodwin, J. S., Atluru, D., Sierakowski, S., & Lianos, E. A. (1986). Mechanism of action of glucocorticosteroids. Inhibition of T cell proliferation and interleukin 2 production by hydrocortisone is reversed by leukotriene B4. *The Journal of Clinical Investigation*, *77*(4), 1244–1250. https://doi.org/10.1172/JCI112427

Hamilton, J. D., Ungar, B., & Guttman-Yassky, E. (2015). Drug evaluation review: dupilumab in atopic dermatitis. *Immunotherapy*, *7*(10), 1043–1058. https://doi.org/10.2217/imt.15.69

Han, S.-C., Kang, G.-J., Ko, Y.-J., Kang, H.-K., Moon, S.-W., Ann, Y.-S., & Yoo, E.-S. (2012). Fermented fish oil suppresses T helper 1/2 cell response in a mouse model of atopic dermatitis via generation of CD4+CD25+Foxp3+ T cells. *BMC Immunology*, *13*, 44. https://doi.org/10.1186/1471-2172-13-44

Harrington, W. F., & Von Hippel, P. H. (1962). *The Structure Of Collagen And Gelatin* (C. B. Anfinsen, M. L. Anson, K. Bailey, & J. T. Edsall (eds.); Vol. 16, pp. 1–138). Academic Press. https://doi.org/https://doi.org/10.1016/S0065-3233(08)60028-5

Hennino, A., Saint-Mezard, P., Nicolas, J. F., Vocanson, M., Dubois, B., Chavagnac, C., & Kaiserlian, D. (2005). Update on the pathophysiology with special emphasis on CD8 effector T cells and CD4 regulatory T cells. *Anais Brasileiros de Dermatologia*, *80*(4), 335–350. https://doi.org/10.1590/s0365-05962005000400003

Hocking, P. J. (1992). The Classification, Preparation, and Utility of Degradable Polymers. *Journal of Macromolecular Science, Part C*, *32*(1), 35–54. https://doi.org/10.1080/15321799208018378

Hoque, M. S., Benjakul, S., & Prodpran, T. (2011). Effects of partial hydrolysis and plasticizer content on the properties of film from cuttlefish (Sepia pharaonis) skin gelatin. *Food Hydrocolloids*, *25*(1), 82–90. https://doi.org/10.1016/j.foodhyd.2010.05.008

Howe, L. M. (1998). Treatment of endotoxic shock: glucocorticoids, lazaroids, nonsteroidals, others. *The Veterinary Clinics of North America. Small Animal Practice*, *28*(2), 249–267. https://doi.org/10.1016/s0195-5616(98)82004-4

Huang, S., & Fu, X. (2010). Naturally derived materials-based cell and drug delivery systems in skin regeneration. *Journal of Controlled Release : Official Journal of the Controlled Release Society*, *142*(2), 149–159. https://doi.org/10.1016/j.jconrel.2009.10.018

Hussain, Z., Katas, H., Mohd Amin, M. C. I., Kumolosasi, E., Buang, F., & Sahudin, S. (2013). Self-assembled polymeric nanoparticles for percutaneous co-delivery of hydrocortisone/hydroxytyrosol: an ex vivo and in vivo study using an NC/Nga mouse model. *International Journal of Pharmaceutics*, *444*(1–2), 109–119. https://doi.org/10.1016/j.ijpharm.2013.01.024

Jacob, J., Haponiuk, J. T., Thomas, S., & Gopi, S. (2018). Biopolymer based nanomaterials in drug delivery systems: A review. *Materials Today Chemistry*, *9*, 43–55. https://doi.org/https://doi.org/10.1016/j.mtchem.2018.05.002

Ji, H., & Li, X. K. (2016). Oxidative Stress in Atopic Dermatitis. *Oxidative Medicine and Cellular Longevity*, *2016*(Figure 1). https://doi.org/10.1155/2016/2721469

Ju Ho, P., Jun Sung, J., Ki Cheon, K., & Jin Tae, H. (2018). Anti-inflammatory effect of Centella asiatica phytosome in a mouse model of phthalic anhydride-induced atopic dermatitis. *Phytomedicine*, *43*, 110–119. https://doi.org/https://doi.org/10.1016/j.phymed.2018.04.013

Jung, M., Lee, T. H., Oh, H. J., Kim, H., Son, Y., Lee, E. H., & Kim, J. (2015). Inhibitory effect of 5,6-dihydroergosteol-glucoside on atopic dermatitis-like skin lesions via suppression of NF-κB and STAT activation. *Journal of Dermatological Science*, *79*(3), 252–261. https://doi.org/10.1016/j.jdermsci.2015.06.005

Kalish, R. S., & Askenase, P. W. (1999). Molecular mechanisms of CD8+ T cell-

mediated delayed hypersensitivity: implications for allergies, asthma, and autoimmunity. *The Journal of Allergy and Clinical Immunology*, *103*(2 Pt 1), 192–199. https://doi.org/10.1016/s0091-6749(99)70489-6

Kaplan, D. H., Igyártó, B. Z., & Gaspari, A. A. (2012). Early immune events in the induction of allergic contact dermatitis. *Nature Reviews Immunology*, *12*(2), 114–124. https://doi.org/10.1038/nri3150

Keet, C. A., & Wood, R. A. (2014). Emerging therapies for food allergy. *The Journal of Clinical Investigation*, *124*(5), 1880–1886. https://doi.org/10.1172/JCI72061

Kieliszek, M., & Błażejak, S. (2016). Current Knowledge on the Importance of Selenium in Food for Living Organisms: A Review. *Molecules (Basel, Switzerland)*, *21*(5). https://doi.org/10.3390/molecules21050609

Kim, D., Kobayashi, T., & Nagao, K. (2019). Research Techniques Made Simple: Mouse Models of Atopic Dermatitis. *The Journal of Investigative Dermatology*, *139*(5), 984-990.e1. https://doi.org/10.1016/j.jid.2019.02.014

Kim, H., Kim, J. R., Kang, H., Choi, J., Yang, H., Lee, P., Kim, J., & Lee, K. W. (2014). 7,8,4'-Trihydroxyisoflavone attenuates DNCB-induced atopic dermatitis-like symptoms in NC/Nga mice. *PloS One*, *9*(8), e104938. https://doi.org/10.1371/journal.pone.0104938

Krogars, K., Heinämäki, J., Karjalainen, M., Rantanen, J., Luukkonen, P., & Yliruusi, J. (2003). Development and characterization of aqueous amylose-rich maize starch dispersion for film formation. *European Journal of Pharmaceutics and Biopharmaceutics : Official Journal of Arbeitsgemeinschaft Fur Pharmazeutische Verfahrenstechnik e.V*, *56*(2), 215–221. https://doi.org/10.1016/s0939-6411(03)00064-x

Lai-Cheong, J. E., & McGrath, J. A. (2017). Structure and function of skin, hair and nails. In *Medicine (United Kingdom)* (Vol. 45, Issue 6, pp. 347–351). Elsevier Ltd. https://doi.org/10.1016/j.mpmed.2017.03.004

Lambeth, J. D. (2007). Nox enzymes, ROS, and chronic disease: An example of antagonistic pleiotropy. *Free Radical Biology and Medicine*, *43*(3), 332–347. https://doi.org/https://doi.org/10.1016/j.freeradbiomed.2007.03.027

Lee, H.-C., & Park, S.-Y. (2019). Preliminary Comparison of the Efficacy and Safety of Needle-Embedding Therapy with Acupuncture for Atopic Dermatitis Patients. *Evidence-Based Complementary and Alternative Medicine*, *2019*,

6937942. https://doi.org/10.1155/2019/6937942

Lee, K. Y., & Mooney, D. J. (2012). Alginate: Properties and biomedical applications. *Progress in Polymer Science*, *37*(1), 106–126. https://doi.org/https://doi.org/10.1016/j.progpolymsci.2011.06.003

Lim, H., Song, K., Kim, R., Sim, J., Park, E., Ahn, K., Kim, J., & Han, Y. (2013). Nutrient intake and food restriction in children with atopic dermatitis. *Clinical Nutrition Research*, *2*(1), 52–58. https://doi.org/10.7762/cnr.2013.2.1.52

Lin, G., Gao, S., Cheng, J., Li, Y., Shan, L., & Hu, Z. (2016). 1β-Hydroxyalantolactone, a sesquiterpene lactone from Inula japonica, attenuates atopic dermatitis-like skin lesions induced by 2,4-dinitrochlorobenzene in the mouse. *Pharmaceutical Biology*, *54*(3), 516–522. https://doi.org/10.3109/13880209.2015.1050745

Lu, J., & Holmgren, A. (2009). Selenoproteins. *The Journal of Biological Chemistry*, *284*(2), 723–727. https://doi.org/10.1074/jbc.R800045200

Malajian, D., & Guttman-Yassky, E. (2015). New pathogenic and therapeutic paradigms in atopic dermatitis. *Cytokine*, *73*(2), 311–318. https://doi.org/10.1016/j.cyto.2014.11.023

Malekhosseini, S., Rezaie, A., Khaledian, S., Abdoli, M., Zangeneh, M. M., Hosseini, A., & Behbood, L. (2020). Fabrication and characterization of hydrocortisone loaded Dextran-Poly Lactic-co-Glycolic acid micelle. *Heliyon*, *6*(5), e03975. https://doi.org/10.1016/j.heliyon.2020.e03975

Meena, S., Gupta, L. K., Khare, A. K., Balai, M., Mittal, A., Mehta, S., & Bhatri, G. (2017). Topical Corticosteroids Abuse: A Clinical Study of Cutaneous Adverse Effects. *Indian Journal of Dermatology*, *62*(6), 675. https://doi.org/10.4103/ijd.IJD_110_17

Moon, G. H., Lee, Y., Kim, E. K., Chung, K. H., Lee, K. J., & An, J. H. (2021). Immunomodulatory and anti-inflammatory effects of asiatic acid in a dncb-induced atopic dermatitis animal model. *Nutrients*, *13*(7). https://doi.org/10.3390/nu13072448

More, R., Haubold, A., & Bokros, J. (1996). Chapter: Biomaterials Science: An Introduction to Materials in Medicine. In *Pyrolytic carbon for long-term medical implants* (pp. 170–180).

Negut, I., Grumezescu, V., & Grumezescu, A. M. (2018). Treatment Strategies for Infected Wounds. *Molecules (Basel, Switzerland)*, *23*(9), 2392.

https://doi.org/10.3390/molecules23092392

Ng, H. H., Leo, C. H., O'Sullivan, K., Alexander, S.-A., Davies, M. J., Schiesser, C. H., & Parry, L. J. (2017). 1,4-Anhydro-4-seleno-d-talitol (SeTal) protects endothelial function in the mouse aorta by scavenging superoxide radicals under conditions of acute oxidative stress. *Biochemical Pharmacology*, *128*, 34–45. https://doi.org/https://doi.org/10.1016/j.bcp.2016.12.019

Nielsen, C. W., Rustad, T., & Holdt, S. L. (2021). Vitamin C from Seaweed: A Review Assessing Seaweed as Contributor to Daily Intake. In *Foods* (Vol. 10, Issue 1). https://doi.org/10.3390/foods10010198

Nogueira, C. W., Zeni, G., & Rocha, J. B. T. (2004). Organoselenium and organotellurium compounds: toxicology and pharmacology. *Chemical Reviews*, *104*(12), 6255–6285. https://doi.org/10.1021/cr0406559

O'Brien, F. J. (2011). Biomaterials & scaffolds for tissue engineering. *Materials Today*, *14*(3), 88–95. https://doi.org/https://doi.org/10.1016/S1369-7021(11)70058-X

Odobasic, D., Kitching, A. R., & Holdsworth, S. R. (2016). Neutrophil-Mediated Regulation of Innate and Adaptive Immunity: The Role of Myeloperoxidase. *Journal of Immunology Research*, *2016*, 2349817. https://doi.org/10.1155/2016/2349817

Ong, P. Y., & Boguniewicz, M. (2008). Atopic Dermatitis. *Primary Care: Clinics in Office Practice*, *35*(1), 105–117. https://doi.org/10.1016/j.pop.2007.09.006

Paller, A. S., Kabashima, K., & Bieber, T. (2017). Therapeutic pipeline for atopic dermatitis: End of the drought? *The Journal of Allergy and Clinical Immunology*, *140*(3), 633–643. https://doi.org/10.1016/j.jaci.2017.07.006

Park, G., & Oh, M. S. (2014). Inhibitory effects of Juglans mandshurica leaf on allergic dermatitis-like skin lesions-induced by 2,4-dinitrochlorobenzene in mice. *Experimental and Toxicologic Pathology : Official Journal of the Gesellschaft Fur Toxikologische Pathologie*, *66*(2–3), 97–101. https://doi.org/10.1016/j.etp.2013.10.001

Park, M. E., & Zippin, J. H. (2014). Allergic Contact Dermatitis to Cosmetics. *Dermatologic Clinics*, *32*(1), 1–11. https://doi.org/https://doi.org/10.1016/j.det.2013.09.006

Patel, N., & Gohil, P. (2012). *A Review on Biomaterials : Scope , Applications & Human Anatomy Significance*.

Pawlowska, E., Szczepanska, J., & Blasiak, J. (2019). Pro- and Antioxidant Effects of Vitamin C in Cancer in correspondence to Its Dietary and Pharmacological Concentrations. *Oxidative Medicine and Cellular Longevity*, *2019*, 7286737. https://doi.org/10.1155/2019/7286737

Peng, W., & Novak, N. (2015). Pathogenesis of atopic dermatitis. *Clinical and Experimental Allergy : Journal of the British Society for Allergy and Clinical Immunology*, *45*(3), 566–574. https://doi.org/10.1111/cea.12495

Pinz, M. P., dos Reis, A. S., Vogt, A. G., Krüger, R., Alves, D., Jesse, C. R., Roman, S. S., Soares, M. P., Wilhelm, E. A., & Luchese, C. (2018). Current advances of pharmacological properties of 7-chloro-4-(phenylselanyl) quinoline: Prevention of cognitive deficit and anxiety in Alzheimer's disease model. *Biomedicine & Pharmacotherapy*, *105*, 1006–1014. https://doi.org/https://doi.org/10.1016/j.biopha.2018.06.049

Pires, A. L. R., Bierhalz, A. C. K., & Moraes, Â. M. (2015). Biomateriais: Tipos, aplicações e mercado. *Quimica Nova*, *38*(7), 957–971. https://doi.org/10.5935/0100-4042.20150094

Podshivalov, A., Zakharova, M., Glazacheva, E., & Uspenskaya, M. (2017). Gelatin/potato starch edible biocomposite films: Correlation between morphology and physical properties. *Carbohydrate Polymers*, *157*, 1162–1172. https://doi.org/10.1016/j.carbpol.2016.10.079

Prete, A., Taylor, A. E., Bancos, I., Smith, D. J., Foster, M. A., Kohler, S., Fazal-Sanderson, V., Komninos, J., O'Neil, D. M., Vassiliadi, D. A., Mowatt, C. J., Mihai, R., Fallowfield, J. L., Annane, D., Lord, J. M., Keevil, B. G., Wass, J. A. H., Karavitaki, N., & Arlt, W. (2020). Prevention of Adrenal Crisis: Cortisol Responses to Major Stress Compared to Stress Dose Hydrocortisone Delivery. *The Journal of Clinical Endocrinology & Metabolism*, *105*(7), 2262–2274. https://doi.org/10.1210/clinem/dgaa133

Quadrado, R. F. N., & Fajardo, A. R. (2020). Microparticles based on carboxymethyl starch/chitosan polyelectrolyte complex as vehicles for drug delivery systems. *Arabian Journal of Chemistry*, *13*(1), 2183–2194. https://doi.org/10.1016/j.arabjc.2018.04.004

Radosinski, L., Labus, K., Zemojtel, P., & Wojciechowski, J. W. (2019). *molecules Development and Validation of a Virtual Gelatin Model Using Molecular Modeling Computational Tools*. https://doi.org/10.3390/molecules24183365

Ratner, B. D., Hoffman, A. S., Schoen, F. J., & Lemons, J. E. (2013). Introduction - Biomaterials Science: An Evolving, Multidisciplinary Endeavor. *Biomaterials Science: An Introduction to Materials: Third Edition*, xxv–xxxix. https://doi.org/10.1016/B978-0-08-087780-8.00153-4

Reis, A. S., Martins, C. C., da Motta, K. P., Paltian, J. J., Costa, G. P., Alves, D., Luchese, C., & Wilhelm, E. A. (2022). Interface of Aging and Acute Peripheral Neuropathy Induced by Oxaliplatin in Mice: Target-Directed Approaches for Na+, K+—ATPase, Oxidative Stress, and 7-Chloro-4-(phenylselanyl) quinoline Therapy. *Molecular Neurobiology*, *59*(3), 1766–1780. https://doi.org/10.1007/s12035-021-02659-5

Ring, J., Alomar, A., Bieber, T., Deleuran, M., Fink-Wagner, A., Gelmetti, C., Gieler, U., Lipozencic, J., Luger, T., Oranje, A. P., Schäfer, T., Schwennesen, T., Seidenari, S., Simon, D., Ständer, S., Stingl, G., Szalai, S., Szepietowski, J. C., Taïeb, A., … Darsow, U. (2012). Guidelines for treatment of atopic eczema (atopic dermatitis) Part II. *Journal of the European Academy of Dermatology and Venereology : JEADV*, *26*(9), 1176–1193. https://doi.org/10.1111/j.1468-3083.2012.04636.x

Rivero, S., García, M. A., & Pinotti, A. (2009). Composite and bi-layer films based on gelatin and chitosan. *Journal of Food Engineering*, *90*(4), 531–539. https://doi.org/https://doi.org/10.1016/j.jfoodeng.2008.07.021

Saito, K., Takenouchi, O., Nukada, Y., Miyazawa, M., & Sakaguchi, H. (2017). An in vitro skin sensitization assay termed EpiSensA for broad sets of chemicals including lipophilic chemicals and pre/pro-haptens. *Toxicology in Vitro*, *40*, 11–25. https://doi.org/10.1016/j.tiv.2016.12.005

Schäcke, H., Döcke, W.-D., & Asadullah, K. (2002). Mechanisms involved in the side effects of glucocorticoids. *Pharmacology & Therapeutics*, *96*(1), 23–43. https://doi.org/https://doi.org/10.1016/S0163-7258(02)00297-8

Schroeder, H. A., Frost, D. V, & Balassa, J. J. (1970). Essential trace metals in man: selenium. *Journal of Chronic Diseases*, *23*(4), 227–243. https://doi.org/10.1016/0021-9681(70)90003-2

Shahid-ul-Islam, Shahid, M., & Mohammad, F. (2013). Green Chemistry Approaches to Develop Antimicrobial Textiles Based on Sustainable Biopolymers—A Review. *Industrial & Engineering Chemistry Research*, *52*(15), 5245–5260. https://doi.org/10.1021/ie303627x

Sharma, S., Sethi, G. S., & Naura, A. S. (2020). Curcumin Ameliorates Ovalbumin-Induced Atopic Dermatitis and Blocks the Progression of Atopic March in Mice. *Inflammation*, *43*(1), 358–369. https://doi.org/10.1007/s10753-019-01126-7

Shin, J., Kim, Y. J., Kwon, O., Kim, N.-I., & Cho, Y. (2016). Associations among plasma vitamin C, epidermal ceramide and clinical severity of atopic dermatitis. *Nutrition Research and Practice*, *10*(4), 398–403. https://doi.org/10.4162/nrp.2016.10.4.398

Sidbury, R., Davis, D. M., Cohen, D. E., Cordoro, K. M., Berger, T. G., Bergman, J. N., Chamlin, S. L., Cooper, K. D., Feldman, S. R., Hanifin, J. M., Krol, A., Margolis, D. J., Paller, A. S., Schwarzenberger, K., Silverman, R. A., Simpson, E. L., Tom, W. L., Williams, H. C., Elmets, C. A., … Eichenfield, L. F. (2014). Guidelines of care for the management of atopic dermatitis: Section 3. Management and treatment with phototherapy and systemic agents. *Journal of the American Academy of Dermatology*, *71*(2), 327–349. https://doi.org/10.1016/j.jaad.2014.03.030

Sies, H. (2014). Role of Metabolic H2O2 Generation: REDOX SIGNALING AND OXIDATIVE STRESS*. *Journal of Biological Chemistry*, *289*(13), 8735–8741. https://doi.org/https://doi.org/10.1074/jbc.R113.544635

Silverberg, J. I., Barbarot, S., Gadkari, A., Simpson, E. L., Weidinger, S., Mina-Osorio, P., Rossi, A. B., Brignoli, L., Saba, G., Guillemin, I., Fenton, M. C., Auziere, S., & Eckert, L. (2021). Atopic dermatitis in the pediatric population. *Annals of Allergy, Asthma & Immunology*. https://doi.org/10.1016/j.anai.2020.12.020

Sionkowska, A. (2011). Current research on the blends of natural and synthetic polymers as new biomaterials: Review. *Progress in Polymer Science - PROG POLYM SCI*, *36*, 1254–1276. https://doi.org/10.1016/j.progpolymsci.2011.05.003

Soliman, E. A., & Furuta, M. (2014). Influence of Phase Behavior and Miscibility on Mechanical, Thermal and Micro-Structure of Soluble Starch-Gelatin Thermoplastic Biodegradable Blend Films. *Food and Nutrition Sciences*, *05*(11), 1040–1055. https://doi.org/10.4236/fns.2014.511115

Suárez-Fariñas, M., Dhingra, N., Gittler, J., Shemer, A., Cardinale, I., de Guzman Strong, C., Krueger, J. G., & Guttman-Yassky, E. (2013). Intrinsic atopic

dermatitis shows similar TH2 and higher TH17 immune activation compared with extrinsic atopic dermatitis. *Journal of Allergy and Clinical Immunology*, *132*(2), 361–370. https://doi.org/https://doi.org/10.1016/j.jaci.2013.04.046

Tan, A. U., & Gonzalez, M. E. (2012). Management of severe atopic dermatitis in children. *Journal of Drugs in Dermatology : JDD*, *11*(10), 1158–1165.

Tanaka, T., Tsutsui, H., Yoshimoto, T., Kotani, M., Matsumoto, M., Fujita, A., Wang, W., Higa, S., Koshimoto, T., Nakanishi, K., & Suemura, M. (2001). Interleukin-18 is elevated in the sera from patients with atopic dermatitis and from atopic dermatitis model mice, NC/Nga. *International Archives of Allergy and Immunology*, *125*(3), 236–240. https://doi.org/10.1159/000053821

Tang, L., Li, X.-L., Deng, Z.-X., Xiao, Y., Cheng, Y.-H., Li, J., & Ding, H. (2020). Conjugated linoleic acid attenuates 2,4-dinitrofluorobenzene-induced atopic dermatitis in mice through dual inhibition of COX-2/5-LOX and TLR4/NF-κB signaling. *The Journal of Nutritional Biochemistry*, *81*, 108379. https://doi.org/https://doi.org/10.1016/j.jnutbio.2020.108379

Taskin, A. K., Yasar, M., Ozaydin, I., Kaya, B., Bat, O., Ankarali, S., Yildirim, U., & Aydin, M. (2013). The hemostatic effect of calcium alginate in experimental splenic injury model. *Ulus Travma Acil Cerrahi Derg*, *19*(3), 195–199. https://doi.org/10.5505/tjtes.2013.30676

Temenoff, J. S., & Mikos, A. G. (2008). *Biomaterials : the intersection of biology and materials science*. Upper Saddle River. http://lib.ugent.be/catalog/rug01:001793207

Tokura, Y. (2010). Extrinsic and intrinsic types of atopic dermatitis. *Journal of Dermatological Science*, *58*(1), 1–7. https://doi.org/10.1016/j.jdermsci.2010.02.008

Touma, C., Sachser, N., Möstl, E., & Palme, R. (2003). Effects of sex and time of day on metabolism and excretion of corticosterone in urine and feces of mice. *General and Comparative Endocrinology*, *130*(3), 267–278. https://doi.org/10.1016/s0016-6480(02)00620-2

Turner, M. J., Travers, J. B., & Kaplan, M. H. (2012). T helper cell subsets in the development of atopic dermatitis. *Journal of Drugs in Dermatology : JDD*, *11*(10), 1174—1178. http://europepmc.org/abstract/MED/23134982

Udompataikul, M., & Limpa-o-vart, D. (2012). Comparative trial of 5% dexpanthenol in water-in-oil formulation with 1% hydrocortisone ointment in

the treatment of childhood atopic dermatitis: a pilot study. *Journal of Drugs in Dermatology : JDD*, *11*(3), 366–374.

Ullah, K., Ali Khan, S., Murtaza, G., Sohail, M., Azizullah, Manan, A., & Afzal, A. (2019). Gelatin-based hydrogels as potential biomaterials for colonic delivery of oxaliplatin. *International Journal of Pharmaceutics*, *556*, 236–245. https://doi.org/https://doi.org/10.1016/j.ijpharm.2018.12.020

Voss, G., Gularte, M., Oliveira, R., Luchese, C., Fajardo, A., & Wilhelm, E. (2020). Biopolymeric films as delivery vehicles for controlled release of hydrocortisone: Promising devices to treat chronic skin diseases. *Materials Science and Engineering: C*, 111074. https://doi.org/10.1016/j.msec.2020.111074

Voss, G. T., de Oliveira, R. L., Davies, M. J., Domingues, W. B., Campos, V. F., Soares, M. P., Luchese, C., Schiesser, C. H., & Wilhelm, E. A. (2021). Suppressive effect of 1,4-anhydro-4-seleno-D-talitol (SeTal) on atopic dermatitis-like skin lesions in mice through regulation of inflammatory mediators. *Journal of Trace Elements in Medicine and Biology*, *67*, 126795. https://doi.org/https://doi.org/10.1016/j.jtemb.2021.126795

Voss, G. T., Oliveira, R. L., de Souza, J. F., Duarte, L. F. B., Fajardo, A. R., Alves, D., Luchese, C., & Wilhelm, E. A. (2018). Therapeutic and technological potential of 7-chloro-4-phenylselanyl quinoline for the treatment of atopic dermatitis-like skin lesions in mice. *Materials Science & Engineering. C, Materials for Biological Applications*, *84*, 90–98. https://doi.org/10.1016/j.msec.2017.11.026

Wang, Kaiqin, Jiang, H., Li, W., Qiang, M., Dong, T., & Li, H. (2018). Role of Vitamin C in Skin Diseases. *Frontiers in Physiology*, *9*, 819. https://doi.org/10.3389/fphys.2018.00819

Wang, Kun, Wang, W., Ye, R., Xiao, J., Liu, Y., Ding, J., Zhang, S., & Liu, A. (2017). Mechanical and barrier properties of maize starch-gelatin composite films: effects of amylose content. *Journal of the Science of Food and Agriculture*, *97*(11), 3613–3622. https://doi.org/10.1002/jsfa.8220

Wilhelm, E. A., Soares, P. S., Reis, A. S., Barth, A., Freitas, B. G., Motta, K. P., Lemos, B. B., Vogt, A. G., da Fonseca, C. A. R., Araujo, D. R., Barcellos, A. M., Perin, G., & Luchese, C. (2019). Se — [(2,2-Dimethyl-1,3-dioxolan-4-yl) methyl] 4-chlorobenzoselenolate reduces the nociceptive and edematogenic

response by chemical noxious stimuli in mice: Implications of multi-target actions. *Pharmacological Reports*, *71*(6), 1201–1209. https://doi.org/10.1016/j.pharep.2019.07.003

Xu, J., Fang, H., Zheng, S., Li, L., Jiao, Z., Wang, H., Nie, Y., Liu, T., & Song, K. (2021). A biological functional hybrid scaffold based on decellularized extracellular matrix/gelatin/chitosan with high biocompatibility and antibacterial activity for skin tissue engineering. *International Journal of Biological Macromolecules*, *187*, 840–849. https://doi.org/https://doi.org/10.1016/j.ijbiomac.2021.07.162

Yarbrough, K. B., Neuhaus, K. J., & Simpson, E. L. (2013). The effects of treatment on itch in atopic dermatitis. *Dermatologic Therapy*, *26*(2), 110–119. https://doi.org/10.1111/dth.12032

Young, S., Wong, M., Tabata, Y., & Mikos, A. G. (2005). Gelatin as a delivery vehicle for the controlled release of bioactive molecules. *Journal of Controlled Release : Official Journal of the Controlled Release Society*, *109*(1–3), 256–274. https://doi.org/10.1016/j.jconrel.2005.09.023

Youssef, A. M., & El-Sayed, S. M. (2018). Bionanocomposites materials for food packaging applications: Concepts and future outlook. *Carbohydrate Polymers*, *193*, 19—27. https://doi.org/10.1016/j.carbpol.2018.03.088

Yuan, L., Pan, M., Lei, M., Zhou, X., Hu, D., Liu, Q., Chen, Y., Li, W., & Qian, Z. (2020). A novel composite of micelles and hydrogel for improving skin delivery of hydrocortisone and application in atopic dermatitis therapy. *Applied Materials Today*, *19*, 100593. https://doi.org/https://doi.org/10.1016/j.apmt.2020.100593

Zacharias, T., Flouda, K., Jepps, T. A., Gammelgaard, B., Schiesser, C. H., & Davies, M. J. (2020). Effects of a novel selenium substituted-sugar (1,4-anhydro-4-seleno-d-talitol, SeTal) on human coronary artery cell lines and mouse aortic rings. *Biochemical Pharmacology*, *173*, 113631. https://doi.org/10.1016/j.bcp.2019.113631

Zanandréa, A., Franceschi, J., & Souza, P. A. de. (2020). The influence of atopic dermatitis on children's lives. *Research, Society and Development*, *9*(8), e99985170. https://doi.org/10.33448/rsd-v9i8.5170

Zdiri, K., Cayla, A., Elamri, A., Erard, A., & Salaun, F. (2022). Alginate-Based Bio-Composites and Their Potential Applications. *Journal of Functional*

Biomaterials, *13*(3), 117. https://doi.org/10.3390/jfb13030117

Zhang, X., Dong, X., Zhao, S., Ke, Y., Wen, K., Zhang, S., Wang, Z., & Shen, J. (2017). Synthesis of haptens and production of antibodies to bisphenol A. *Frontiers of Agricultural Science and Engineering*, *4*(3), 366–372. https://doi.org/10.15302/J-FASE-2017132

Zia, K. M., Tabasum, S., Nasif, M., Sultan, N., Aslam, N., Noreen, A., & Zuber, M. (2017). A review on synthesis, properties and applications of natural polymer based carrageenan blends and composites. *International Journal of Biological Macromolecules*, *96*, 282–301. https://doi.org/https://doi.org/10.1016/j.ijbiomac.2016.11.095

ANEXO A

Carta de aprovação dos protocolos experimentais pela Comissão de Ética em Experimentação Animal da Universidade Federal de Pelotas

UNIVERSIDADE FEDERAL DE PELOTAS

PARECER Nº 62/2018/CEEA/REITORIA
PROCESSO Nº 23110.025357/2018-96

Pelotas, 14 de junho de 2018

Certificado

Certificamos que a proposta intitulada "**Avaliação do efeito de compostos sintéticos inéditos na dermatite atópica induzida por 2,4-dinitroclorobenzeno em camundongos",** processo n° **23110.023357/2018-96**, sob a responsabilidade de **Ethel Antunes Wilhelm** - que envolve a produção, manutenção ou utilização de animais pertencentes ao filo Chordata, subfilo Vertebrata (exceto humanos), para fins de pesquisa científica (ou ensino) – encontra-se de acordo com os preceitos da Lei nº 11.794, de 8 de outubro de 2008, do Decreto nº 6.899, de 15 de julho de 2009, e com as normas editadas pelo Conselho Nacional de Controle de Experimentação Animal (CONCEA), e recebeu parecer **FAVORÁVEL** a sua execução pela Comissão de Ética em Experimentação Animal, em reunião de 11/06/2018.

Solicitamos que no TCLE seja assinado pelo Chefe do Biotério (fornecedor dos animais).

Finalidade	(X) Pesquisa ( ) Ensino
Vigência da autorização	15/07/2018 a 15/07/2023
Espécie/linhagem/raça	*Mus musculus*/Balb/c
N° de animais	208
Idade	60 dias
Sexo	Fêmeas
Origem	Biotério Central - UFPel

Número para cadastro: **23357-2018**

M.V. Dra. Anelize de Oliveira Campello Felix

Presidente da CEEA

Documento assinado eletronicamente por **ANELIZE DE OLIVEIRA CAMPELLO FELIX**, **Médico Veterinário**, em 14/06/2018, às 10:45, conforme horário oficial de Brasília, com fundamento no art. 6º, § 1º, do Decreto nº 8.539, de 8 de outubro de 2015.

A autenticidade deste documento pode ser conferida no site http://sei.ufpel.edu.br/sei/controlador_externo.php?acao=documento_conferir&id_orgao_acesso_externo=0, informando o código verificador **0178016** e o código CRC **8E1D3652**.

Referência: Processo nº 23110.025357/2018-96 SEI nº 0178016

ANEXO B

Permissão do periódico científico International Journal of Trace Elements in Medicine and Biology para a reprodução do material

Re: Authorization to insert article in the Thesis

DS **Dirk Schaumlöffel <dirk.schaumloeffel@univ-pau.fr>**
24/11/2022 10:27

Para: svc-scielsjournals@elsevier.com; gui_voss@hotmail.com

Authorization granted to attach the mentioned article in your thesis.

Dirk Schaumlöffel

Editor-in-Chief

Le 24.11.2022 à 14:13, svc-scielsjournals@elsevier.com a écrit :
> This email has been sent from the editor contact form on journals.elsevier.com by Guilherme Teixeira Voss. You can reply to Guilherme Teixeira Voss via gui_voss@hotmail.com.
>
> Suppressive effect of 1,4-anhydro-4-seleno-D-talitol (SeTal) on atopic
> dermatitis-like skin lesions in mice through regulation of
> inflammatory mediators.
> Guilherme T. Voss a, Renata L. de Oliveira a, Michael J. Davies b,c, William B. Domingues d,
> Vinicius F. Campos d, Mauro P. Soares e, Cristiane Luchese a, Carl H. Schiesser c,**,
> Ethel A. Wilhelm a,*
>
> I come through this email to request the authorization document to attach the aforementioned article in my thesis.
>
> Att.
> Guilherme Teixeira Voss

ANEXO C

Permissão do periódico científico International *Materials Science & Engineering C* para a reprodução do material

Dear Guilherme Teixeira Voss

We hereby grant you permission to reprint the material below at no charge in your thesis subject to the following conditions:

RE: Biopolymeric films as delivery vehicles for controlled release of hydrocortisone: Promising devices to treat chronic skin diseases, Materials Science and Engineering: C, Volume 114, 2020, Voss et al

1. If any part of the material to be used (for example, figures) has appeared in our publication with credit or acknowledgement to another source, permission must also be sought from that source. If such permission is not obtained then that material may not be included in your publication/copies.

2. Suitable acknowledgment to the source must be made, either as a footnote or in a reference list at the end of your publication, as follows:

"This article was published in Publication title, Vol number, Author(s), Title of article, Page Nos, Copyright Elsevier (or appropriate Society name) (Year)."

3. Your thesis may be submitted to your institution in either print or electronic form.

4. Reproduction of this material is confined to the purpose for which permission is hereby given.

5. This permission is granted for non-exclusive world English rights only. For other languages please reapply separately for each one required. Permission excludes use in an electronic form other than submission. Should you have a specific electronic project in mind please reapply for permission.

6. As long as the article is embedded in your thesis, you can post/share your thesis in the University repository.

7. Should your thesis be published commercially, please reapply for permission.

8. Posting of the full article/ chapter online is not permitted. You may post an abstract with a link to the Elsevier website www.elsevier.com, or to the article on ScienceDirect if it is available on that platform.

Kind regards,

Roopa Lingayath

ANEXO D

Comprovante de submissão do manuscrito na revista *Biomaterials Advances*

This is an automated message.

Journal: Biomaterials Advances
Title: Treating atopic-dermatitis-like skin lesions in mice with gelatin-alginate films containing 1,4-anhydro-4-seleno-d-talitol (SeTal)
Corresponding Author: Dr Ethel Wilhelm
Co-Authors: Guilherme T Voss; Michael J. Davies; Carl H. Schiesser; Renata L. de Oliveira; Andresa B. Nornberg; Victória R. Soares; Angelita M. Barcellos; Cristiane Luchese; André R. Fajardo
Manuscript Number: BIOADV-D-23-00268

Dear Guilherme T Voss,

The corresponding author Dr Ethel Wilhelm has listed you as a contributing author of the following submission via Elsevier's online submission system for Biomaterials Advances.

Submission Title: Treating atopic-dermatitis-like skin lesions in mice with gelatin-alginate films containing 1,4-anhydro-4-seleno-d-talitol (SeTal)

Elsevier asks all authors to verify their co-authorship by confirming agreement to publish this article if it is accepted for publication.